GRI-00/0123

# DEVELOPMENT OF A LOW COST INFERENTIAL NATURAL GAS ENERGY FLOW RATE PROTOTYPE RETROFIT MODULE

FINAL REPORT


*Prepared by:*

T. B. Morrow
E. Kelner
A. Minachi

SOUTHWEST RESEARCH INSTITUTE
Mechanical and Fluids Engineering Division
6220 Culebra Road
San Antonio, Texas, USA 78238-5166



SwRI Project Nos. 18-8890 (GRI) and 18-8627 (DOE)


*Prepared for:*


GAS RESEARCH INSTITUTE
GRI Contract No. 5097-270-3937

GRI Project Manager
Charles E. French
Pipeline Business Unit

U.S. DEPARTMENT OF ENERGY
DOE Cooperative Agreement No. DE-FC21-96M33033

DOE Technical Monitor
James Ammer
Gas Supply Projects

October 2000

*This page is intentionally blank.*

## GRI Disclaimer

LEGAL NOTICE: This report was prepared by Southwest Research Institute (SwRI) as an account of work sponsored by the Gas Research Institute (GRI) and the U.S. Department of Energy (DOE). Neither SwRI, GRI, members of these companies, DOE, nor any person acting on their behalf:

a. Makes any warranty or representation, expressed or implied, with respect to the accuracy, completeness, or usefulness of the information contained in this report, or that the use of any apparatus, methods, or process disclosed in this report may not infringe upon privately owned rights; or

b. Assumes any liability with respect to the use of, or for damages resulting from the use of, any information, apparatus, method, or process disclosed in this report.

*This page is intentionally blank.*

# REPORT DOCUMENTATION PAGE

Form Approved
OMB No. 0704-0188



| 1. AGENCY USE ONLY (Leave blank) | 2. REPORT DATE | 3. REPORT TYPE AND DATES COVERED |
|---|---|---|
| | October 2000 | Final Report (05/99-06/00) |

**4. TITLE AND SUBTITLE**
Development of a Low Cost Inferential Natural Gas Energy Flow Rate Prototype Retrofit Module

**5. FUNDING NUMBERS**
GRI Contract No. 5097-270-3937
DOE Cooperative Agreement No. DE-FC21-96MC33033

**6. AUTHOR(S)**
Thomas B. Morrow, Eric Kelner, Ali Minachi

**7. PERFORMING ORGANIZATION NAME(S) AND ADDRESS(ES)**
Southwest Research Institute
6220 Culebra Road
San Antonio, Texas 78238-5166

**8. PERFORMING ORGANIZATION REPORT NUMBER**
18.08890 (GRI)
18.08627 (DOE)

**9. SPONSORING ORGANIZATION NAMES AND ADDRESSES**
Gas Research Institute
8600 Bryn Mawr Avenue
Chicago, IL 60631-3562

U.S. Department of Energy
National Energy Technology Laboratory
P.O. Box 880
Morgantown, WV 26507-0880

**10. SPONSORING/MONITORING AGENCY REPORT NUMBER**
GRI-00/0123

**11. SUPPLEMENTARY NOTES**

**12a. DISTRIBUTION/AVAILABILITY STATEMENT**

**12b. DISTRIBUTION CODE**

**13. ABSTRACT (Maximum 200 words)**

The goal was to develop a prototype instrument module to retrofit a natural gas custody transfer flow meter for energy measurement, at a cost an order-of-magnitude lower than a gas chromatograph. Objectives were to: (1) revise the inferential property approach to allow use of the speed of sound at pipeline pressure and temperature as a correlation variable together with the carbon dioxide and nitrogen concentrations; (2) design and build a prototype instrument module for energy measurement; and (3) test the prototype module at various flowing natural gas conditions in the GRI Metering Research Facility (MRF).

The inferential approach was revised to use the speed of sound at arbitrary pressure and temperature as a correlation variable. An energy meter module was built to measure the inferential properties on a sample gas stream at reduced pressure. $CO_2$ and ultrasonic transducers were selected and installed in the prototype module. An ACCOL computer code was developed to calculate the heating value and energy flow rate on a Bristol Babcock model 3330 flow computer, which is commonly used for flow metering installations in the field. Abbreviated tests were performed with a 12-inch ultrasonic flow meter in the MRF High Pressure Loop (HPL) and with a 4-inch orifice meter in the MRF Low Pressure Loop (LPL).

**14. SUBJECT TERMS**
Energy Meter
Energy Flow Rate Measurement
Ultrasonic Meter
Orifice Meter
Heating Value
Metering Research Facility
Custody Transfer
Flow Computer

**15. NUMBER OF PAGES**
98

**16. PRICE CODE**

| 17. SECURITY CLASSIFICATION OF REPORT | 18. SECURITY CLASSIFICATION OF THIS PAGE | 19. SECURITY CLASSIFICATION OF ABSTRACT | 20. LIMITATION OF ABSTRACT |
|---|---|---|---|
| Unclassified | Unclassified | Unclassified | |

NSN 7540-01-280-5500

Standard Form 298 (Rev. 2-89)
Prescribed by ANSI Std. Z39-18
298-102

*This page is intentionally blank.*

# Research Summary

| | |
|---|---|
| **Title:** | Development of a Low Cost Inferential Natural Gas Energy Flow Rate Prototype Retrofit Module |
| **Contractor:** | Southwest Research Institute (SwRI) |
| **GRI Contract No.** | 5097-270-3937<br>(Also DOE Cooperative Agreement No. DE-FC21-96MC33033) |
| **Principal Investigator(s):** | Thomas B. Morrow, Eric Kelner, Ali Minachi |
| **Report Period:** | May 1999 – June 2000<br>Final Report |

**Objectives:**

The project goal was to develop a working prototype instrument module, for retrofitting a natural gas custody transfer flow meter for energy measurement, at a cost an order-of-magnitude lower than the gas chromatograph.

The project had three specific objectives:

- Refine and extend the fundamental technology of inferential property sensing. Specifically, revise the inferential correlation approach to allow use of the speed of sound at arbitrary pressure and temperature as a correlation variable together with the carbon dioxide and nitrogen concentrations.
- Design and build a prototype instrument module for energy measurement.
- Test the prototype at various flowing natural gas conditions in the GRI Metering Research Facility (MRF).

**Technical Perspective:**

The cost to upgrade an existing meter station to energy measurement by gas chromatography (GC) composition assay is currently $60,000 - $100,000. The complexity of the GC requires sustained maintenance by highly trained staff. A prior project for the U.S. Department of Energy (DOE) identified a simpler, inferential approach with the potential to reduce costs for energy measurement by an order of magnitude. The inferential approach used the AGA Report No. 8 Gross Method Equation of State and measured the sound speed, nitrogen ($N_2$), and carbon dioxide ($CO_2$) concentrations at standard temperature, 60ºF, and at standard pressure, 14.73 psia, abbreviated as STP. This approach was shown to be technically feasible for a broad range of gas compositions through the development of least-square-error regression equations and

by laboratory tests. DOE and GRI agreed to co-fund a second project phase to design, build and test a prototype energy meter module that would be compatible with existing volumetric flow meters for natural gas service.

**Technical Approach:**

The GRI Measurement Technical Advisor Group (MTAG) recommended that the approach be revised to permit using the speed of sound signal from an ultrasonic flow meter in place of the measured value of sound speed at STP. In response to this request, the inferential correlations were reformulated to employ the sound speed at arbitrary temperature and pressure and the $N_2$ and $CO_2$ concentrations without significant loss of accuracy. For applications not involving an ultrasonic meter, a separate energy meter module was designed and fabricated to measure the speed of sound, and $N_2$ and $CO_2$ concentrations on a sample gas stream at reduced pressure. $CO_2$ and ultrasonic transducers were selected and installed in the prototype module. Smart transmitters were used to measure temperature and pressure. A FORTRAN computer code was written to perform the energy and flow rate calculations. The FORTRAN code was translated into ACCOL to run on a Bristol Babcock model 3330 flow computer, which is commonly used for flow metering installations in the field. Tests were scheduled with a 12-inch ultrasonic flow meter in the Metering Research Facility (MRF) High Pressure Loop (HPL) and with a 4-inch orifice meter in the MRF Low Pressure Loop (LPL).

**Results:**

An unexpected communication problem arose between the ultrasonic flowmeter and the flow computer. Although the difficulty was eventually corrected, it limited the number of energy meter performance tests within the period of time reserved for testing in the MRF. Abbreviated tests with the 12-inch ultrasonic meter in the HPL indicated that the standard volumetric heating value was determined accurately to within about ±1 Btu/SCF. A similar abbreviated test using the energy meter module to measure sound speed with the 4-inch orifice meter in the LPL appeared to show that the system for measuring gas temperature within the energy meter module needs to be improved. The energy meter module sensor for measuring $CO_2$ concentration performed well, as expected.

**Project Implications:**

Successful development and implementation of a low cost inferential energy measurement prototype will benefit the U.S. natural gas industry. Widespread implementation of a low cost energy measurement instrument will:

- Facilitate improved gas network inventory control by reducing imbalances and inequities in energy transfers across system boundaries, and to and from bulk storage facilities.

- Facilitate the use of thermal energy balances to optimize the fuel efficiency of industrial plants that are fueled by natural gas.
- Facilitate equitable fuel energy transfer to motorists at compressed natural gas (CNG) dispensing stations.

This technology will also allow real-time energy rate measurement at many more field meter sites due to its cost effectiveness.

GRI Project Manager
Charles E. French
Program Manager – Measurement
Pipeline Business Unit

*This page is intentionally blank.*

# Table of Contents

# Table of Contents (continued)

# List of Figures

# List of Figures (continued)

# List of Figures (continued)

*This page is intentionally blank.*

# List of Tables

*This page is intentionally blank.*

# 1.0 EXECUTIVE SUMMARY

A natural gas technology assessment and feasibility evaluation (Behring et al., 1999) was performed by Southwest Research Institute for the U.S. Department of Energy (DOE) in 1998. In the assessment phase of the project, the needs and potential benefits of widespread energy measurement in the U.S. natural gas industry were identified. The project found that deregulation and open access have increased the need for widespread energy measurement. However, energy measurement has had limited implementation. Traditional gas composition assay equipment (gas chromatography) is expensive to install ($60,000 - $100,000 per meter station), and operating economics limit these installations.

Behring et al. also identified the fact that a full composition assay is not required at every meter station to measure flow rate or energy flow rate. Flow and energy measurement properties may be determined with just a few inferential measurements that characterize the natural gas composition without a full composition analysis. The practical feasibility of that approach was demonstrated with least-square-error regression correlations that predict the energy measurement properties of a natural gas database with accuracy equivalent to a detailed composition assay, and $500 worth of commercially available on-line sensors.

DOE and Gas Research Institute (GRI)* agreed to co-fund a second project phase to design, build and test a prototype energy meter module that would be compatible with existing volumetric flow meters for natural gas service.

## 1.1 Objectives

The project goal was to develop a working prototype instrument module, with performance capable of retrofitting a natural gas custody transfer flow meter for energy measurement, at an order-of-magnitude lower cost than the gas chromatograph.

This research project had three specific objectives:

- Refine and extend the fundamental technology of inferential property sensing. Specifically, extend the inferential correlation approach to permit using the speed of sound at arbitrary pressure and temperature as a correlation variable.
- Design and construct a working retrofit instrument module for energy measurement.
- Test the working prototype at various flowing natural gas conditions in the GRI Metering Research Facility (MRF).

## 1.2 Gas Quality Tariffs

Behring et al. developed a database of 102 natural gas mixtures. This database is a modified subset of an earlier gas mixture database used by Starling et al. (1991) in the development of the AGA equation of state for natural gas mixtures (AGA, 1994). The inferential correlations developed by Behring et al. are least-square-error regression fits to 102 natural gas mixtures that cover a range of heating values from 987 Btu/SCF to 1151 Btu/SCF.

* In April 2000, Gas Research Institute (GRI) and the Institute of Gas Technology (IGT) combined to form Gas Technology Institute (GTI).

The nitrogen and carbon dioxide concentrations ranged separately from 0.44% to 6.00%, while the sum of the diluent gases ranged from 0.97% to 7.40%. To determine whether the range of heating values or the range of diluent concentrations should be extended, gas quality tariff limits for interstate gas pipelines were investigated. Pipelines reserve the right to refuse gas that is outside gas quality tariff limits.

Miller (1995) reported the results of the Grid Integration Project Task Force that assessed the impact of gas quality as it affects gas movements across the interstate pipeline grid. The Task Force found that gas quality problems affected less than 2% of the average 50+ BCFD of gas moved across the grid. The quality characteristics most significant to pipeline operation are Btu content, and concentrations of carbon dioxide, hydrogen sulfide and water vapor. The Task Force's report adds that "other characteristics have lesser impact on operations but may affect production (e.g., nitrogen), pipeline economics (e.g., inerts transportation), end-use (e.g., sulfur, inerts) or cause environmental concerns (e.g., trace contaminants)."

The Task Force found that most pipeline companies surveyed reported a minimum Btu limit between 950 to 970 Btu/SCF. Of the companies that reported a maximum Btu limit, the majority set limits between 1050 Btu/SCF and 1200 Btu/SCF (some companies limit hydrocarbon dew point or liquid hydrocarbon content rather than the energy content). The current tariff limits for carbon dioxide concentration are in the range between 1% and 3%, based primarily on corrosion considerations. Tariff limits for hydrogen sulfide are much lower, in the range of 4 ppm to 16 ppm. At these low levels, hydrogen sulfide will not significantly affect the natural gas energy content. Tariff limits for water vapor range from 4 –7 lb/million SCF. Rather than specify a separate tariff for nitrogen, it is customary to specify an upper limit for “total inerts,” which includes the combination of carbon dioxide, nitrogen, carbon monoxide, and any other gas that does not have a heating value. Just under one-half of the companies surveyed limit total inerts in the range of 3% to 5%.

In summary, the gas composition database developed by Behring et al. covers the heating value range from 987 Btu/SCF to 1151 Btu/SCF compared to the tariff limit range from 950 – 970 Btu/SCF to 1050 - 1200 Btu/SCF. The database covers the range of total inerts from 0.97% to 7.40% compared to the tariff limit for total inerts of 3% to 5%. The nitrogen and carbon dioxide concentrations in the database range separately from 0.44% to 6.00% compared to the tariff upper limit for carbon dioxide of 1% to 3%. We can expect that the inferential least-square-error correlations developed by Behring et al. will accurately predict the heating value and thermodynamic properties of natural gas mixtures bounded by the gas quality tariffs.

## 1.3 Summary

The GRI Measurement Technical Advisor Group (MTAG) recommended that the approach be revised to permit using the speed of sound signal from an ultrasonic flow meter in place of the measured value of sound speed at STP. In response to this recommendation, the inferential correlations were reformulated to employ the sound speed and the $N_2$ and $CO_2$ concentrations at arbitrary temperature and pressure without significant loss of accuracy. For applications not involving an ultrasonic meter, a separate energy meter module was designed and fabricated to measure the speed of sound and $N_2$ and $CO_2$ concentrations on a sample gas stream at reduced pressure. $CO_2$ and ultrasonic transducers were selected and installed in the prototype module. Smart transmitters were used to measure temperature and pressure. A FORTRAN

computer code was written to perform the energy and flow rate calculations. The FORTRAN code was translated into ACCOL to run on a Bristol Babcock model 3330 flow computer, which is commonly used for flow metering installations in the field. Tests were scheduled with a 12-inch ultrasonic flow meter in the MRF High Pressure Loop (HPL) and with a 4-inch orifice meter in the MRF Low Pressure Loop (LPL).

As the ultrasonic meter tests got under way, an unexpected communications problem arose between the ultrasonic flowmeter and the flow computer. Although the difficulty was eventually corrected, it limited the number of energy meter performance tests within the period of time reserved for testing in the MRF. Abbreviated tests with the 12-inch ultrasonic meter in the HPL indicated that the standard volumetric heating value was determined accurately to within ±1 Btu/SCF. A second test was performed using the energy meter module to measure the speed of sound and $CO_2$ concentration for gas flowing through a 4-inch orifice meter in the LPL. Data collection was delayed initially by a communications problem between the energy meter module and the flow computer. Communication was established by correcting an error in the computer code. Tests of the energy meter module showed a +47 Btu/SCF difference between the measured heating value and the known reference value. However, the measured value of $CO_2$ concentration was within an average of 0.054 mole% of the known value determined by gas chromatograph, well within the allowable error of ±0.3 mole% for this measurement.

Attention was focused on the measurements of sound speed and temperature in the energy meter module to resolve the heating value error. Two adjustments were made to the measured data that reduce the heating value error to 2.3 Btu/SCF. The first adjustment is a 1-cycle correction of –5 μsecond to the ultrasonic signal transit time. This correction reduced the error to +15.2 Btu/SCF, demonstrating the importance of accurate sound speed measurement. The second adjustment is to the measured value of gas temperature, which was influenced by the ambient temperature (over 90ºF on the day of the test). When the gas temperature was reduced from the recorded values of over 90ºF to 73ºF, a value slightly above the gas temperature in the orifice meter tube, the error in heating value was reduced to –2.3 Btu/SCF. This demonstrates the need to insulate the energy meter module from ambient heating and/or cooling effects.

The original energy meter development goal for accuracy was ±5 Btu/SCF. While an accuracy level of ±1 Btu/SCF is probably needed for the energy meter to be considered as a replacement for a gas chromatograph, at the accuracy level of ±5 Btu/SCF the energy meter will be used in applications where the Btu content of the gas stream is needed, but the cost of a gas chromatograph is prohibitive. Also, an uncertainty in energy content of ±5 Btu/SCF (about 0.5%) is not inappropriate when the energy meter is used together with a flow meter of similar or higher percentage uncertainty in volumetric flow rate.

## 1.4 Recommendations for Further Work

1. Improve the design and operation of the system used to measure the speed of sound in the gas stream flowing through the energy meter module. The goal is to measure the sound speed to an accuracy of 1 ft/s.
2. Improve the design and operation of the system used to measure the temperature of the gas stream flowing through the energy meter module. Eliminate the influence of ambient temperature on the measured gas temperature.

3. Select, develop, and evaluate the design of a system for determining the $N_2$ concentration in the gas stream flowing through the energy meter module by the measurement of a thermo-physical property such as the specific heat. A strong candidate is the apparatus and method described in GRI Patent US5,932,793 (Drayton, 1999) for determining thermophysical properties using an isochoric (constant volume) approach.
4. Successfully complete the ultrasonic meter test and the orifice meter test, and review the results with GRI/DOE.
5. Evaluate the performance of the energy meter module for a range of gas mixtures with heating values in the range from 950 Btu/SCF to 1100 Btu/SCF.
6. Recruit a commercial partner to assess the commercial potential of the energy meter module.
7. Schedule and complete field tests of the energy meter module with an ultrasonic flow meter and a second class of meter such as turbine meter, orifice meter, or Coriolis meter.

## 2.0 Correlating Chemical Properties to Standard Sound Speed

Behring et al. (1999) identified a promising technique to characterize natural gas hydrocarbon mixtures with a single inferential property when the concentrations of the diluent gases (carbon dioxide and nitrogen) are known. The single inferential property was the speed of sound in the natural gas mixture at standard pressure and temperature conditions of 14.73 psia and 60ºF. Successful data correlations were developed for chemical properties such as molecular weight, $MW$, mass-based heating value, $H_m$, standard density, $\rho_{std}$, molar ideal gross heating value, $H_{n,ref}$, and standard volumetric heating value, $H_{v,std}$, which is the product of the standard density and the mass-based heating value. The correlations have now been extended to include speed of sound measured at arbitrary values of temperature and pressure. However, before explaining the extensions, it is helpful to review the work accomplished on the previous phase of this project and the modified approach developed on the current project.

Behring et al. reviewed prior research on inferential methods for determining gas density and heating value. Relationships between the gas density, molecular weight, and/or heating value and the speed of sound had been discovered and discussed before. Lueptow and Phillips (1994) noted that the speed of sound had been used to determine the composition of binary (two-constituent) gas mixtures successfully. These authors observed that natural gas mixtures with low quantities of inerts had a greater heating value at a particular sound speed than gas mixtures with high level of inerts. They found that the spread of heating values at constant sound speed was of the order of 7% (approximately 70 Btu/SCF) for gases with inert concentrations ranging from 0% to 5%. Lueptow and Phillips did not attempt to compensate for the diluent constituents.

Watson and White (1981) devised a correlation for the natural gas heating value at standard pressure and temperature to the sound speed. They assumed that natural gas could be represented as a blend of methane, ethane, propane and butane with negligible amounts of $CO_2$ and $N_2$. In the absence of diluents, they claimed that the heating value of the blend could be monitored acoustically with 0.4% accuracy (approximately 4 Btu/SCF). These authors noted that non-combustible gases ($N_2$, $CO_2$) introduced an ambiguity in the energy content determination. They concluded, "… a means for segregating or otherwise knowing the non-combustible gas fractions is required. A method for achieving this identification acoustically has not been defined as yet."

Kristensen et al. (1998) developed a proprietary thermodynamic correlation between the flowing gas density and the sound speed. The correlation required the use of known diluent concentrations, and was able to predict density from sound speed (measured by an ultrasonic flow meter) to within an accuracy of 1% over several different natural gas compositions.

Behring et al. developed correlations for standard heating value, mass-based heating value, molecular weight, standard density, etc. as a function of the sound speed at standard temperature and pressure, and the mole fractions of $CO_2$ and $N_2$. Also, he showed how the standard sound speed could be substituted for the relative density of the natural gas mixture so that the AGA-8 equation of state (Gross Method; AGA, 1994) could be used to calculate thermodynamic properties such as density and compressibility.

Figure 1a shows the behavior of the standard density, $\rho_{std}$, as a function of the standard sound speed, $S_{std}$, for 86 different natural gas mixtures. The values of $\rho_{std}$ and $S_{std}$ were

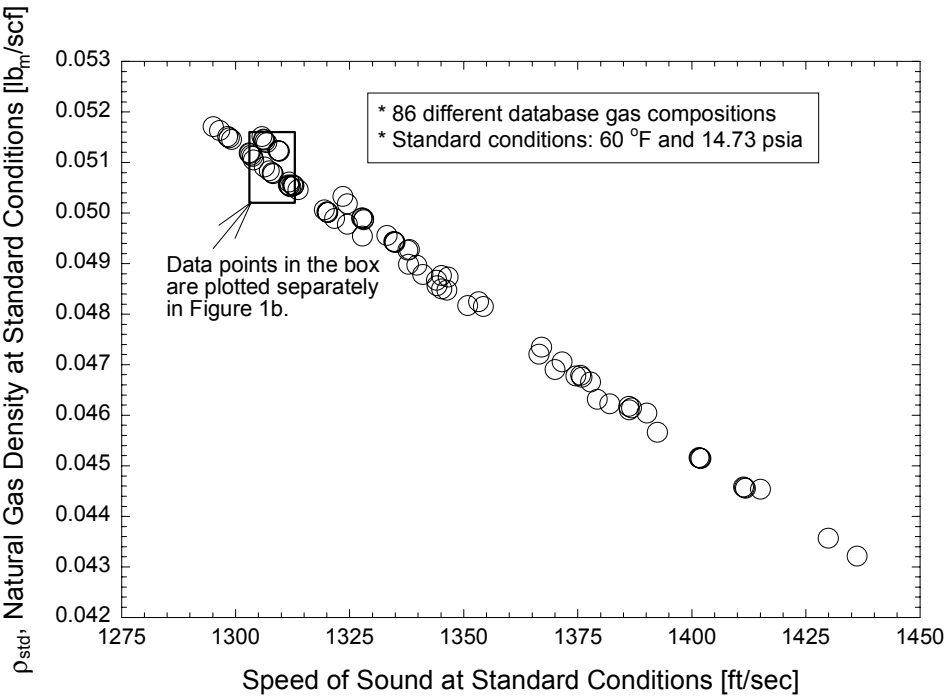


**Figure 1a. Natural gas density at standard conditions as a function of speed of sound.**

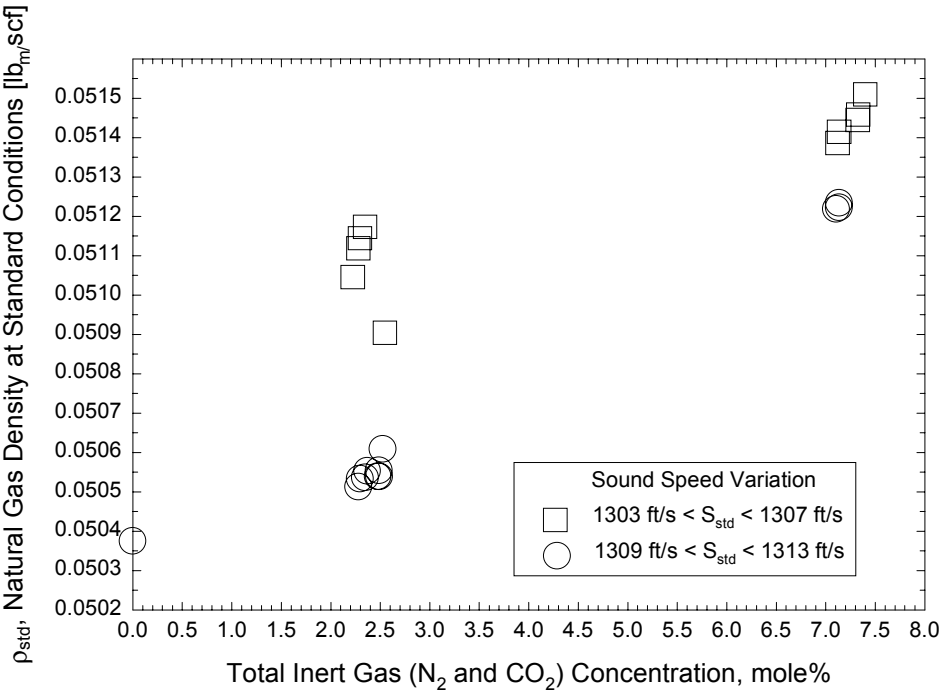


**Figure 1b. Natural gas density at standard conditions as a function of diluent gas concentration.**

calculated using Lomic SonicWare® (1997) from the detailed composition analysis listed in Table 1. The scatter of the data points for the same value of standard sound speed is caused by the presence of non-hydrocarbon gases, up to 6% by volume of carbon dioxide and/or nitrogen. It may not be obvious that the scatter shown in Figure 1a is caused mainly by the inert gas concentrations rather than by the combination of hydrocarbon gases. To clarify this point, let's look specifically at the data points for $\rho_{std}$ in the range of standard sound speed values from 1303 ft/s to 1313 ft/s. Figure 1b shows 21 data points from Table 1 and one data point from Table 2 plotted as standard density as a function of total inert concentration. Data points for sound speeds between 1303 ft/s and 1307 ft/s are plotted as squares. Data points for sound speeds between 1309 ft/s and 1313 ft/s are plotted as circles. The effect of sound speed on density can be seen clearly in Figure 1b. However, a second effect is also present. For each sound speed range, the density is proportional to the total inert gas concentration (nitrogen and methane together). The data correlation will be improved if the functional dependence on nitrogen and carbon dioxide concentrations is accounted for explicitly.

As a first approximation, natural gas mixtures at standard pressure and temperature can be represented by an ideal gas equation of state.

$$\rho_{std} = P_{std} \Big/ RT_{std} \tag{1}$$

where $\rho_{std}$ = standard density, $P_{std}$ = 14.73 psia, $R$ = gas constant, and $T_{std}$ = 520ºR.

For an ideal gas, the standard sound speed, $S_{std}$, is related to the gas temperature as:

$$S_{std}^{\ 2} = kRT_{std} \tag{2}$$

where $k$ = ratio of specific heats. Combining equations (1) and (2), we obtain

$$\rho_{std} = kP_{std} \Big/ S_{std}^{\ 2} \tag{3}$$

Since the pressure is constant, $P$ = 14.73 psia, we might expect that the standard density would vary inversely as the square of the standard sound speed. However, the ratio of specific heats, $k$, increases linearly as a function of standard sound speed, as shown in Figure 2. The "scatter" of data points at constant values of sound speed in Figure 2 shows that the ratio of specific heats is also affected by the diluent gas concentration.

An approximate functional form for the standard density as a function of the standard speed of sound would be:

$$\rho_{std} = A + B / S_{std} + C / S_{std}^{\ 2} \tag{4}$$

Behring et al. used a similar functional form that is second order in standard sound speed with good results.

$$\rho_{std} = A + B * S_{std} + C * S_{std}^{\ 2} \tag{5}$$

## Table 1. Natural gas mixture composition database.

| ID# | Sstd | $_{\rho}$std | MW | Hv | nitrogen | carbon dioxide | methane | ethane | propane | i-butane | n-butane | i-pentane | n-pentane | n-hexane | n-heptane | n-octane |
|---|---|---|---|---|---|---|---|---|---|---|---|---|---|---|---|---|
| | (ft/s) | lbm/ft3 | | (Btu/scf) | (mole%) | (mole%) | (mole%) | (mole%) | (mole%) | (mole%) | (mole%) | (mole%) | (mole%) | (mole%) | (mole%) | (mole%) |
| 1 | 1302.94 | 0.0511865 | 19.3241 | 1136.7 | 0.4422 | 1.9285 | 84.3361 | 8.8946 | 3.1919 | 0.59064 | 0.39376 | 0.10950 | 0.07300 | 0.0325 | 0.0061 | 0.0012 |
| 52 | 1311.63 | 0.0505531 | 19.0864 | 1136.6 | 1.9285 | 0.4422 | 84.3361 | 8.8946 | 3.1919 | 0.59064 | 0.39376 | 0.10950 | 0.07300 | 0.0325 | 0.0061 | 0.0012 |
| 2 | 1411.57 | 0.0445646 | 16.8372 | 1024.9 | 1.6004 | 0.2331 | 95.5340 | 1.8790 | 0.4926 | 0.09066 | 0.06044 | 0.03522 | 0.02348 | 0.0309 | 0.0168 | 0.0034 |
| 53 | 1401.83 | 0.0451462 | 17.0559 | 1025.0 | 0.2331 | 1.6004 | 95.5340 | 1.8790 | 0.4926 | 0.09066 | 0.06044 | 0.03522 | 0.02348 | 0.0309 | 0.0168 | 0.0034 |
| 3 | 1334.70 | 0.0494356 | 18.6729 | 1025.9 | 5.6769 | 1.4546 | 85.1473 | 5.4174 | 1.5968 | 0.30438 | 0.20292 | 0.08694 | 0.05796 | 0.0391 | 0.0138 | 0.0019 |
| 54 | 1309.38 | 0.0512337 | 19.3483 | 1026.1 | 1.4546 | 5.6769 | 85.1473 | 5.4174 | 1.5968 | 0.30438 | 0.20292 | 0.08694 | 0.05796 | 0.0391 | 0.0138 | 0.0019 |
| 4 | 1312.77 | 0.0505387 | 19.0814 | 1122.1 | 0.6224 | 1.8643 | 85.4814 | 8.0607 | 2.8624 | 0.52170 | 0.34780 | 0.11346 | 0.07564 | 0.0398 | 0.0096 | 0.0008 |
| 55 | 1320.16 | 0.0500096 | 18.8827 | 1122.0 | 1.8643 | 0.6224 | 85.4814 | 8.0607 | 2.8624 | 0.52170 | 0.34780 | 0.11346 | 0.07564 | 0.0398 | 0.0096 | 0.0008 |
| 5 | 1328.07 | 0.0498841 | 18.8415 | 1028.6 | 5.4939 | 1.8292 | 84.3931 | 5.8857 | 1.6910 | 0.32742 | 0.21828 | 0.06942 | 0.04628 | 0.0296 | 0.0128 | 0.0033 |
| 56 | 1306.32 | 0.0514449 | 19.4277 | 1028.8 | 1.8292 | 5.4929 | 84.3931 | 5.8857 | 1.6910 | 0.32742 | 0.21828 | 0.06942 | 0.04628 | 0.0296 | 0.0128 | 0.0033 |
| 6 | 1327.69 | 0.0498922 | 18.8443 | 1032.3 | 5.3551 | 1.7802 | 84.4786 | 5.8782 | 1.7778 | 0.34002 | 0.22668 | 0.07050 | 0.04700 | 0.0309 | 0.0116 | 0.0034 |
| 57 | 1306.48 | 0.0514147 | 19.4162 | 1032.5 | 1.7802 | 5.3551 | 84.4786 | 5.8782 | 1.7778 | 0.34002 | 0.22668 | 0.07050 | 0.04700 | 0.0309 | 0.0116 | 0.0034 |
| 7 | 1411.36 | 0.0445763 | 16.8416 | 1025.1 | 1.6052 | 0.2339 | 95.5192 | 1.8835 | 0.4933 | 0.09108 | 0.06072 | 0.03546 | 0.02364 | 0.0326 | 0.0176 | 0.0038 |
| 58 | 1401.59 | 0.0451596 | 17.0610 | 1025.1 | 0.2339 | 1.6052 | 95.5192 | 1.8835 | 0.4933 | 0.09108 | 0.06072 | 0.03546 | 0.02364 | 0.0326 | 0.0176 | 0.0038 |
| 8 | 1303.80 | 0.0511191 | 19.2987 | 1137.6 | 0.4278 | 1.8497 | 84.4678 | 8.8604 | 3.1831 | 0.58008 | 0.38672 | 0.11994 | 0.07996 | 0.0369 | 0.0068 | 0.0008 |
| 59 | 1312.12 | 0.0505132 | 19.0713 | 1137.5 | 1.8497 | 0.4278 | 84.4678 | 8.8604 | 3.1831 | 0.58008 | 0.38672 | 0.11994 | 0.07996 | 0.0369 | 0.0068 | 0.0008 |
| 9 | 1334.86 | 0.0494259 | 18.6692 | 1025.6 | 5.6760 | 1.4579 | 85.1666 | 5.4022 | 1.5922 | 0.30366 | 0.20244 | 0.08706 | 0.05804 | 0.0385 | 0.0134 | 0.0020 |
| 60 | 1309.56 | 0.0512222 | 19.3440 | 1025.8 | 1.4579 | 5.6760 | 85.1666 | 5.4022 | 1.5922 | 0.30366 | 0.20244 | 0.08706 | 0.05804 | 0.0385 | 0.0134 | 0.0020 |
| 10 | 1312.75 | 0.0505390 | 19.0814 | 1122.3 | 0.6122 | 1.8630 | 85.4915 | 8.0626 | 2.8576 | 0.52254 | 0.34836 | 0.11412 | 0.07608 | 0.0404 | 0.0100 | 0.0016 |
| 61 | 1320.20 | 0.0500061 | 18.8814 | 1122.2 | 1.8630 | 0.6122 | 85.4915 | 8.0626 | 2.8576 | 0.52254 | 0.34836 | 0.11412 | 0.07608 | 0.0404 | 0.0100 | 0.0016 |
| 15 | 1411.78 | 0.0445535 | 16.8330 | 1024.7 | 1.6032 | 0.2299 | 95.5480 | 1.8724 | 0.4883 | 0.08982 | 0.05988 | 0.03462 | 0.02308 | 0.0312 | 0.0164 | 0.0032 |
| 66 | 1401.99 | 0.0451377 | 17.0527 | 1024.8 | 0.2299 | 1.6032 | 95.5480 | 1.8724 | 0.4883 | 0.08982 | 0.05988 | 0.03462 | 0.02308 | 0.0312 | 0.0164 | 0.0032 |
| 16 | 1303.45 | 0.0511445 | 19.3083 | 1137.7 | 0.4293 | 1.8647 | 84.4333 | 8.8669 | 3.1897 | 0.58182 | 0.38788 | 0.12066 | 0.08044 | 0.0377 | 0.0072 | 0.0004 |
| 67 | 1311.84 | 0.0505328 | 19.0787 | 1137.6 | 1.8647 | 0.4293 | 84.4333 | 8.8669 | 3.1897 | 0.58182 | 0.38788 | 0.12066 | 0.08044 | 0.0377 | 0.0072 | 0.0004 |
| 17 | 1334.97 | 0.0494159 | 18.6655 | 1026.1 | 5.6680 | 1.4349 | 85.1784 | 5.4163 | 1.5962 | 0.30426 | 0.20284 | 0.08706 | 0.05804 | 0.0387 | 0.0131 | 0.0022 |
| 68 | 1309.58 | 0.0512186 | 19.3426 | 1026.3 | 1.4349 | 5.6680 | 85.1784 | 5.4163 | 1.5962 | 0.30426 | 0.20284 | 0.08706 | 0.05804 | 0.0387 | 0.0131 | 0.0022 |
| 18 | 1312.53 | 0.0505545 | 19.0873 | 1122.4 | 0.6137 | 1.8710 | 85.4620 | 8.0768 | 2.8634 | 0.52272 | 0.34848 | 0.11412 | 0.07608 | 0.0405 | 0.0101 | 0.0011 |
| 69 | 1320.01 | 0.0500188 | 18.8861 | 1122.3 | 1.8710 | 0.6137 | 85.4620 | 8.0768 | 2.8634 | 0.52272 | 0.34848 | 0.11412 | 0.07608 | 0.0405 | 0.0101 | 0.0011 |
| 19 | 1382.00 | 0.0462233 | 17.4611 | 1051.2 | 2.3535 | 0.0401 | 92.2794 | 3.7252 | 0.9170 | 0.26166 | 0.17444 | 0.08898 | 0.05932 | 0.0654 | 0.0115 | 0.0235 |
| 70 | 1366.54 | 0.0472077 | 17.8311 | 1051.3 | 0.0401 | 2.3535 | 92.2794 | 3.7252 | 0.9170 | 0.26166 | 0.17444 | 0.08898 | 0.05932 | 0.0654 | 0.0115 | 0.0235 |
| 20 | 1392.51 | 0.0456565 | 17.2485 | 1034.3 | 2.6733 | 0.0402 | 93.0357 | 3.1217 | 0.6420 | 0.16896 | 0.11264 | 0.06930 | 0.04620 | 0.0436 | 0.0229 | 0.0235 |
| 71 | 1374.59 | 0.0467768 | 17.6697 | 1034.4 | 0.0402 | 2.6733 | 93.0357 | 3.1217 | 0.6420 | 0.16896 | 0.11264 | 0.06930 | 0.04620 | 0.0436 | 0.0229 | 0.0235 |
| 21 | 1377.80 | 0.0466533 | 17.6244 | 1020.7 | 2.4630 | 1.5280 | 90.8251 | 4.4050 | 0.6420 | 0.06774 | 0.04516 | 0.01386 | 0.00924 | 0.0003 | 0.0006 | 0.0000 |
| 72 | 1371.56 | 0.0470512 | 17.7739 | 1020.7 | 1.5280 | 2.4630 | 90.8251 | 4.4050 | 0.6420 | 0.06774 | 0.04516 | 0.01386 | 0.00924 | 0.0003 | 0.0006 | 0.0000 |
| 22 | 1299.09 | 0.0514480 | 19.4222 | 1141.2 | 0.4040 | 1.9870 | 83.9520 | 9.1380 | 3.2590 | 0.59340 | 0.39560 | 0.12540 | 0.08360 | 0.0473 | 0.0139 | 0.0008 |
| 73 | 1308.27 | 0.0507734 | 19.1690 | 1141.1 | 1.9870 | 0.4040 | 83.9520 | 9.1380 | 3.2590 | 0.59340 | 0.39560 | 0.12540 | 0.08360 | 0.0473 | 0.0139 | 0.0008 |
| 23 | 1298.63 | 0.0514839 | 19.4357 | 1140.9 | 0.4050 | 2.0270 | 83.8681 | 9.1800 | 3.2790 | 0.58560 | 0.39040 | 0.12294 | 0.08196 | 0.0459 | 0.0136 | 0.0005 |
| 74 | 1308.03 | 0.0507926 | 19.1763 | 1140.8 | 2.0270 | 0.4050 | 83.8681 | 9.1800 | 3.2790 | 0.58560 | 0.39040 | 0.12294 | 0.08196 | 0.0459 | 0.0136 | 0.0005 |
| 24 | 1298.24 | 0.0515052 | 19.4436 | 1142.9 | 0.3940 | 1.9730 | 83.7500 | 9.3490 | 3.3080 | 0.58080 | 0.38720 | 0.11976 | 0.07984 | 0.0447 | 0.0133 | 0.0004 |
| 75 | 1307.38 | 0.0508323 | 19.1910 | 1142.8 | 1.9730 | 0.3940 | 83.7500 | 9.3490 | 3.3080 | 0.58080 | 0.38720 | 0.11976 | 0.07984 | 0.0447 | 0.0133 | 0.0004 |
| 25 | 1346.30 | 0.0484706 | 18.3062 | 1066.2 | 1.2630 | 1.9820 | 88.9650 | 5.4550 | 1.6160 | 0.30780 | 0.20520 | 0.09780 | 0.06520 | 0.0310 | 0.0120 | 0.0000 |
| 76 | 1350.87 | 0.0481644 | 18.1912 | 1066.2 | 1.9820 | 1.2630 | 88.9650 | 5.4550 | 1.6160 | 0.30780 | 0.20520 | 0.09780 | 0.06520 | 0.0310 | 0.0120 | 0.0000 |

## Table 1. Natural gas mixture composition database (continued).

| ID# | Sstd | $\rho$std | MW | Hv | nitrogen | carbon dioxide | methane | ethane | propane | i-butane | n-butane | i-pentane | n-pentane | n-hexane | n-heptane | n-octane |
|---|---|---|---|---|---|---|---|---|---|---|---|---|---|---|---|---|
| | (ft/s) | lbm/ft3 | | (Btu/scf) | (mole%) | (mole%) | (mole%) | (mole%) | (mole%) | (mole%) | (mole%) | (mole%) | (mole%) | (mole%) | (mole%) | (mole%) |
| 26 | 1354.30 | 0.0481456 | 18.1869 | 1021.2 | 4.1950 | 1.5730 | 87.9810 | 4.8020 | 0.9080 | 0.18840 | 0.12560 | 0.09300 | 0.06200 | 0.0450 | 0.0260 | 0.0010 |
| 77 | 1337.77 | 0.0492617 | 18.6063 | 1021.3 | 1.5730 | 4.1950 | 87.9810 | 4.8020 | 0.9080 | 0.18840 | 0.12560 | 0.09300 | 0.06200 | 0.0450 | 0.0260 | 0.0010 |
| 27 | 1386.26 | 0.0461729 | 17.4439 | 1008.4 | 1.9080 | 1.9860 | 92.7220 | 2.7990 | 0.3430 | 0.06180 | 0.04120 | 0.06420 | 0.04280 | 0.0150 | 0.0170 | 0.0000 |
| 78 | 1386.79 | 0.0461398 | 17.4314 | 1008.4 | 1.9860 | 1.9080 | 92.7220 | 2.7990 | 0.3430 | 0.06180 | 0.04120 | 0.06420 | 0.04280 | 0.0150 | 0.0170 | 0.0000 |
| 28 | 1367.09 | 0.0473409 | 17.8845 | 1014.4 | 5.1240 | 0.5810 | 88.8020 | 4.1500 | 0.8580 | 0.17940 | 0.11960 | 0.07320 | 0.04880 | 0.0400 | 0.0220 | 0.0020 |
| 79 | 1338.09 | 0.0492746 | 18.6112 | 1014.6 | 0.5810 | 5.1240 | 88.8020 | 4.1500 | 0.8580 | 0.17940 | 0.11960 | 0.07320 | 0.04880 | 0.0400 | 0.0220 | 0.0020 |
| 29 | 1345.11 | 0.0487582 | 18.4179 | 1020.4 | 4.9480 | 1.6030 | 86.6460 | 4.9600 | 1.2440 | 0.24180 | 0.16120 | 0.08640 | 0.05760 | 0.0340 | 0.0170 | 0.0010 |
| 80 | 1324.52 | 0.0501823 | 18.9529 | 1020.6 | 1.6030 | 4.9480 | 86.6460 | 4.9600 | 1.2440 | 0.24180 | 0.16120 | 0.08640 | 0.05760 | 0.0340 | 0.0170 | 0.0010 |
| 30 | 1296.55 | 0.0516298 | 19.4907 | 1141.1 | 0.4230 | 2.1250 | 84.0050 | 8.7790 | 3.2380 | 0.64740 | 0.43160 | 0.16740 | 0.11160 | 0.0590 | 0.0130 | 0.0000 |
| 81 | 1306.37 | 0.0509044 | 19.2184 | 1141.0 | 2.1250 | 0.4230 | 84.0050 | 8.7790 | 3.2380 | 0.64740 | 0.43160 | 0.16740 | 0.11160 | 0.0590 | 0.0130 | 0.0000 |
| 31 | 1344.10 | 0.0486669 | 18.3810 | 1055.2 | 2.4750 | 1.7790 | 87.9700 | 5.5520 | 1.5120 | 0.29520 | 0.19680 | 0.09840 | 0.06560 | 0.0360 | 0.0190 | 0.0010 |
| 82 | 1339.74 | 0.0489632 | 18.4924 | 1055.2 | 1.7790 | 2.4750 | 87.9700 | 5.5520 | 1.5120 | 0.29520 | 0.19680 | 0.09840 | 0.06560 | 0.0360 | 0.0190 | 0.0010 |
| 32 | 1346.59 | 0.0487312 | 18.4086 | 1005.2 | 5.5400 | 1.7960 | 86.4450 | 4.7560 | 0.9140 | 0.19860 | 0.13240 | 0.08580 | 0.05720 | 0.0460 | 0.0260 | 0.0030 |
| 83 | 1323.54 | 0.0503251 | 19.0075 | 1005.3 | 1.7960 | 5.5400 | 86.4450 | 4.7560 | 0.9140 | 0.19860 | 0.13240 | 0.08580 | 0.05720 | 0.0460 | 0.0260 | 0.0030 |
| 33 | 1386.30 | 0.0460996 | 17.4158 | 1022.6 | 2.5050 | 0.9750 | 92.3210 | 3.2850 | 0.5690 | 0.11100 | 0.07400 | 0.06000 | 0.04000 | 0.0350 | 0.0230 | 0.0020 |
| 84 | 1375.95 | 0.0467506 | 17.6605 | 1022.6 | 0.9750 | 2.5050 | 92.3210 | 3.2850 | 0.5690 | 0.11100 | 0.07400 | 0.06000 | 0.04000 | 0.0350 | 0.0230 | 0.0020 |
| 34 | 1375.63 | 0.0467867 | 17.6753 | 1016.5 | 4.1230 | 0.7040 | 90.4400 | 3.5110 | 0.7500 | 0.17040 | 0.11360 | 0.07140 | 0.04760 | 0.0410 | 0.0250 | 0.0030 |
| 85 | 1353.26 | 0.0482417 | 18.2223 | 1016.7 | 0.7040 | 4.1230 | 90.4400 | 3.5110 | 0.7500 | 0.17040 | 0.11360 | 0.07140 | 0.04760 | 0.0410 | 0.0250 | 0.0030 |
| 35 | 1337.89 | 0.0489815 | 18.4978 | 1079.0 | 1.0370 | 2.0360 | 88.0480 | 6.2390 | 1.8390 | 0.36780 | 0.24520 | 0.09120 | 0.06080 | 0.0260 | 0.0080 | 0.0020 |
| 86 | 1344.14 | 0.0485561 | 18.3380 | 1079.0 | 2.0360 | 1.0370 | 88.0480 | 6.2390 | 1.8390 | 0.36780 | 0.24520 | 0.09120 | 0.06080 | 0.0260 | 0.0080 | 0.0020 |
| 38 | 1311.77 | 0.0506087 | 19.1076 | 1122.6 | 0.6178 | 1.9051 | 85.3453 | 8.1433 | 2.8692 | 0.53850 | 0.35900 | 0.10470 | 0.06980 | 0.0345 | 0.0117 | 0.0011 |
| 89 | 1319.42 | 0.0500602 | 18.9017 | 1122.5 | 1.9051 | 0.6178 | 85.3453 | 8.1433 | 2.8692 | 0.53850 | 0.35900 | 0.10470 | 0.06980 | 0.0345 | 0.0117 | 0.0011 |
| 39 | 1415.05 | 0.0445340 | 16.8278 | 987.2 | 3.7924 | 0.2609 | 94.6077 | 1.0118 | 0.2128 | 0.04572 | 0.03048 | 0.01464 | 0.00976 | 0.0086 | 0.0044 | 0.0008 |
| 90 | 1390.14 | 0.0460360 | 17.3928 | 987.3 | 0.2609 | 3.7924 | 94.6077 | 1.0118 | 0.2128 | 0.04572 | 0.03048 | 0.01464 | 0.00976 | 0.0086 | 0.0044 | 0.0008 |
| 40 | 1436.21 | 0.0432094 | 16.3285 | 1013.1 | 0.9015 | 0.0668 | 98.2722 | 0.5159 | 0.1607 | 0.03552 | 0.02368 | 0.00942 | 0.00628 | 0.0055 | 0.0016 | 0.0009 |
| 91 | 1429.95 | 0.0435644 | 16.4604 | 1013.1 | 0.0668 | 0.9015 | 98.2722 | 0.5159 | 0.1607 | 0.03552 | 0.02368 | 0.00942 | 0.00628 | 0.0055 | 0.0016 | 0.0009 |
| 41 | 1313.72 | 0.0504571 | 19.0503 | 1126.0 | 0.4313 | 1.7708 | 85.4560 | 8.4983 | 2.7421 | 0.53706 | 0.35804 | 0.10038 | 0.06692 | 0.0315 | 0.0068 | 0.0008 |
| 92 | 1321.72 | 0.0498864 | 18.8360 | 1125.9 | 1.7708 | 0.4313 | 85.4560 | 8.4983 | 2.7421 | 0.53706 | 0.35804 | 0.10038 | 0.06692 | 0.0315 | 0.0068 | 0.0008 |
| 44 | 1328.09 | 0.0498658 | 18.8344 | 1032.1 | 5.3452 | 1.7745 | 84.5143 | 5.8831 | 1.7596 | 0.33582 | 0.22388 | 0.07044 | 0.04696 | 0.0309 | 0.0119 | 0.0034 |
| 95 | 1306.88 | 0.0513865 | 19.4056 | 1032.3 | 1.7745 | 5.3452 | 84.5143 | 5.8831 | 1.7596 | 0.33582 | 0.22388 | 0.07044 | 0.04696 | 0.0309 | 0.0119 | 0.0034 |
| 45 | 1327.85 | 0.0498985 | 18.8469 | 1028.8 | 5.4952 | 1.8318 | 84.3746 | 5.8795 | 1.7111 | 0.32880 | 0.21920 | 0.06906 | 0.04604 | 0.0297 | 0.0117 | 0.0033 |
| 96 | 1306.12 | 0.0514588 | 19.4330 | 1029.0 | 1.8318 | 5.4952 | 84.3746 | 5.8795 | 1.7111 | 0.32880 | 0.21920 | 0.06906 | 0.04604 | 0.0297 | 0.0117 | 0.0033 |
| 46 | 1324.52 | 0.0497726 | 18.7938 | 1110.0 | 0.9617 | 1.5021 | 85.9284 | 8.4563 | 2.3022 | 0.41910 | 0.27940 | 0.07308 | 0.04872 | 0.0228 | 0.0057 | 0.0005 |
| 97 | 1327.80 | 0.0495424 | 18.7073 | 1110.0 | 1.5021 | 0.9617 | 85.9284 | 8.4563 | 2.3022 | 0.41910 | 0.27940 | 0.07308 | 0.04872 | 0.0228 | 0.0057 | 0.0005 |
| 47 | 1303.11 | 0.0511733 | 19.3191 | 1136.9 | 0.4264 | 1.9201 | 84.3789 | 8.8749 | 3.1776 | 0.60132 | 0.40088 | 0.10872 | 0.07248 | 0.0310 | 0.0065 | 0.0012 |
| 98 | 1311.83 | 0.0505367 | 19.0802 | 1136.8 | 1.9201 | 0.4264 | 84.3789 | 8.8749 | 3.1776 | 0.60132 | 0.40088 | 0.10872 | 0.07248 | 0.0310 | 0.0065 | 0.0012 |
| 48 | 1341.09 | 0.0487764 | 18.4208 | 1076.7 | 1.2010 | 1.8560 | 88.2210 | 6.1190 | 1.8840 | 0.35340 | 0.23560 | 0.05580 | 0.03720 | 0.0230 | 0.0130 | 0.0010 |
| 99 | 1345.21 | 0.0484975 | 18.3160 | 1076.7 | 1.8560 | 1.2010 | 88.2210 | 6.1190 | 1.8840 | 0.35340 | 0.23560 | 0.05580 | 0.03720 | 0.0230 | 0.0130 | 0.0010 |
| 49 | 1295.14 | 0.0517027 | 19.5175 | 1151.1 | 0.3407 | 1.8816 | 83.4187 | 9.5284 | 3.5694 | 0.62190 | 0.41460 | 0.10968 | 0.07312 | 0.0327 | 0.0081 | 0.0011 |
| 100 | 1304.00 | 0.0510459 | 19.2710 | 1150.1 | 1.8816 | 0.3407 | 83.4187 | 9.5284 | 3.5694 | 0.62190 | 0.41460 | 0.10968 | 0.07312 | 0.0327 | 0.0081 | 0.0011 |
| 50 | 1333.21 | 0.0495504 | 18.7162 | 1024.3 | 5.9990 | 1.3984 | 84.4872 | 5.9271 | 1.5364 | 0.30534 | 0.20356 | 0.06342 | 0.04228 | 0.0251 | 0.0101 | 0.0021 |
| 101 | 1305.78 | 0.0515096 | 19.4522 | 1024.5 | 1.3984 | 5.9990 | 84.4872 | 5.9271 | 1.5364 | 0.30534 | 0.20356 | 0.06342 | 0.04228 | 0.0251 | 0.0101 | 0.0021 |
| 51 | 1379.30 | 0.0463119 | 17.4935 | 1068.6 | 1.4200 | 0.0330 | 93.3240 | 1.7800 | 3.2000 | 0.08700 | 0.05800 | 0.02520 | 0.01680 | 0.0560 | 0.0000 | 0.0000 |
| 102 | 1370.01 | 0.0469022 | 17.7154 | 1068.7 | 0.0330 | 1.4200 | 93.3240 | 1.7800 | 3.2000 | 0.08700 | 0.05800 | 0.02520 | 0.01680 | 0.0560 | 0.0000 | 0.0000 |

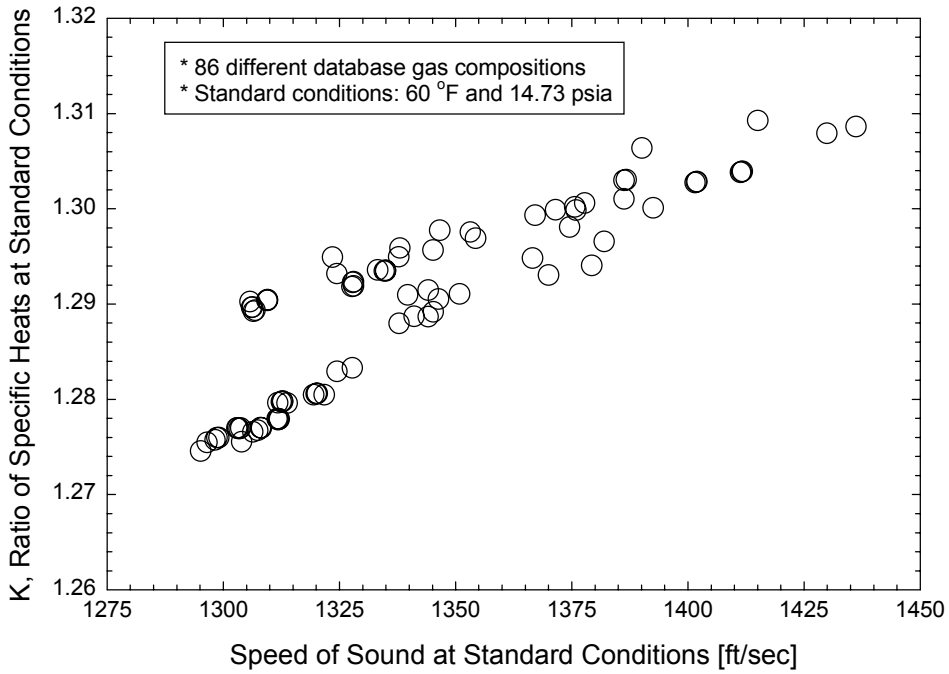


**Figure 2. Specific heat ratio for natural gas mixtures at standard conditions as a function of speed of sound.**

To help in determining values of the coefficients in equation (5), Behring et al. used the natural gas mixture database developed by Starling et al. to form a set of 102 gas mixture compositions that appears in Appendix A in the Tasks A and B DOE final report. As Figure 1b suggests, the coefficients in equation (5) will be functions of the diluent gas concentrations.

A close inspection of the set of 102 gas mixture compositions used by Behring et al. showed that 16 of the 102 compositions were duplicated inadvertently. Only 86 of the 102 mixture compositions are unique. Further investigation showed that several of the 86 mixture compositions vary only slightly from one another. In fact, the distribution of values for the standard heating value is strongly bimodal as shown below. The overweighting of gas mixture samples means that the least-square-error regression fit described in the next section can be expected to give better results in these two regions than in the other three regions.

| 985 – 1005 Btu/SCF | 1005 – 1035 Btu/SCF | 1035 – 1115 Btu/SCF | 1115 – 1145 Btu/SCF | 1145 – 1155 Btu/SCF |
|---|---|---|---|---|
| 2 samples | 42 samples | 14 samples | 26 samples | 2 samples |

The reduced database of 86 different natural gas mixture compositions is shown in Table 1 of this report. Four new columns were added to supplement the columns that list the mole fraction composition. The new columns show the values of standard sound speed, standard density, molecular weight, and volumetric heating value for each natural gas mixture. The values of standard sound speed and standard density were calculated using Lomic SonicWare.

The values of molecular weight and volumetric heating value were calculated using standard methods and the physical constant data in GPA Standard 2145 (GPA, 1994).

## 2.1 Regression Correlation for Standard Density

Behring et al. developed the following regression correlation for standard density:

$$\rho_{std} = A + B * S_{std} + C * S_{std}^{\ 2} \tag{6}$$

where

$$A = A_0 + A_1 * X_{N2} + A_2 * X_{CO2}$$

$$B = B_0 + B_1 * X_{N2} + B_2 * X_{CO2}$$

$$C = C_0 + C_1 * X_{N2} + C_2 * X_{CO2}$$

Here, $X_{CO2}$ is the mole fraction concentration of carbon dioxide, and $X_{N2}$ is the mole fraction concentration of nitrogen. Values for the nine unknown coefficients were calculated by least-square-error regression fit to the data, values of $\rho_{std}$, $S_{std}$, $X_{N2}$, and $X_{CO2}$ for the 102 gas mixtures in the data set. The values reported by Behring et al. are:

$$A_0 = 0.2395147\,,\ A_1 = 7.067074e^{-4}\,,\ A_2 = 2.334917e^{-3}$$

$$B_0 = -2.228333e^{-4}\,,\ B_1 = -9.87042e^{-7}\,,\ B_2 = -3.35135e^{-6}$$

$$C_0 = 5.99480e^{-8}\,,\ C_1 = 3.81330e^{-10}\,,\ C_2 = 1.26106e^{-9}$$

Regression residuals for $\rho_{std}$ are plotted in Figure 3a versus gas ID number, and in Figure 3b versus $\rho_{std}$. The residuals for each gas mixture are computed as the calculated value minus the actual value, expressed as a percentage of the actual value. As shown in Figure 3a, the magnitudes of the residuals are of the order of 0.02% or less for each gas mixture. This implies that the correlation between the model, equation (6), and the data is approaching 1.0, and the root-mean-square error is approaching zero. Figure 3b shows that the gas mixture database is over-weighted towards higher values of standard density. Figure 1a also had more points concentrated at higher values of the standard density and lower values of the standard sound speed.

## 2.2 Alternate Approach to Calculating Standard Density

Our goal is to develop a modified procedure for calculating gas mixture density for arbitrary values of pressure and temperature. A least-square-error regression fit to 102 gas mixtures isn't practical at the infinite number of combinations of pressure and temperature. However, equation (6), which arose from the regression fit to 102 gas mixtures, is a quadratic model with linear corrections for diluent concentrations. The number of empirical coefficients that must be determined from data is exactly nine regardless of whether they are determined from a least-square-error regression fit to 102 gas mixtures or from an exact fit to a subset of nine gas mixtures. Since Figure 3b shows very low values of correlation residuals over the entire

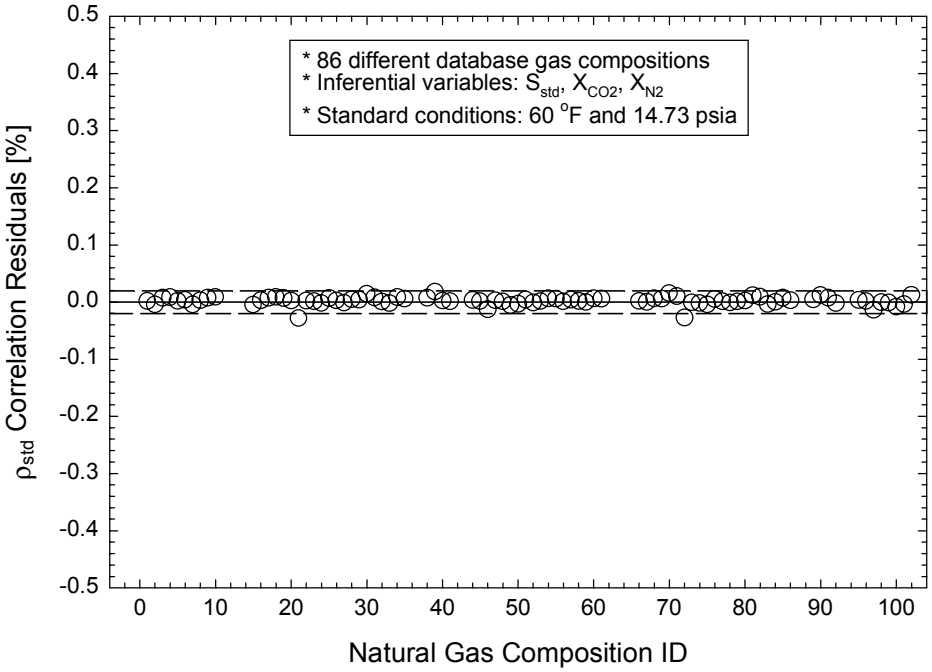


**Figure 3a. Correlation residuals for the standard density, $\rho_{std}$, as a function of natural gas composition ID number.**

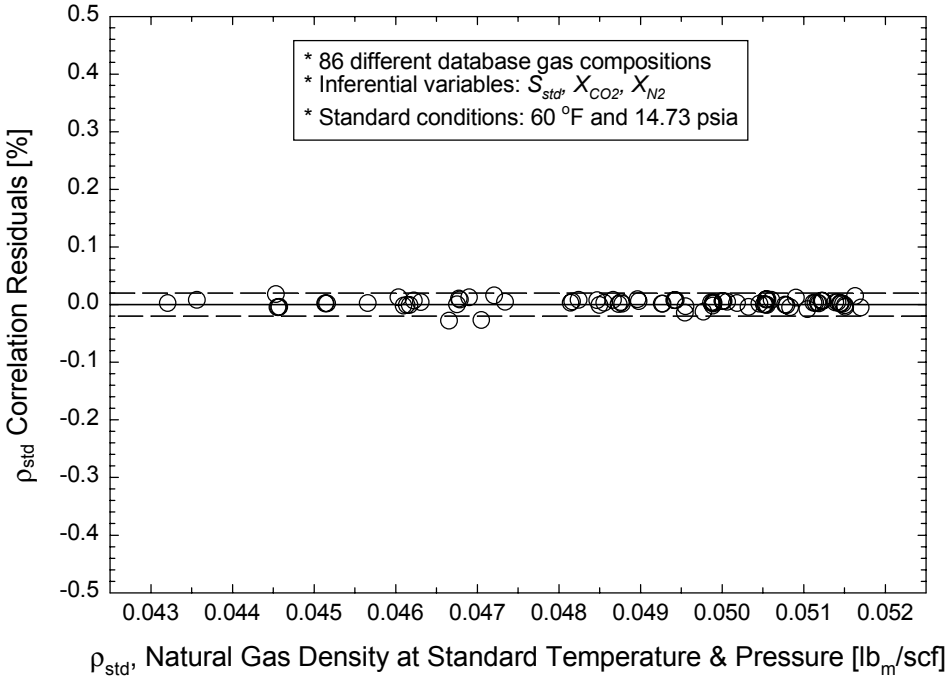


**Figure 3b. Correlation residuals for the standard density, $\rho_{std}$, as a function of natural gas standard density.**

range of standard density, let's see whether we can achieve the same results with an *exact fit* to data from only nine gas mixtures. The strategy to be followed is outlined below.

1. Identify three reference gas mixtures with 0% carbon dioxide and 0% nitrogen that will cover the full range of interest for standard heating value, molecular weight, and standard density.
2. For each of the three reference gas mixtures, reduce the hydrocarbon mixture concentration from 100% to 94% and add in 2% carbon dioxide and 4% nitrogen.
3. Repeat step 2, but delete the 2% carbon dioxide and 4% nitrogen, and add in 4% carbon dioxide and 2% nitrogen. We now have the nine reference gas mixtures.
4. Calculate the values of molecular weight for each of the nine reference gas mixtures.
5. Since values of density and sound speed are needed for arbitrary pressure and pressure, use an equation of state, such as the Lomic SonicWare computer program or the GRI Extended Thermodynamic Properties Computer Program developed by Savidge (1989) to calculate these properties for the nine reference gas mixtures at increments of temperature and pressure. The detailed composition method is used to calculate properties for each of the nine reference gas mixtures.
6. Develop cubic-spline fit approximations for the sound speed as a function of temperature and pressure, and for the density as a function of pressure and temperature for each of the nine reference gas mixtures. The cubic-spline fit "models" the response of the detailed equation of state for the reference gas mixture. Once the cubic-spline fit approximations have been developed for each of the nine reference gas mixtures, the detailed equation of state is no longer used.
7. For the measured values of pressure and temperature, use the cubic-spline fit approximations to calculate values of density and sound speed for each of the nine reference gas mixtures.
8. Use the calculated values of density and sound speed for the nine reference gas mixtures to determine the nine coefficients in equation (11) in Section 3.0.
9. Use the calculated values of sound speed and the values of molecular weight calculated in step 4 to determine the nine coefficients in equation (13) in Section 3.5.
10. Use the sound speed value measured by an ultrasonic sensor for the gas mixture of unknown composition to calculate the mixture gas density from equation (11), and the mixture molecular weight from equation (13).

These steps will be described below in greater detail.

Table 2 lists the physical properties and composition of nine reference gas mixtures covering a slightly larger range of standard density and standard sound speed than the 82 distinct gas mixtures listed in Table 1. (The reference gas mixtures are based upon, but are different than, gas ID numbers 40, 26 and 49 from Table 1.) The first three reference gas mixtures, labeled 40_00_00, 26_00_00 and 49_00_00, are formed by rebalancing the hydrocarbon gas and diluent concentrations to force the carbon dioxide and nitrogen concentrations to 0%. Three more reference gas mixtures, labeled 40_02_04, 26_02_04 and 49_02_04, were formed by reducing the hydrocarbon concentrations by a factor of 0.94 and adding 2% carbon dioxide and 4% nitrogen. Finally the last three reference gas mixtures, labeled 40_04_02, 26_04_02 and 49_04_02, were formed by swapping the carbon dioxide and nitrogen concentrations.

**Table 2. Database of nine reference natural gas compositions.**

| ID# | 40_00_00 | 40_02_04 | 40_04_02 | 26_00_00 | 26_02_04 | 26_04_02 | 49_00_00 | 49_02_04 | 49_04_02 |
|---|---|---|---|---|---|---|---|---|---|
| Sstd (ft/s) | 1441.37 | 1399.16 | 1385.36 | 1385.91 | 1350.75 | 1338.19 | 1311.74 | 1285.18 | 1274.19 |
| $\rho_{std}$ ($lb_m/ft^3$) | 0.042879 | 0.045599 | 0.04645 | 0.04585 | 0.048393 | 0.049244 | 0.050375 | 0.052646 | 0.053499 |
| MW | 16.2018 | 17.2304 | 17.5504 | 17.3184 | 18.2800 | 18.6000 | 19.0165 | 19.8763 | 20.1962 |
| Hv (Btu/SCF) | 1023.0 | 961.5 | 961.6 | 1083.8 | 1018.7 | 1018.8 | 1176.3 | 1105.6 | 1105.7 |
| nitrogen (%) | 0.0000 | 4.0000 | 2.0000 | 0.0000 | 4.0000 | 2.0000 | 0.0000 | 4.0000 | 2.0000 |
| carbon dioxide (%) | 0.0000 | 2.0000 | 4.0000 | 0.0000 | 2.0000 | 4.0000 | 0.0000 | 2.0000 | 4.0000 |
| methane (%) | 99.2331 | 93.2791 | 93.2791 | 93.3664 | 87.7644 | 87.7644 | 85.3147 | 80.1958 | 80.1958 |
| ethane (%) | 0.5209 | 0.4897 | 0.4897 | 5.0959 | 4.7902 | 4.7902 | 9.7450 | 9.1603 | 9.1603 |
| propane (%) | 0.1623 | 0.1525 | 0.1525 | 0.9636 | 0.9058 | 0.9058 | 3.6505 | 3.4315 | 3.4315 |
| i-butane (%) | 0.0359 | 0.0337 | 0.0337 | 0.1999 | 0.1879 | 0.1879 | 0.636 | 0.5979 | 0.5979 |
| n-butane (%) | 0.0239 | 0.0225 | 0.0225 | 0.1333 | 0.1253 | 0.1253 | 0.424 | 0.3986 | 0.3986 |
| i-pentane (%) | 0.00951 | 0.00894 | 0.00894 | 0.09869 | 0.09277 | 0.09277 | 0.11217 | 0.10544 | 0.10544 |
| n-pentane (%) | 0.00634 | 0.00596 | 0.00596 | 0.0658 | 0.06185 | 0.06185 | 0.07478 | 0.07029 | 0.07029 |
| n-hexane (%) | 0.0056 | 0.0052 | 0.0052 | 0.0478 | 0.0449 | 0.0449 | 0.0334 | 0.0314 | 0.0314 |
| n-heptane (%) | 0.0016 | 0.0152 | 0.0152 | 0.0276 | 0.0259 | 0.0259 | 0.0083 | 0.0078 | 0.0078 |
| n-octane (%) | 0.0009 | 0.0009 | 0.0009 | 0.0011 | 0.001 | 0.001 | 0.0011 | 0.0011 | 0.0011 |

We will assume a functional form for a model equation similar to equation (4).

$$\rho_{std} = \left( A_\rho + B_\rho / S_{std} + C_\rho / S_{std}^{\,2} \right) * \left( 1 + D_\rho * X_{CO2} + E_\rho * X_{N2} \right) \tag{7}$$

where

$$D_\rho = D_1 + D_2 / S_{std} + D_3 / S_{std}^{\,2}$$

$$E_\rho = E_1 + E_2 / S_{std} + E_3 / S_{std}^{\,2}$$

The first three coefficients of the model equation are calculated using the values of $\rho_{std}$ and $S_{std}$ for reference gas mixtures 40_00_00, 29_00_00 and 49_00_00. The other six coefficients are calculated by solving a set of six simultaneous equations using values of $\rho_{std}$ and $S_{std}$ for reference gas mixtures 40_02_04, 40_04_02, 29_02_04, 29_04_02, 49_02_04 and 49_04_02. The calculated coefficient values are:

$$A_\rho = -2.96476e^{-3}, B_\rho = 2.67159e^{1}, C_\rho = 5.67358e^{4}$$

$$D_1 = 1.24381e^{-2}, D_2 = -2.13555e^{1}, D_3 = 1.02455e^{4}$$

$$E_1 = 7.03503e^{-3}, E_2 = -1.12843e^{1}, E_3 = 4.95709e^{3}$$

Let's compare model equation (7) to the database of 86 natural gas mixtures from Table 1. Model equation (7) fits the density values for the 86 natural gas mixtures nearly as well as the least-square-error regression equation (6). The model equation fits the database values for $\rho_{std}$ with a mean error of +0.007% and a standard deviation of 0.013%. The 95% confidence interval extends from -0.020% to +0.034% as shown in Figure 4.

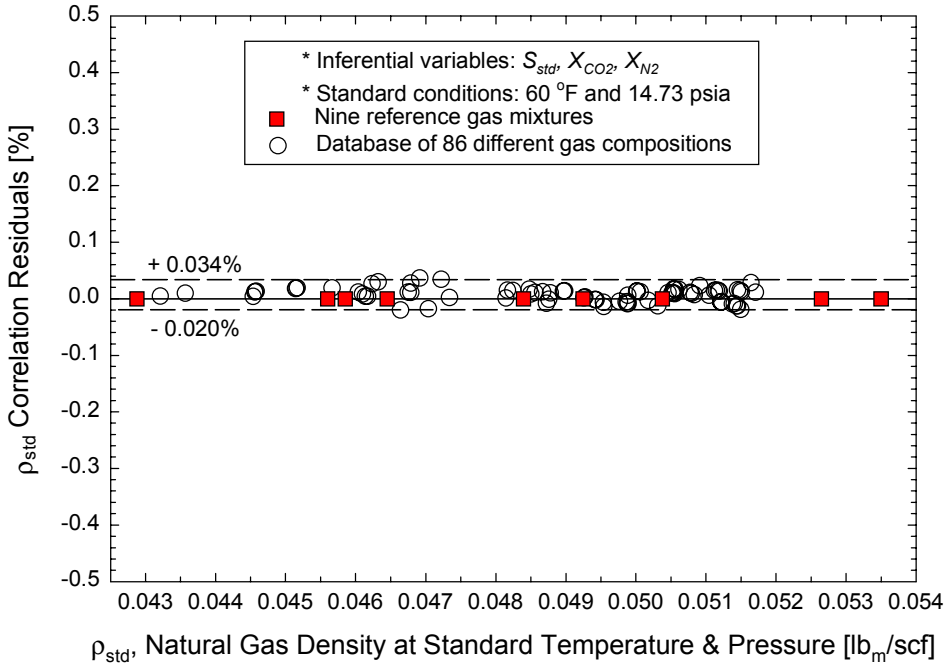


**Figure 4. Residuals for the standard density, $\rho_{std}$ , calculated from an exact fit to nine reference natural gas mixtures as a function of natural gas standard density.**

## 2.3 Regression Correlation for Molecular Weight

Behring et al. reported the following correlation for molecular weight:

$$MW = A + B * S_{std} + C * S_{std}^{\ 2} \tag{8}$$

where

$$A = A_0 + A_1 * X_{N2} + A_2 * X_{CO2}$$

$$B = B_0 + B_1 * X_{N2} + B_2 * X_{CO2}$$

$$C = C_0 + C_1 * X_{N2} + C_2 * X_{CO2}$$

The values for the nine regression coefficients were determined by least-square-error regression fit to values of *MW* and $S_{std}$ for the set of 102 natural gas mixtures. The coefficient values reported by Behring et al. are:

$$A_0 = 89.59987,\ A_1 = 0.2595616,\ A_2 = 0.8420112$$

$$B_0 = -0.08303539,\ B_1 = -3.57614e^{-4},\ B_2 = -1.20199e^{-3}$$

$$C_0 = 2.22787e^{-5},\ C_1 = 1.37342e^{-7},\ C_2 = 4.51462e^{-7}$$

The regression fit residuals for *MW* are plotted in Figure 5a versus gas ID number, and in Figure 5b versus *MW*. As shown in Figure 5a, the magnitude of the correlation residuals is of the order of 0.02% or less for each gas mixture.

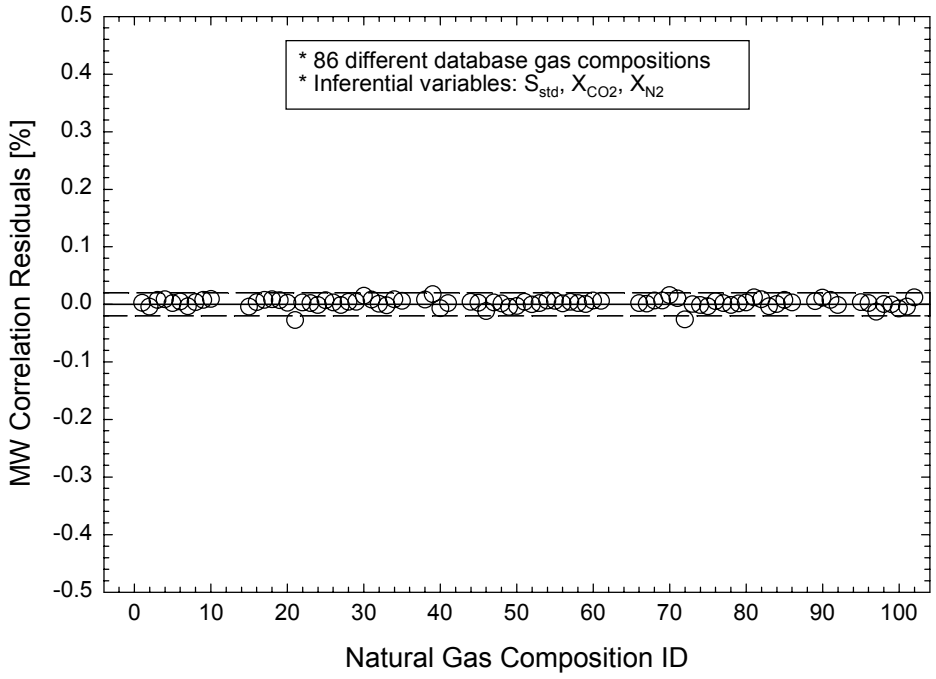


**Figure 5a. Correlation residuals for the molecular weight, *MW*, as a function of the natural gas composition ID number.**

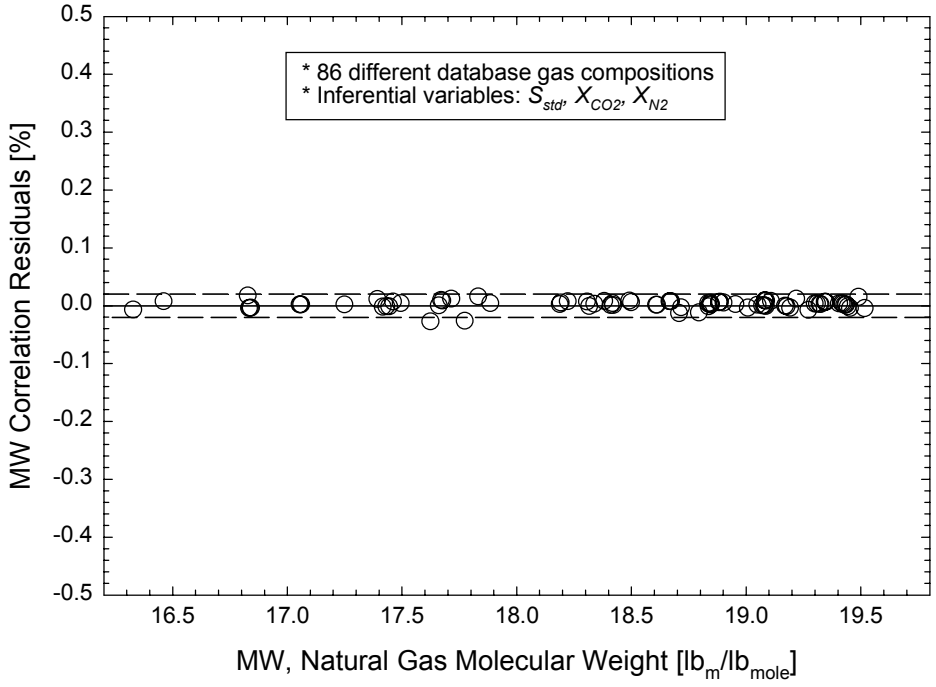


**Figure 5b. Correlation residuals for the molecular weight, *MW*, as a function of the molecular weight of the natural gas mixtures.**

## 2.4 Alternate Approach to Calculating Molecular Weight

It is useful to have a procedure for calculating the molecular weight of a natural gas mixture as a function of sound speed and diluent concentrations based on an exact fit to the nine reference gas mixtures. In this section, we will demonstrate the procedure using values of the standard sound speed. However, the method can be used at any temperature and pressure if the sound speed values at those conditions are known for the nine reference gas mixtures.

We will assume a functional form similar to equation (7), with $MW$ replacing $\rho_{std}$.

$$MW = \left( A_{MW} + B_{MW} / S_{std} + C_{MW} / S_{std}^{\,2} \right) * \left( 1 + D_{MW} * X_{CO2} + E_{MW} * X_{N2} \right) \tag{9}$$

where

$$D_{MW} = D_{MW1} + D_{MW2} / S_{std} + D_{MW3} / S_{std}^{\,2}$$

$$E_{MW} = E_{MW1} + E_{MW2} / S_{std} + E_{MW3} / S_{std}^{\,2}$$

Table 2 gives the values of $MW$, $S_{std}$, carbon dioxide and nitrogen concentration for the nine reference gas mixtures. A spreadsheet was used to calculate values of the nine coefficients:

$$A_{MW} = -1.45902,\ B_{MW} = 1.12609e^{4},\ C_{MW} = 2.04601e^{7}$$

$$D_{MW1} = 1.13286e^{-2},\ D_{MW2} = -1.83504e^{1},\ D_{MW3} = 8.31724e^{3}$$

$$E_{MW1} = 7.50343e^{-3},\ E_{MW2} = -1.25503e^{1},\ E_{MW3} = 5.91045e^{3}.$$

Model equation (9), an exact fit to molecular weight and standard sound speed data for nine reference gas mixtures, provides nearly as good a fit to the 86 different gas mixtures as regression equation (8), which used the complete database of 102 gas mixtures to calculate the regression coefficients. The mean error for equation (9) applied to the 86 natural gas mixtures in Table 1 is +0.007% and the standard deviation is 0.013%. The 95% confidence interval extends from –0.019% to +0.032% as shown in Figure 6.

## 2.5 Regression Correlation for Mass-Based Heating Value

Behring et al (1999) reported the following correlation for the mixture heating value per unit mass, $H_m$.

$$H_m = \left( \frac{A + B * MW_{HC}}{MW} \right) \tag{10}$$

where $MW_{HC}$ is the hydrocarbon molecular weight, defined as

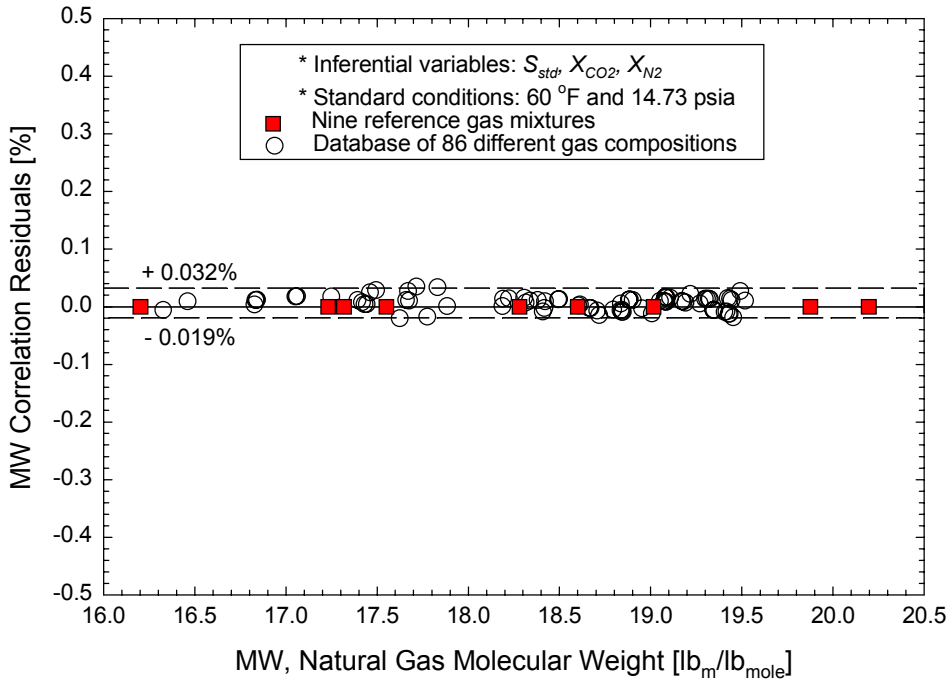


**Figure 6. Residuals for the mixture molecular weight, *MW,* calculated from an exact fit to nine reference gas mixtures as a function of mixture molecular weight.**

$$MW_{HC} = MW - \left(\frac{X_{CO2}}{100} * 44.010\right) - \left(\frac{X_{N2}}{100} * 28.0134\right), \text{ and}$$

$$B = B_0 + B_1 * S_{std}$$

$$B_1 = B_2 + B_3 * X_{N2} + B_4 * X_{CO2}$$

This set of equations has five coefficients that were determined by least-square-error regression fit to the 102 natural gas mixtures. The regression coefficient values reported by Behring et al. are:

$$A = 54,343.048\,,\ B_0 = 20,442.406$$

$$B_2 = 0.04552871\,,\ B_3 = -0.02523803\,,\ B_4 = -0.02568212$$

The regression fit residuals for mass-based heating value are plotted in Figures 7a and Figure 7b. The magnitude of the correlation residuals is of the order of 0.02%.

Figure 8 shows the values of $H_m$ plotted against $S_{std}$ for all 86 gas mixtures in Table 1. The values of $H_m$ vary by approximately 15%, from about 23,500 Btu/lb$_m$ to less than 20,000 Btu/lb$_m$. Values of $H_m$ were calculated using equation (10) and the values of $S_{std}$ from Table 2 for reference gas compositions 40_00_00, 26_00_00 and 49_00_00. Figure 8 shows that these values, for hydrocarbon gas mixtures with 0 mole% diluents, lie above the values of $H_m$ for the

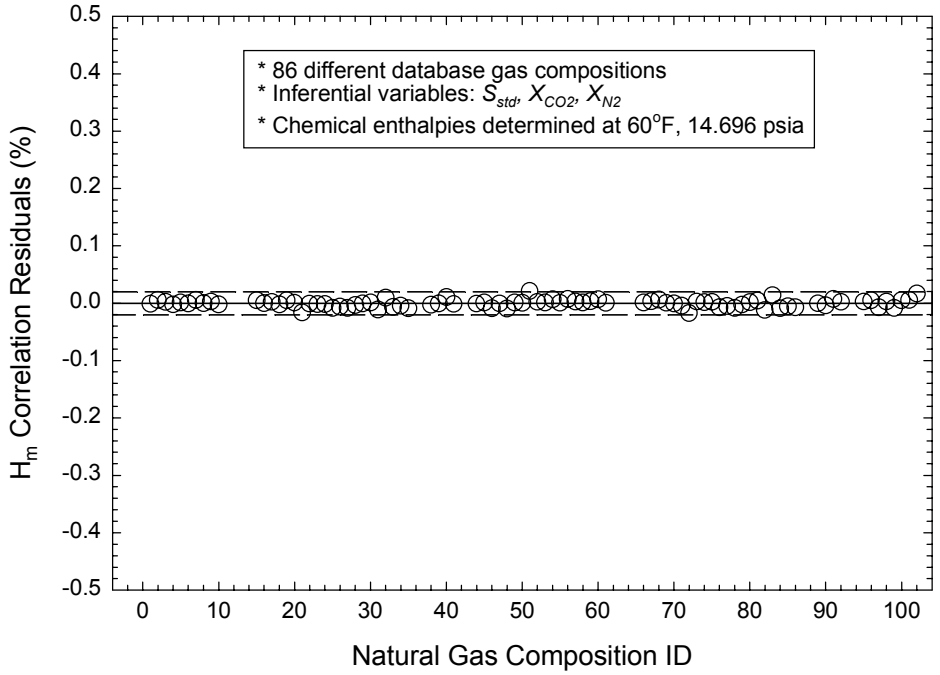


**Figure 7a. Correlation residuals for the mass-based heating value, $H_m$, as a function of the natural gas composition ID number.**

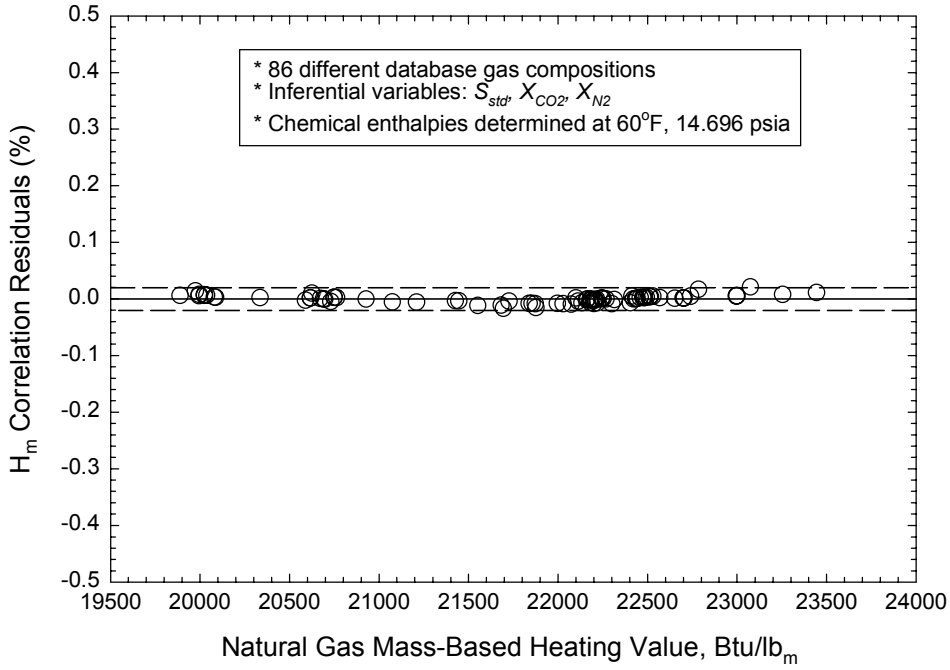


**Figure 7b. Correlation residuals for the mass-based heating value, $H_m$, as a function of the mass-based heating value of the natural gas mixture.**

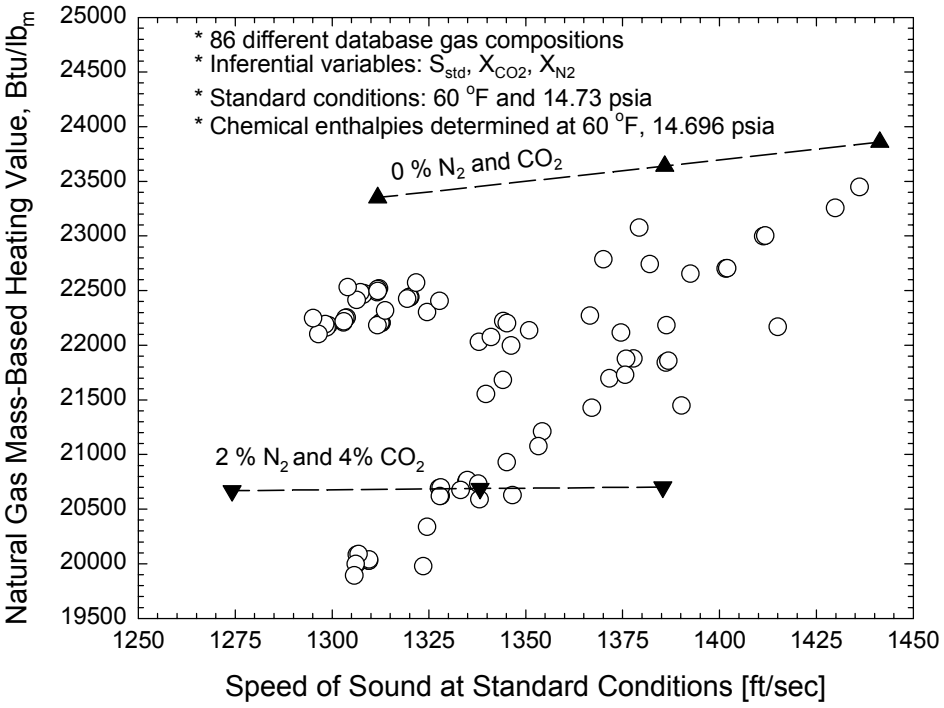


**Figure 8. Mass-based heating value as a function of standard sound speed.**

86 natural gas mixtures with diluents. Note also the small change in heating value with standard sound speed. Most of the data scatter in Figure 8 is caused by different concentrations of carbon dioxide and/or nitrogen. To demonstrate this point, values of $H_m$ were calculated for reference gas compositions 40_04_02, 26_04_02 and 49_04_02. Figure 8 shows that these values are nearly independent of sound speed, and are displaced downwards and to the left of the values for the reference gas mixtures 40_00_00, 26_00_00 and 49_00_00 without diluents.

Equation (10), the correlation for mass-based heating value, $H_m$, does not need to be modified. However, while the values of carbon dioxide and nitrogen concentrations are assumed to be known or measured, the value of the standard sound speed is unknown. Behring et al. proposed that the sound speed be measured at standard temperature and pressure. However, if the gas mixture molecular weight, *MW*, is known through measurements at another combination of pressure and temperature, then either equation (8) or equation (9) can be used to calculate $S_{std}$.

The new computational procedure developed on this project is to determine the gas mixture molecular weight, *MW*, from a correlation similar to equation (9), but based on sound speed values for the nine reference gas mixtures at temperature and pressure conditions that are different from standard temperature and pressure. Because the gas mixture molecular weight is a chemical property, it is independent of pressure and temperature. Assuming that condensation of vapor into liquid does not occur, the value of *MW* calculated at arbitrary pressure and temperature conditions is the same as the value at standard pressure and temperature.

Let's assume that a value of *MW* has been determined experimentally from the value of sound speed measured at pipeline conditions. Since the model equation coefficients have already been calculated for equation (9), this equation can be used to solve for $S_{std}$ in terms of the experimentally determined value of *MW* and the values of $X_{CO2}$ and $X_{N2}$. Since the sound speed

appears in the equations for $D_{MW}$ and $E_{MW}$, it is easiest to solve equation (9) iteratively. On the first iteration, the diluent correction term ($1 + D_{MW} * X_{CO2} + E_{MW} * X_{N2}$) is omitted and the quadratic equation is solved for $S_{std}$. Although there are two roots to the quadratic equation for $S_{std}$, only one root is a physically realistic value. This value of $S_{std}$ is then used to calculate values of $D_{MW}$ and $E_{MW}$. On the second iteration, the diluent correction term is included and a new value of $S_{std}$ is calculated from the quadratic equation. The new value of $S_{std}$ is used to update the estimate of the diluent correction term, and the procedure is repeated until new and old values of $S_{std}$ are within 0.01 ft/sec. of each other. The converged value of $S_{std}$ is used to calculate the value of mass-based heating value, $H_m$. It is also used to calculate the value of standard density, $\rho_{std}$, using either equation (6) or equation (7).

## 2.6 Calculation of Standard Volumetric Heating Value

Behring et al. found that a separate regression correlation equation for the standard volumetric heating value, $H_v$, was unnecessary. $H_v$ is calculated simply as the product of the mass-based heating value, $H_m$, and the standard density, $\rho_{std}$. Therefore, using equation (6) and its coefficients for the standard density, $\rho_{std}$, and equation (10) and its coefficients for the mass-based heating value, $H_m$, values of the standard volumetric heating value, $H_v$, can be calculated as a function of the standard sound speed, $S_{std}$, the mole fraction of carbon dioxide, $X_{CO2}$, and the mole fraction of nitrogen, $X_{N2}$. The regression fit residuals for the standard volumetric heating value are plotted in Figure 9a and Figure 9b.

As an alternative, we may use the model equation (7) for standard density, $\rho_{std}$, and regression equation (10) for the mass-based heating value, $H_m$. Since equation (10) requires the value of molecular weight, *MW*, we may also require that model equation (9) be used to calculate *MW*.

Figure 10 shows the results of using model equations (7) and (9) together with equation (10) to calculate the standard volumetric heating value as the product of $H_v = \rho_{std} * H_m$. For the database of 86 different natural gas compositions, the mean error is +0.013% and the standard deviation is 0.016%. The 95% confidence interval extends from +0.045% to –0.019%. Expressed as an interval around the value of standard volumetric heating value, the 95% confidence interval is from +0.48 Btu/SCF to –0.20 Btu/SCF around the indicated value.

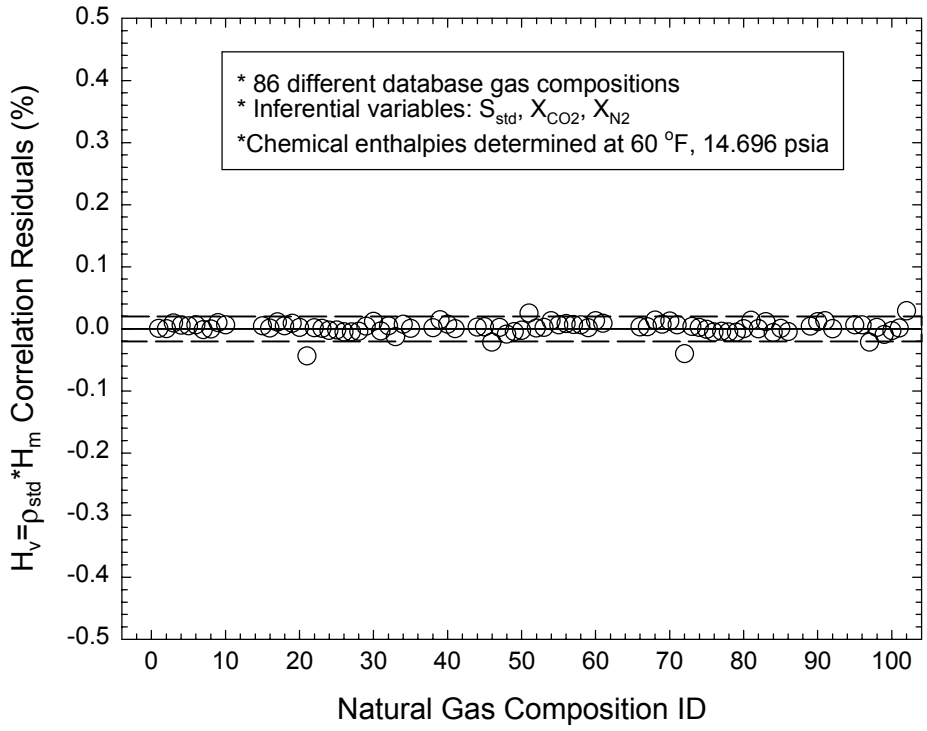


**Figure 9a. Correlation residuals for the standard volumetric heating value, $H_v$, as a function of the natural gas composition ID number.**

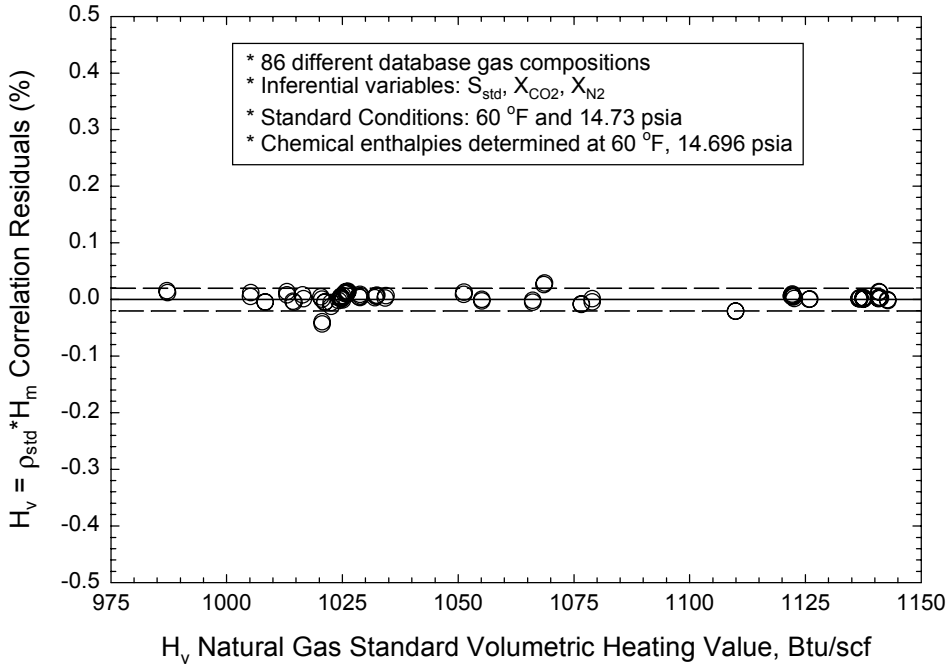


**Figure 9b. Correlation residuals for the standard volumetric heating value, $H_v$, as a function of the standard volumetric heating value, $H_v$.**

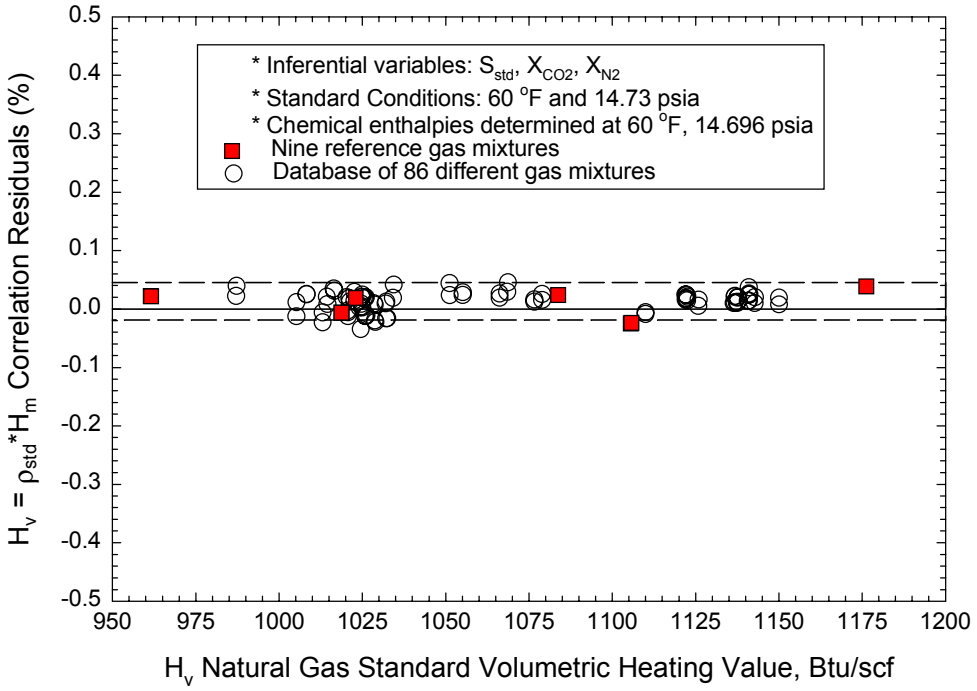


**Figure 10. Residuals for the standard volumetric heating value, $H_v$, calculated using $\rho_{std}$ and *MW* values calculated from the nine reference gas mixture equations.**

*This page is intentionally blank.*

## 3.0 Extension to Arbitrary Pressure and Temperature

Behring et al. (1999) showed that the standard sound speed, $S_{std}$, together with the carbon dioxide concentration, $X_{CO2}$, and the nitrogen concentration, $X_{N2}$, could be used as input variables for the Gross Characterization method of the AGA 8 (1994) density equation of state. The natural gas density at pipeline conditions, which is needed to calculate the energy flow rate for all meters except those that measure mass flow rate, would be calculated by specifying $S_{std}$, $X_{CO2}$, $X_{N2}$, pipeline static pressure, $P$, and pipeline static temperature, $T$.

One disadvantage of the method described by Behring et al. is that the speed of sound must be measured at standard pressure, $P_{std}$ = 14.73 psia, and at standard temperature, $T_{std}$ = 60°F. Single-path and multipath ultrasonic flow meters provide a measured value of the speed of sound in the flowing gas at pipeline pressure and temperature. Unfortunately, there was no way to relate this measured value to the standard sound speed.

In the previous section we showed that the standard density, $\rho_{std}$, could be modeled successfully by equation (7) as a function of $S_{std}$, $X_{CO2}$, and $X_{N2}$. We will extend our model equation (7) to arbitrary pressure and temperature as:

$$\rho_{calc} = \left( A_\rho + {B_\rho}/{S} + {C_\rho}/{S^2} \right) * \left( 1 + D_\rho * X_{CO2} + E_\rho * X_{N2} \right)$$

$$D_\rho = D_1 + {D_2}/{S} + {D_3}/{S^2} \qquad (11)$$

$$E_\rho = E_1 + {E_2}/{S} + {E_3}/{S^2}$$

where $\rho_{calc}$ and $S$ are the density and sound speed at the pipeline temperature and pressure.

The nine coefficients in equation (11) are functions of the temperature and pressure. However, the coefficients can be calculated for a specific combination of pressure and temperature if the values of density and sound speed are known for the nine reference gases whose compositions are given in Table 2.

### 3.1 Numerical Example for Amarillo Gas

We will demonstrate the use of equation (11) to calculate the density at pipeline conditions for Amarillo gas, one of the six reference gas compositions used in AGA Report No. 8 (1994), and furnished as a reference gas in Lomic SonicWare® (1997). Amarillo gas is composed of 90.6724% methane, 4.5279% ethane, 0.8280% propane, 0.1037% i-butane, 0.1563% n-butane, 0.0321% i-pentane, 0.0443% n-pentane, 0.0393% n-hexane, 3.1284% nitrogen, and 0.4676% carbon dioxide. Let's assume that we want to calculate the density at a pressure of 930 psia and a temperature of 75°F. Lomic SonicWare gives a value of sound speed, $S$, of 1,346.03 ft/sec and a value of density, $\rho$, of 3.24335 $lb_m/ft^3$ for Amarillo gas at this temperature and pressure.

The first step is to calculate the values of $\rho$ and $S$ for the nine reference gas mixtures in Table 2 for a pressure of 930 psia and a temperature of 75°F. SonicWare was used for these

reference gas calculations with the compositions listed in Table 2. The results for density, $\rho$, and sound speed, *S*, are listed in Table 3 below.

**Table 3. Reference gas properties at 930 psia and 75°F.**

| Gas ID | $N_2$ (%) | $CO_2$ (%) | $\rho$ ($lb_m/ft^3$) | *S* (ft/sec) |
|---|---|---|---|---|
| 40_00_00 | 0.0000 | 0.0000 | 2.94372 | 1418.84 |
| 26_00_00 | 0.0000 | 0.0000 | 3.22370 | 1346.06 |
| 49_00_00 | 0.0000 | 0.0000 | 3.69687 | 1244.22 |
| 40_02_04 | 4.0000 | 2.0000 | 3.11875 | 1381.02 |
| 40_04_02 | 2.0000 | 4.0000 | 3.19675 | 1362.36 |
| 26_02_04 | 4.0000 | 2.0000 | 3.38267 | 1317.05 |
| 26_04_02 | 2.0000 | 4.0000 | 3.46614 | 1299.44 |
| 49_02_04 | 4.0000 | 2.0000 | 3.82503 | 1226.68 |
| 49_04_02 | 2.0000 | 4.0000 | 3.91975 | 1210.21 |
| Amarillo gas | 3.1284 | 0.4676 | 3.24335 | 1346.03 |

When the values of $\rho$, *S*, $X_{CO2}$, and $X_{N2}$ are inserted into equation (11) for the nine reference gases, we have a system of nine algebraic equations and nine unknown coefficients. For this example, values of the unknown coefficients were calculated using matrix operations within a spreadsheet. Coefficient values are:

$$A_\rho = 6.76349e^{-2},\ B_\rho = 9.82126e^{2},\ C_\rho = 4.39636e^{6}$$

$$D_1 = 1.63933e^{-2},\ D_2 = -3.12772e^{1},\ D_3 = 1.65121e^{4}$$

$$E_1 = 6.68038e^{-3},\ E_2 = -1.08333e^{1},\ E_3 = 5.31502e^{3}$$

Using these coefficient values in equation (11), together with the values of *S*, $X_{CO2}$, and $X_{N2}$ listed in Table 3 for Amarillo gas gives a value for the gas density of $\rho = 3.24303$ $lb_m/ft^3$. This value is 0.010% lower than the value listed in Table 3 and calculated by SonicWare, using the detailed composition method.

## 3.2 Generating a Reference Gas Data Base

To solve the numerical example for Amarillo gas, we used the detailed composition method in Lomic SonicWare to calculate values of gas density and sound speed for each of the nine reference gases at the actual pipeline pressure and temperature. For online energy meter operation, these values are calculated in advance and stored in computer memory. Since it is not feasible to perform calculations for every possible combination of pressure and temperature, a matrix of pressure and temperature values was selected and Lomic SonicWare was used to perform the calculations for these values. In general, the actual pipeline pressure and/or temperature will lie between the values used in the calculations. In this event, cubic-spline interpolation is used to estimate values of density and sound speed from the calculated values.

Let's see how this works for Gas ID#26_00_00, one of the nine reference gas mixtures. The detailed gas composition (listed in Table 2) was input into Lomic SonicWare, and physical properties (speed of sound, density, molar specific heats, ratio of specific heats, and viscosity) were calculated for different combinations of pressure and temperature. Lomic SonicWare permits holding the pressure constant, and varying the temperature in fixed increments between an upper and lower limit. Properties were calculated for temperatures between 20°F and 150°F in steps of 10°F for pressure values of 14.73 psia, 50 psia, and from 100 psia to 1400 psia in increments of 100 psia.

Figure 11a shows the variation of gas mixture density, $\rho$, as a function of pressure and temperature. For clarity, calculated values are not plotted for some isotherms. Figure 11b shows the variation of sound speed, *S*, as a function of pressure and temperature. Again, calculated values for some isotherms are left off the plot for clarity. The density and sound speed vary smoothly as a function of pressure and temperature with no visible discontinuities. The same observation is true for the other eight reference gases. Therefore, it should be possible to use cubic-spline interpolation to calculate intermediate values with good results.

### 3.3 Cubic-Spline Interpolation

Ferziger (1981) writes that cubic-spline interpolation produces a smooth curve similar to that drawn by a draftsman. The term "spline" relates to a draftsman's spline, a thin flexible rod that can be bent to fit through given data points on a graph. A cubic-spline has three properties.

1. The curve is piecewise cubic; the polynomial coefficients are different on each interval.
2. The curve passes through the given data exactly.
3. The first and second derivatives are continuous at the node points.

Let's represent the cubic-spline function as $y = f_i(x)$ over the "i$^{th}$" interval, $x_i \le x \le x_{i+1}$. Following Ferziger, the cubic-spline function can be written as:

$$f_i(x) = f''(x_i)\frac{(x_{i+1}-x)^3}{6\Delta_i} + f''(x_{i+1})\frac{(x-x_i)^3}{6\Delta_i} + \left[\frac{f(x_i)}{\Delta_i} - \frac{\Delta_i}{6}f''(x_i)\right](x_{i+1}-x) + \left[\frac{f(x_{i+1})}{\Delta_i} - \frac{\Delta_i}{6}f''(x_{i+1})\right](x-x_i) \tag{12}$$

In this equation, the symbol $f''$ represents the second derivative of $f_i(x)$ with respect to $x$, and $\Delta_i = (x_{i+1} - x_i)$ is the length of the i$^{th}$ interval.

Ferziger presents sample FORTRAN computer programs for computing a cubic-spline fit to input data, $y_i = f(x_i)$ in one-dimension. The cubic polynomial coefficients in equation (12) for each interval are determined by requiring (1) that the first derivatives, $f'$, be continuous at $x_2 \le x_i \le x_{n-1}$, and (2) that the second derivatives, $f''$, be specified at the end points, $x_1$ and $x_n$. Following Ferziger, we shall use a *cantilever* end condition and set $f_1'' = f_2''$ and $f_n'' = f_{n-1}''$. These conditions lead to a tri-diagonal set of algebraic equations for the values of the second derivatives at each point that are solved by standard matrix operation methods.

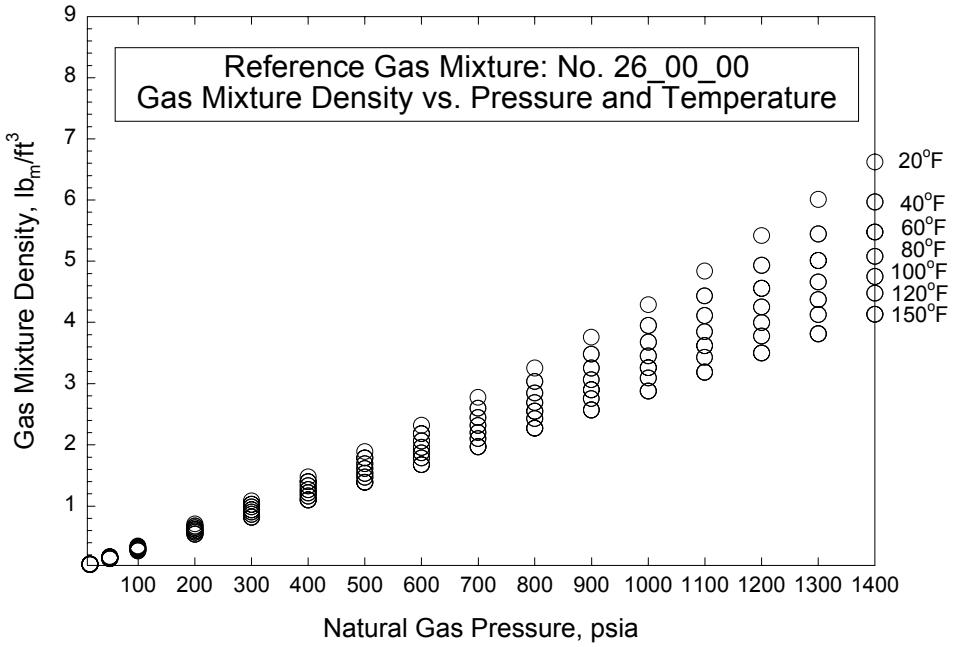


**Figure 11a. Variation of gas mixture density, $\rho$, as a function of pressure and temperature for reference gas 26_00_00.**

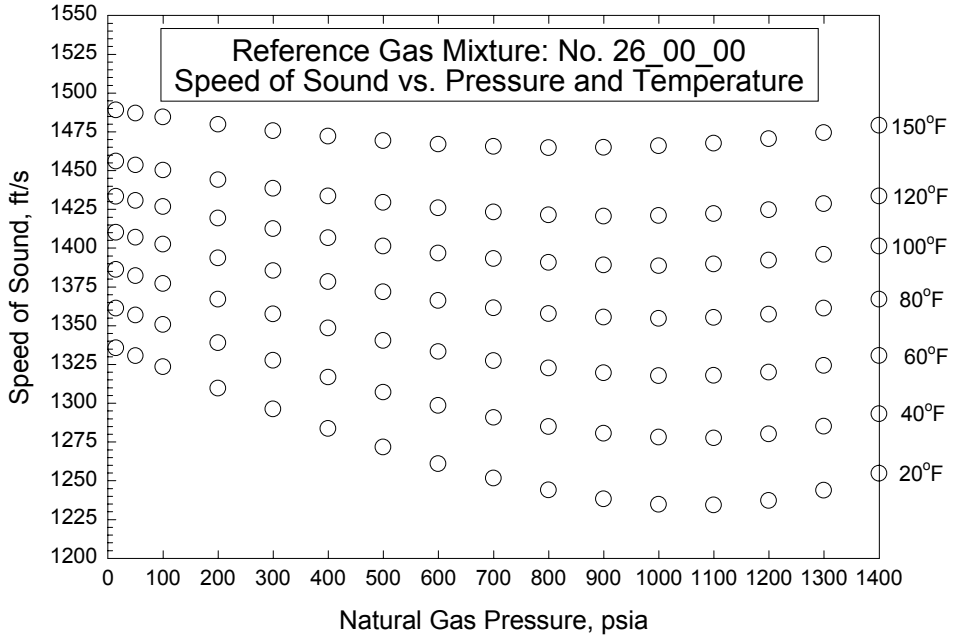


**Figure 11b. Variation of sound speed, *S*, as a function of pressure and temperature for reference gas 26_00_00.**

A one-dimensional cubic-spline fit, $y = f(x)$, allows us to fit the sound speed or the gas mixture density as a function of pressure for constant values of temperature. However, we need cubic-spline curve fits for sound speed or density as a function of both independent variables, temperature and pressure. Ferziger recommends a procedure to follow for multi-dimensional cubic-spline interpolation. The first step is to calculate cubic-spline fits for density or sound speed as a function of pressure while holding the values of temperature constant. Then, for each value of pressure, $P_i$, the values of the second derivatives, $f'' = d^2 f / dP^2$, are known for several values of temperature, $T_j$. These second derivatives are now considered to be functions of temperature for each of the $P_i$, and a cubic-spline fit is calculated for the second derivatives as a function of temperature. Since the temperature and pressure are known, we can determine the intervals, $T_j \le T \le T_{j+1}$, and $P_i \le P \le P_{i+1}$ in which the temperature and pressure are contained. The cubic-spline fit for $f''$ is evaluated to give $f''(P_i, T)$ and $f''(P_{i+1}, T)$. Now, the values of $f''$ are used in the interval $P_i \le P \le P_{i+1}$ to calculate the value of $f(P,T)$.

Table 4 compares interpolated values of sound speed, $S_i$, and gas mixture density, $\rho_i$, for a pressure of 950 psia and temperature of 35°F with values calculated by Lomic SonicWare. The magnitude of the interpolation error is of the order of 0.01% or less for all nine of the reference gas mixtures.

**Table 4. Comparison of interpolated and calculated values of sound speed and density at 950 psia and 35°F for the nine reference gas mixtures.**

| Gas ID | $S_i$ (ft/s) | $S_{cal}$ (ft/s) | % error | $\rho_i$ ($lb_m/ft^3$) | $\rho_{cal}$ ($lb_m/ft^3$) | % error |
|---|---|---|---|---|---|---|
| 40_00_00 | 1342.69 | 1342.81 | -0.009 | 3.41480 | 3.41445 | 0.010 |
| 26_00_00 | 1268.47 | 1268.48 | -0.001 | 3.78178 | 3.78176 | 0.001 |
| 49_00_00 | 1162.94 | 1162.93 | 0.001 | 4.44055 | 4.44068 | -0.003 |
| 26_02_04 | 1242.64 | 1242.62 | 0.002 | 3.95780 | 3.95779 | 0.000 |
| 26_04_02 | 1224.24 | 1224.21 | 0.002 | 4.06903 | 4.06902 | 0.000 |
| 40_02_04 | 1307.93 | 1307.94 | -0.001 | 3.61222 | 3.61224 | -0.001 |
| 40_04_02 | 1288.70 | 1288.70 | 0.000 | 3.71258 | 3.71260 | -0.001 |
| 49_02_04 | 1149.13 | 1149.13 | 0.000 | 4.56842 | 4.56849 | -0.002 |
| 49_04_02 | 1131.42 | 1131.42 | 0.000 | 4.70464 | 4.70473 | -0.002 |

## 3.4 Calculation of Gas Mixture Density

As a further example, let's use equation (11) to calculate the gas mixture density at a pressure of 950 psia and a temperature of 65°F. These values are reasonable choices for pipeline transportation of natural gas. The values of density and sound speed for the nine reference gases were calculated by cubic-spline interpolation from the database of values as a function of pressure and temperature. Then, the nine coefficients in equation (11) were calculated from the nine interpolated values of gas mixture density and sound speed.

For this example, we've selected eight natural gas mixtures. The first five gas mixtures (*Amarillo* gas, *Gulf Coast* gas, *Ekofisk* gas, *High* $CO_2$ *&* $N_2$, and *High* $N_2$) are also used as example mixtures in AGA Report No. 8 and in the Lomic SonicWare computer code. The sixth gas mixture is pure methane. The seventh and eighth gas mixtures are taken from the set of 86 gas mixtures listed in Table 1. Gas ID#39 and 49 were selected because they had the lowest and highest values of standard heating value, $H_v$. Detailed compositions for all eight gas mixtures are listed in Table 5. Lomic SonicWare was used to calculate the value of sound speed, $S$, and gas mixture density, $\rho$, at a pressure of 950 psia and temperature of 65°F. Values of standard sound speed, $S_{std}$, and standard density, $\rho_{std}$, were also calculated using Lomic SonicWare. These values are listed in Table 5 together with values of the molecular weight, $MW$, the mass-based heating value, $H_m$, and the standard volumetric heating value, $H_v$.

To test our calculation methods, equation (11) was used together with the values of sound speed, $S$, nitrogen concentration, $X_{N2}$, and carbon dioxide concentration, $X_{CO2}$, listed in Table 5 to calculate values of the gas mixture density, $\rho_{calc}$, for all eight gas mixtures. The density error magnitude is less than 0.02% for all gas mixtures except *High* $CO_2$ *&* $N_2$ and *High* $N_2$ where the magnitude of the error is of the order of 0.10%

## 3.5 Calculation of Molecular Weight

Equation (9) can be extended to arbitrary pressure and temperature by replacing the standard sound speed, $S_{std}$, by the actual sound speed, $S$, and by calculating the nine coefficients from values of $MW$ and $S$ for the nine reference gas mixtures. The equation for molecular weight becomes:

$$MW_{calc} = \left( A_{MW} + B_{MW}/S + C_{MW}/S^2 \right) * \left(1 + D_{MW} * X_{CO2} + E_{MW} * X_{N2}\right) \qquad (13)$$

where $D_{MW} = D_{MW1} + D_{MW2}/S + D_{MW3}/S^2$, and $E_{MW} = E_{MW1} + E_{MW2}/S + E_{MW3}/S^2$.

The values of sound speed, $S$, needed for equation (13) are the same ones computed by cubic-spline fit and used to calculate the coefficients in equation (11). Of course, the values of molecular weight, $MW$, for the nine reference gases are not functions of pressure and temperature, but are constants listed in Table 2.

Values of molecular weight for the eight natural gas mixtures were calculated using equation (13) together with the data for sound speed, $S$, nitrogen concentration, $X_{N2}$, and carbon dioxide concentration, $X_{CO2}$ listed in Table 5. The magnitude of the error in the molecular weight calculation is of the order of 0.02% or less for all gas mixtures except *High* $CO_2$ *&* $N_2$ and *High* $N_2$. For the latter two mixtures, the error is of the order of 0.10%.

## 3.6 Calculation of Standard Sound Speed

Before we can use either equation (6) or (7) to calculate the standard density, and equation (10) to calculate the mass-based heating value, we need to know the value of the standard sound speed, $S_{std}$. In the method developed by Behring et al., it was assumed that the standard sound speed would be measured experimentally. Now, however, we want to be able to

calculate the standard sound speed using the value of molecular weight, *MW*, computed at pipeline pressure and temperature.

**Table 5. Calculations of gas density, molecular weight, standard sound speed, and heating value.**

| | Values of S, Sstd, $\rho$, $\rho$std Calculated by SonicWare™ Detailed Composition Method | | | | | | | |
|---|---|---|---|---|---|---|---|---|
| **ID#** | **Amarillo** | **Gulf Coast** | **Ekofisk** | **High $CO_2$ & $N_2$** | **High $N_2$** | **Methane** | **ID#39** | **ID#49** |
| **Pressure (psia)** | 950 | 950 | 950 | 950 | 950 | 950 | 950 | 950 |
| **Temperature (°F)** | 65 | 65 | 65 | 65 | 65 | 65 | 65 | 65 |
| **S (ft/s)** | 1,328.18 | 1,365.60 | 1,252.59 | 1,248.13 | 1,316.18 | 1,411.72 | 1,379.19 | 1,208.52 |
| **Sstd (ft/s)** | 1,377.77 | 1,412.38 | 1,325.65 | 1,298.63 | 1,344.53 | 1,449.78 | 1,415.05 | 1,295.14 |
| **$\rho$ ($lb_m/ft^3$)** | 3.423668 | 3.248156 | 3.789474 | 3.884008 | 3.536385 | 3.061223 | 3.208673 | 4.036393 |
| **$\rho$std (lbm/ft3)** | 0.046578 | 0.044467 | 0.0497045 | 0.052495 | 0.049350 | 0.042457 | 0.044534 | 0.0517027 |
| **MW** | 17.5955 | 16.7994 | 18.7683 | 19.8291 | 18.6488 | 16.0430 | 16.8278 | 19.5175 |
| **Hm (Btu/lbm)** | 22,217.6 | 23,299.4 | 22,293.6 | 17,774.9 | 18,371.7 | 23,891.0 | 22,166.9 | 22,245.2 |
| **Hv (Btu/SCF)** | 1034.85 | 1036.05 | 1108.09 | 933.10 | 906.65 | 1014.34 | 987.18 | 1150.14 |
| **nitrogen (%)** | 3.1284 | 0.2595 | 1.0068 | 5.70206 | 13.4650 | 0.0000 | 3.7924 | 0.3407 |
| **carbon dioxide (%)** | 0.4676 | 0.5956 | 1.4954 | 7.58508 | 0.9850 | 0.0000 | 0.2609 | 1.8816 |
| **methane (%)** | 90.6724 | 96.5222 | 85.9063 | 81.21181 | 81.4410 | 100.0000 | 94.6077 | 83.4187 |
| **ethane (%)** | 4.5279 | 1.8186 | 8.4919 | 4.30304 | 3.3000 | 0.0000 | 1.0118 | 9.5284 |
| **propane (%)** | 0.8280 | 0.4596 | 2.3015 | 0.89501 | 0.6050 | 0.0000 | 0.2128 | 3.5694 |
| **i-butane (%)** | 0.1037 | 0.0977 | 0.3486 | 0.15100 | 0.1000 | 0.0000 | 0.04572 | 0.6219 |
| **n-butane (%)** | 0.1563 | 0.1007 | 0.3506 | 0.15200 | 0.1040 | 0.0000 | 0.03048 | 0.4146 |
| **i-pentane (%)** | 0.0321 | 0.0473 | 0.0509 | 0.00000 | 0.0000 | 0.0000 | 0.01464 | 0.10968 |
| **n-pentane (%)** | 0.0443 | 0.0324 | 0.0480 | 0.00000 | 0.0000 | 0.0000 | 0.00976 | 0.07312 |
| **n-hexane (%)** | 0.0393 | 0.0664 | 0.0000 | 0.00000 | 0.0000 | 0.0000 | 0.0086 | 0.0327 |
| **n-heptane (%)** | 0.0000 | 0.0000 | 0.0000 | 0.00000 | 0.0000 | 0.0000 | 0.0044 | 0.0081 |
| **n-octane (%)** | 0.0000 | 0.0000 | 0.0000 | 0.00000 | 0.0000 | 0.0000 | 0.0008 | 0.0011 |
| | **Values of Density Calculated Using Equation (11) and Actual Sound Speed** | | | | | | | |
| **Pressure (psia)** | 950 | 950 | 950 | 950 | 950 | 950 | 950 | 950 |
| **Temperature (°F)** | 65 | 65 | 65 | 65 | 65 | 65 | 65 | 65 |
| **S (ft/s)** | 1,328.18 | 1,365.60 | 1,252.59 | 1,248.13 | 1,316.18 | 1,411.72 | 1,379.19 | 1,208.52 |
| **nitrogen (%)** | 3.1284 | 0.2595 | 1.0068 | 5.70206 | 13.4650 | 0.0000 | 3.7924 | 0.3407 |
| **carbon dioxide (%)** | 0.4676 | 0.5956 | 1.4954 | 7.58508 | 0.9850 | 0.0000 | 0.2609 | 1.8816 |
| **$\rho_{calc}$ ($lb_m/ft^3$)** | 3.423293 | 3.248623 | 3.7898805 | 3.880360 | 3.5338361 | 3.0611714 | 3.208209 | 4.0368728 |
| **Error in $\rho_{calc}$ (%)** | -0.011 | 0.014 | 0.011 | -0.094 | -0.072 | -0.002 | -0.014 | 0.012 |
| | **Values of Molecular Weight Calculated Using Equation (12) and Actual Sound Speed** | | | | | | | |
| **$MW_{calc}$** | 17.5975 | 16.8000 | 18.7723 | 19.8478 | 18.6671 | 16.0425 | 16.8262 | 19.5173 |
| **Error in Mwcalc (%)** | 0.011 | 0.004 | 0.021 | 0.094 | 0.098 | -0.003 | -0.010 | -0.001 |
| | **Values of Standard Sound Speed Calculated from Molecular Weight Using Equation (8)** | | | | | | | |
| **$Sstd_{calc}$ (ft/s)** | 1377.66 | 1412.33 | 1325.52 | 1298.03 | 1343.98 | 1449.81 | 1415.20 | 1295.10 |
| **Error in $Sstd_{calc}$ (%)** | -0.008 | -0.004 | -0.010 | -0.046 | -0.041 | 0.002 | 0.011 | -0.003 |
| | **Values of Standard Sound Speed Calculated from Molecular Weight Using Equation (9)** | | | | | | | |
| **$Sstd_{calc}$ (ft/s)** | 1377.73 | 1412.53 | 1325.57 | 1297.69 | 1343.65 | 1449.76 | 1415.08 | 1295.22 |
| **Error in $Sstd_{calc}$ (%)** | -0.003 | 0.011 | -0.006 | -0.072 | -0.066 | -0.001 | 0.002 | 0.006 |
| | **Values of Standard Density, Mass-Based and Standard Volumetric Heating Value** | | | | | | | |
| **$\rho std_{calc}$ ($lbm/ft^3$)** | 0.046577 | 0.044456 | 0.0497125 | 0.052562 | 0.0494066 | 0.042456 | 0.0445358 | 0.0516961 |
| **Error in $\rho std_{calc}$ (%)** | -0.002 | -0.024 | 0.016 | 0.129 | 0.114 | -0.002 | 0.004 | -0.013 |
| **$Hm_{calc}$ (Btu/lbm)** | 22,214.7 | 23,302.5 | 22,290.4 | 17,811.3 | 18,415.6 | 23,895.8 | 22,167.0 | 22,245.4 |
| **Error in $Hm_{calc}$ (%)** | -0.013 | 0.013 | -0.015 | 0.205 | 0.239 | 0.020 | 0.001 | 0.001 |
| **$Hv_{calc}$ (Btu/SCF)** | 1034.70 | 1035.94 | 1108.11 | 936.20 | 909.85 | 1014.52 | 987.23 | 1150.00 |
| **Error in Hvcalc (%)** | -0.014 | -0.011 | 0.002 | 0.333 | 0.353 | 0.018 | 0.005 | -0.012 |
| **Error in Hvcalc (Btu/SCF)** | -0.15 | -0.11 | 0.02 | 3.10 | 3.20 | 0.18 | 0.05 | -0.14 |

Equation (8) is a least-square-error regression fit that relates the molecular weight to the standard sound speed, the carbon dioxide concentration and the nitrogen concentration. This equation can be used to calculate $S_{std}$ if the other three variables are known. Using the terminology of equation (8):

$$S_{std} = \frac{-B \pm \sqrt{B^2 - 4C(A - MW)}}{2C}$$

$$A = A_0 + A_1 * X_{N2} + A_2 * X_{CO2}, \qquad (14)$$

$$B = B_0 + B_1 * X_{N2} + B_2 * X_{CO2},$$

$$C = C_0 + C_1 * X_{N2} + C_2 * X_{CO2}$$

The coefficients in the linear expressions for $A$, $B$, and $C$ are constants and are listed in the paragraph following equation (8). Equation (14) has two solutions, but only one of the solutions is physically realistic. Table 5 lists the value of $S_{std}$ calculated for the eight example gas mixtures. The magnitude of the calculation error in $S_{std}$ is of the order of 0.01%, except for the two examples with high diluent concentrations. For these gas mixtures, the magnitude of the error in $S_{std}$ is less than 0.05%.

Another option available is to use equation (9) to calculate the standard sound speed. Using the terminology of equation (9):

$$S_{std} = \frac{-B_{MW} \pm \sqrt{B_{MW}{}^2 - 4aC_{MW}}}{2a}$$

$$a = A_{MW} - \frac{MW}{(1 + D_{MW} * X_{CO2} + E_{MW} * X_{N2})} \qquad (15)$$

$$D_{MW} = D_{MW1} + D_{MW2}/S_{std} + D_{MW3}/S_{std}^2$$

$$E_{MW} = E_{MW1} + E_{MW2}/S_{std} + E_{MW3}/S_{std}^2$$

Since $S_{std}$ appears in the expressions for $D_{MW}$ and $E_{MW}$ on the right hand side of equation (15), this equation must be solved iteratively. For the first iteration, we assume that $D_{MW} \cong D_{MW1}$ and $E_{MW} \cong E_{MW1}$ and solve for $S_{std}$. For the second and higher numbered iterations, the value of $S_{std}$ computed in the previous iteration is used to evaluate $D_{MW}$ and $E_{MW}$. For the eight example gas mixtures in Table 5, convergence was achieved within four iterations. Equation (15) also has two solutions, but only one of these solutions is physically realistic. Table 5 shows that the magnitudes of the error in standard sound speed are comparable when using either equation (8) or equation (9). For the two gas mixtures with high diluent concentrations, the error magnitude is about 30% smaller if equation (8) is used rather than equation (9). Since equation (8) is simpler to program and does not require iteration, it is preferred for energy meter module calculations.

## 3.7 Calculation of Standard Volumetric Heating Value

Further calculations of standard density, $\rho_{std}$, using either equation (6) or equation (7), and the mass-based heating value, $H_m$, using equation (10), are straightforward. The standard volumetric heating value, $H_v$, is simply the product of $\rho_{std} * H_m$. Table 5 lists the values of $\rho_{std}$, $H_m$, and $H_v$ calculated for the eight-gas mixture examples and the error associated with each calculation. For the six example gas mixtures with total diluent concentrations of 4.0 mole% or less, the magnitude of the error in calculating $H_v$ is less than 0.02%. This corresponds to an actual error magnitude in $H_v$ of less than 0.2 Btu/SCF. For the two gas mixtures with total diluent concentrations between 13 mole% and 15 mole%, the error in $H_v$ is of the order of 0.35%, equivalent to an actual error of about 3.2 Btu/SCF.

## 3.8 Energy Meter Module Computer Code

A digital computer code was written in FORTRAN to perform all of the calculations required for an energy meter module. Two distinct measurement scenarios are anticipated.

### 3.8.1 Sound Speed Measured by an Ultrasonic Flow Meter

In this scenario, the speed of sound indication and the measured values for gas temperature and gas pressure are provided by an ultrasonic flow meter. The ultrasonic flow meter also provides a value for the volumetric flow rate. Since an ultrasonic flow meter does not measure the concentrations of carbon dioxide and nitrogen, a stream of natural gas will be drawn off through a pipe fitting located downstream of the flow meter. The gas stream passes through a pressure regulation valve, into an energy meter module that contains the carbon dioxide sensor, and a connection to an apparatus for determining the nitrogen concentration.

The composition of dry natural gas is a chemical property, and the concentrations of carbon dioxide and nitrogen are not functions of temperature and pressure. The FORTRAN computer code calculates the density and molecular weight of the natural gas mixture at the pressure and temperature measured at the ultrasonic flow meter. The computer code also calculates the standard sound speed, and the mass-based heating value. The energy flow rate is calculated as the volumetric flow rate measured by the ultrasonic flow meter multiplied by the product of the gas density and the mass-based heating value. The units of the energy flow rate are Btu/hour.

### 3.8.2 Sound Speed Measured by the Energy Meter Module

A second measurement scenario includes all flow meter types (orifice meter, V-cone meter, turbine meter, Coriolis meter, etc.) that do not measure the speed of sound in the flowing gas stream. For these meters, the sound speed will be measured separately using acoustic sensors installed inside the energy meter module. The pressure and temperature of the gas stream flowing through the energy meter module will be measured also. Note that in this scenario, the pressure and temperature at the location where the speed of sound is measured in the energy meter module may be very different from the gas pressure and temperature in the flow meter. Concentrations of carbon dioxide and nitrogen typical of the gas in the flow meter will be measured by sensors in the energy meter module or in a second apparatus connected to the energy meter module. The FORTRAN computer code first calculates the density and molecular

weight of the natural gas mixture in the energy meter module. Next, the computer code calculates the standard sound speed and the mass-based heating value. Finally, the computer code calculates the natural gas density at the gas pressure and temperature in the flow meter. The energy flow rate is calculated as the volumetric flow rate through the flow meter multiplied by the product of the natural gas density in the flow meter and the mass-based heating value.

## 3.9 Flow Computer

The FORTRAN computer code was developed and debugged using DIGITAL Visual Fortran 5.0 on a desktop PC running under Windows 95. However, this is not a realistic platform for a flow measurement system to be used in the field by the natural gas industry. Because the project objective was to evaluate the energy meter concept while acquiring experimental data from actual flow meters, it was decided to move the software onto a flow computer suitable for field measurements.

A meeting was held with Bristol Babcock Inc. in Houston to discuss the use of a Bristol Babcock model 3330 flow computer as a platform that would be compatible with existing flow meters and with the energy meter software. Several advantages were identified: (1) the model 3330 flow computer is commonly used in the natural gas transmission industry; (2) the ACCOL software used to program the flow computer also has wide acceptance in the industry; (3) model 3330 flow computers are currently used to communicate with and process data from ultrasonic, turbine and orifice flow meters; (4) Bristol Babcock does not manufacture or sell an energy measurement system (such as a gas chromatograph) that might be expected to compete with energy meter development; and (5) the choice of a general purpose flow computer as a platform for the MRF demonstration would not prejudice the selection of a commercialization partner at a later time.

Bristol Babcock signed a non-disclosure agreement with Southwest Research Institute to safeguard the confidentiality of the energy meter software development. An order was placed with Bristol Babcock to furnish a model 3330 flow computer and programmer support to translate the energy module computer code from FORTRAN into ACCOL. Bristol Babcock and SwRI engineers worked closely together to debug the ACCOL code and to assure that values of chemical and thermodynamic properties calculated by the ACCOL and FORTRAN codes were substantially the same.

# 4.0 Uncertainty Considerations

Behring et al. (1999) reported preliminary estimates for the uncertainty limits needed to achieve a measurement uncertainty of 0.5% in the mass-based heating value, the standard density, and the standard volumetric heating value. The uncertainty limit for $X_{CO2}$ was ±0.2 mole%. The uncertainty limit for $X_{N2}$ was ±0.3 mole%. The uncertainty limit for $S_{std}$ was ±0.5% which is equivalent to about ±7 ft/s. No preliminary uncertainty estimates were made for the gas mixture pressure or temperature. The use of the least-square-error regression correlations developed by Behring et al. assumes that the gas pressure will be controlled at 14.73 psia and the gas temperature at 60°F.

Behring et al. state "the 0.5% specification was arbitrarily chosen based on the general industry effort to reduce custody transfer measurements to (uncertainty) levels below 1%." An uncertainty level of ±0.5% in the standard volumetric heating value would correspond to approximately ±5 Btu/SCF. For an energy meter module to be effective as a replacement for a gas chromatograph, the goal uncertainty level should be reduced from approximately ±5 Btu/SCF to the order of ±1 Btu/SCF. However, not all applications require accuracy of ±1 Btu/SCF. An accuracy of ±5 Btu/SCF will still allow use of the energy measurement method in situations where the cost of a gas chromatograph can not be justified.

## 4.1 Sensitivity Calculation – Standard Volumetric Heating Value, $H_v$

To estimate the sensitivity of the standard volumetric heating value to errors in the measured variables, sensitivity calculations were performed using the energy meter computer code. It was assumed that the energy meter module was operating in association with an ultrasonic flow meter. The ultrasonic flow meter, pressure, temperature, and $N_2$ and $CO_2$ sensors would provide measured values of (1) average flow velocity, (2) local gas temperature, (3) speed of sound, (4) mole% concentration of nitrogen, (5) mole% concentration of carbon dioxide, and (6) local gas pressure in the gas mixture flowing through the flow meter. The sensitivity analysis was performed by running the computer code for a set of *base conditions*, then changing the values of the input variables. The average flow velocity measurement does not affect the calculation of energy content in the gas, so it was omitted from the sensitivity analysis. Between six and nine runs were made for different values for each of the other five variable. Only one variable was changed at a time.

In order to determine the *actual values* of gas density, mass-based heating value and standard volumetric heating value, a gas chromatograph analysis of the natural gas mixture circulating in the MRF high pressure loop on June 6, 2000, was performed. The *base condition* gas mixture is composed of 96.023872% methane, 1.534452% ethane, 1.255016% carbon dioxide, 0.914424% nitrogen, 0.176326% propane, 0.020447% i-butane, 0.033854% n-butane, 0.010620% i-pentane, 0.009403% n-pentane, 0.008653% hexane, 0.009206% heptane, 0.002627% octane, and 0.001102% nonane. The standard volumetric heating value is 1009.54 Btu/SCF. Other *base conditions* are: gas mixture sound speed = 1387.46 ft/s, local gas temperature = 70°F, local gas pressure = 620 psia.

The results of the sensitivity calculations are shown in Figures 12 through 16, and the sensitivity factors are listed in Table 6.

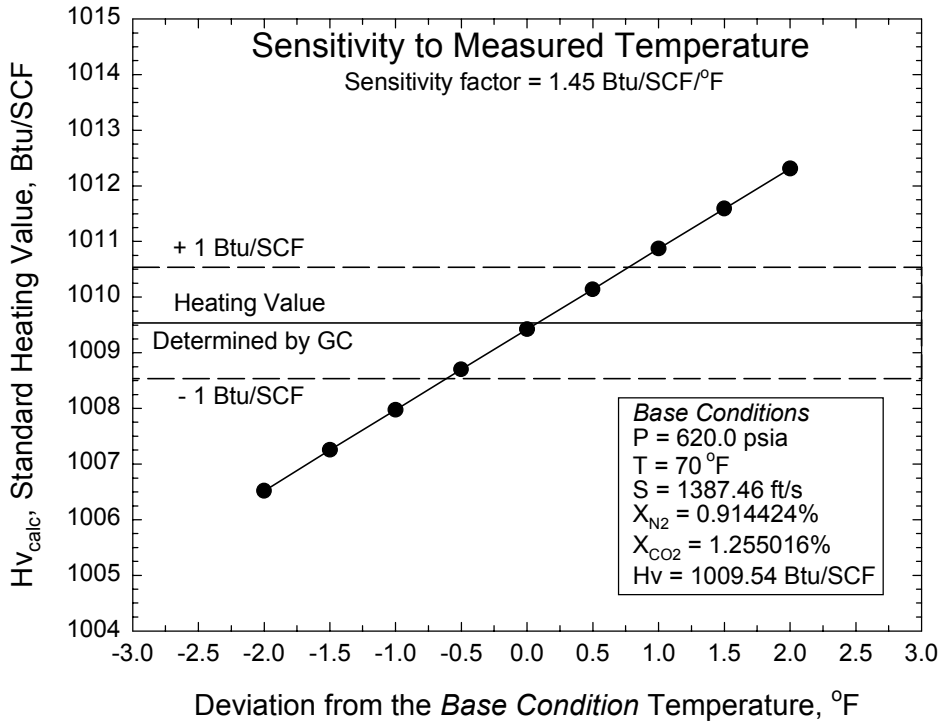


**Figure 12. Sensitivity of the standard heating value calculated by the energy meter algorithm to an error in the measured value of temperature.**

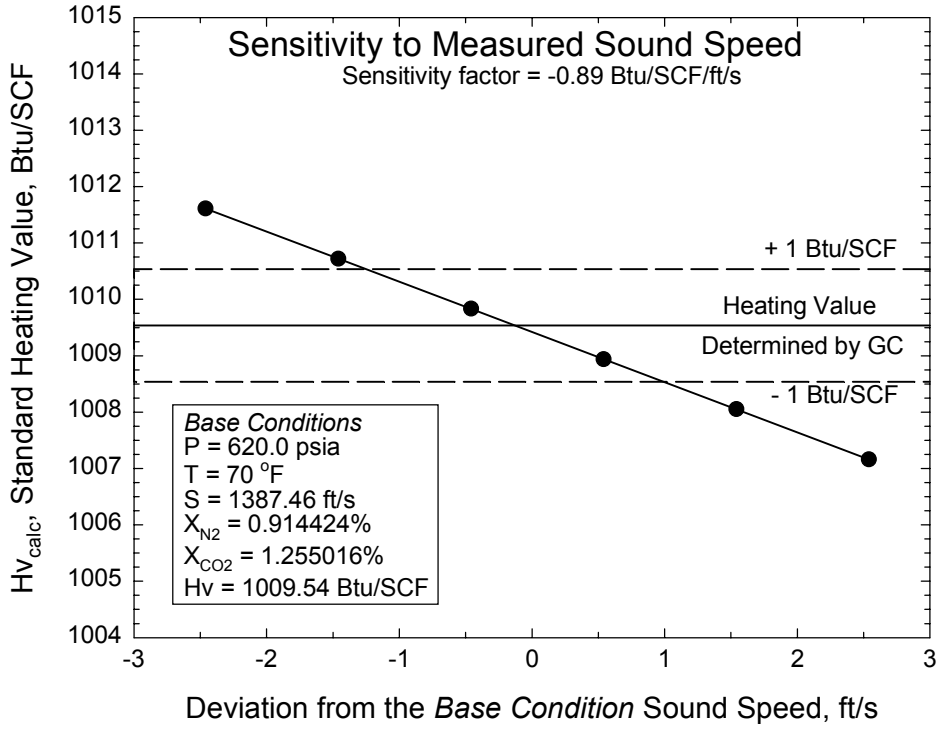


**Figure 13. Sensitivity of the standard heating value calculated by the energy meter algorithm to an error in the measured value of sound speed.**

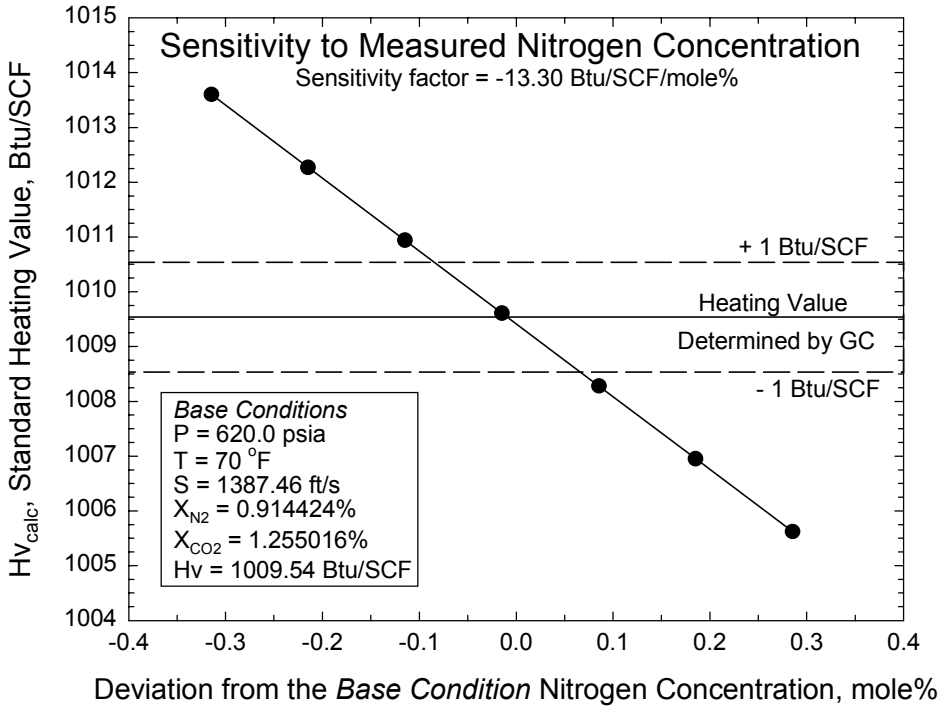


**Figure 14. Sensitivity of the standard heating value calculated by the energy meter algorithm to an error in the measured value of nitrogen concentration.**

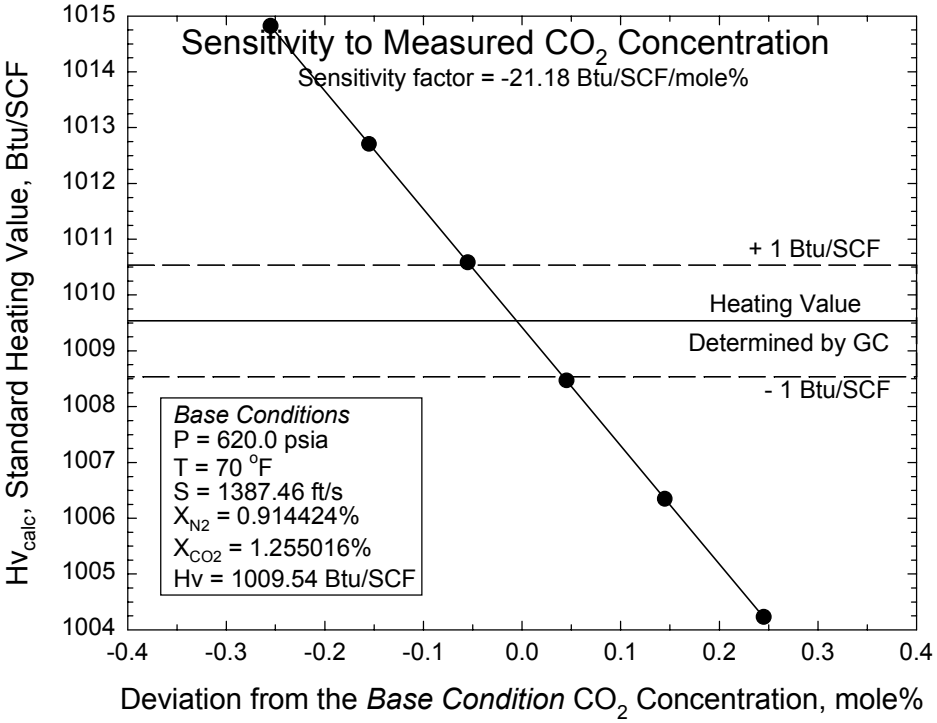


**Figure 15. Sensitivity of the standard heating value calculated by the energy meter algorithm to an error in the measured value of carbon dioxide concentration.**

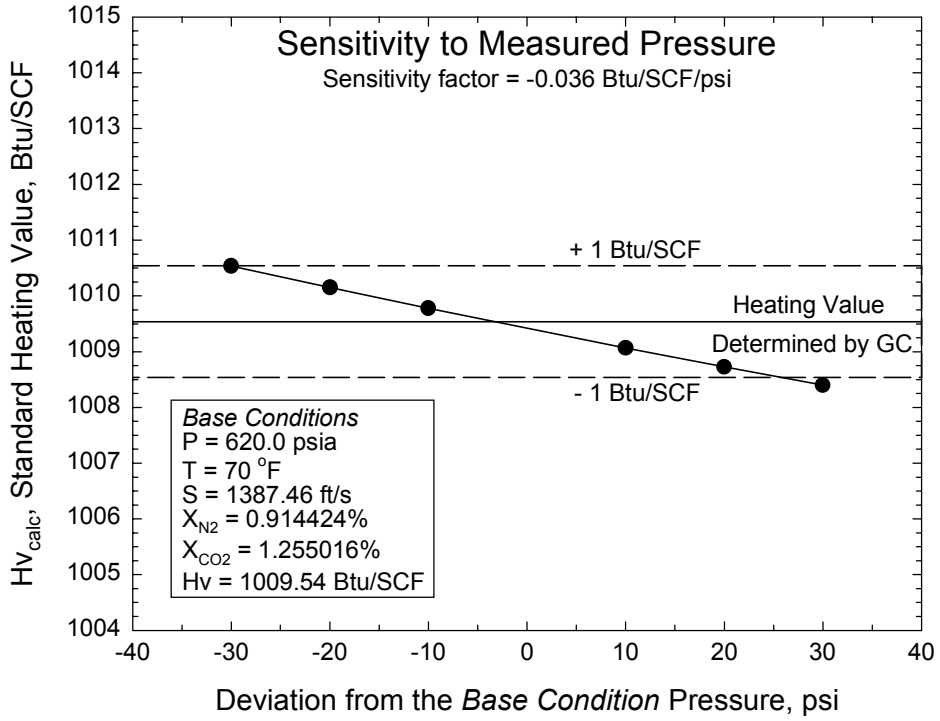


**Figure 16. Sensitivity of the standard heating value calculated by the energy meter algorithm to an error in the measured value of pressure.**

**Table 6. Sensitivity factors for calculated values of standard volumetric heating value.**

| *Sensitivity to* | *Value* | *Units* |
|---|---|---|
| Temperature | $\partial H_v / \partial T = 1.45$ | (Btu/SCF)/°F |
| Speed of Sound | $\partial H_v / \partial S = -0.89$ | (Btu/SCF)/(ft/s) |
| Nitrogen Concentration | $\partial H_v / \partial X_{N2} = -13.30$ | (Btu/SCF)/mole% |
| Carbon Dioxide Concentration | $\partial H_v / \partial X_{CO2} = -21.18$ | (Btu/SCF)/mole% |
| Pressure | $\partial H_v / \partial P = -0.036$ | (Btu/SCF)/psi |

The sensitivity factors can be used to calculate the magnitude of a measurement error for each variable that would lead to an error of ±1 Btu/SCF in the standard heating value. The gas temperature would have to be measured to an accuracy of ±0.7°F as shown in Figure 12. For the same uncertainty level of ±1 Btu/SCF, the uncertainty limits for the other measured variables are ±1.1 ft/s for sound speed, ±0.08 mole% for the nitrogen concentration, ±0.05 mole% for the carbon dioxide concentration, and ±25 psi for the gas pressure.

## 4.2 Sensitivity Calculation – Natural Gas Energy Content, $\rho * H_m$

The standard volumetric heating value, $H_v$, is a convenient measure of the energy content of a cubic foot of natural gas at standard pressure, 14.73 psia and standard temperature, 60°F. Behring et al. show that the energy flow rate, $Q_{energy}$, with units of Btu/hr can be calculated as the product of the standard volumetric flow rate, $Q_{v,std}$, with units of SCF/hr and the standard volumetric heating value, $H_v$, with units of Btu/SCF.

$$Q_{energy} = Q_{v,std} * H_v = \left( \frac{Q_m}{\rho_{std}} \right) * \left( \rho_{std} * H_m \right) = Q_m * H_m \tag{16}$$

Volumetric flow meters, such as an ultrasonic flow meter or a turbine flow meter, do not measure $Q_{v,std}$ directly. Instead, they measure the volumetric flow rate, $Q_v$, with units of "actual" cubic feet of gas/hr. The standard volumetric flow rate, $Q_{v,std}$, can be calculated by multiplying the actual volumetric flow rate, $Q_v$, by the ratio of the actual density divided by the standard density:

$$Q_{v,std} = Q_v * \left( \frac{\rho}{\rho_{std}} \right) \tag{17}$$

The ratio of the gas densities can be calculated as:

$$\frac{\rho}{\rho_{std}} = \left( \frac{P}{14.73 psia} \right) * \left( \frac{519.67°R}{T} \right) * \left( \frac{Z_{std}}{Z} \right) \tag{18}$$

The values of $P$ and $T$ are the pressure and temperature of the gas mixture at flow meter conditions. These two quantities will be measured with pressure and temperature transmitters. However, the ratio of the natural gas compressibility will have to be calculated. The usual procedure is to use the AGA Report No. 8 (1994) equation of state and the detailed gas composition method using the composition measured by a gas chromatograph.

We would like to avoid the requirement for a gas chromatograph and to use the correlations described earlier. Let's rewrite equation (16) as

$$Q_{energy} = Q_{v,std} * H_v = Q_v * \left( \frac{\rho}{\rho_{std}} \right) * \left( \rho_{std} * H_m \right) = Q_v * \rho * H_m \tag{19}$$

Since the actual volumetric flow rate, $Q_v$, is measured by the flow meter, we can use equations (10) and (11) to calculate the mass-based heating value, $H_m$, and the flowing gas density, $\rho$, needed to calculate the energy rate.

The sensitivity of the $\left( \rho * H_m \right)$ product to errors in the measured variables was calculated in the same manner as the sensitivity in the standard volumetric heating value, $H_v$. The results of the sensitivity calculations are shown in Figures 17 through 21, and the sensitivity factors are listed in Table 7. The sensitivity factors can be used to calculate the magnitude of a measurement error for each variable that would lead to an error of ± 0.5% in the energy content

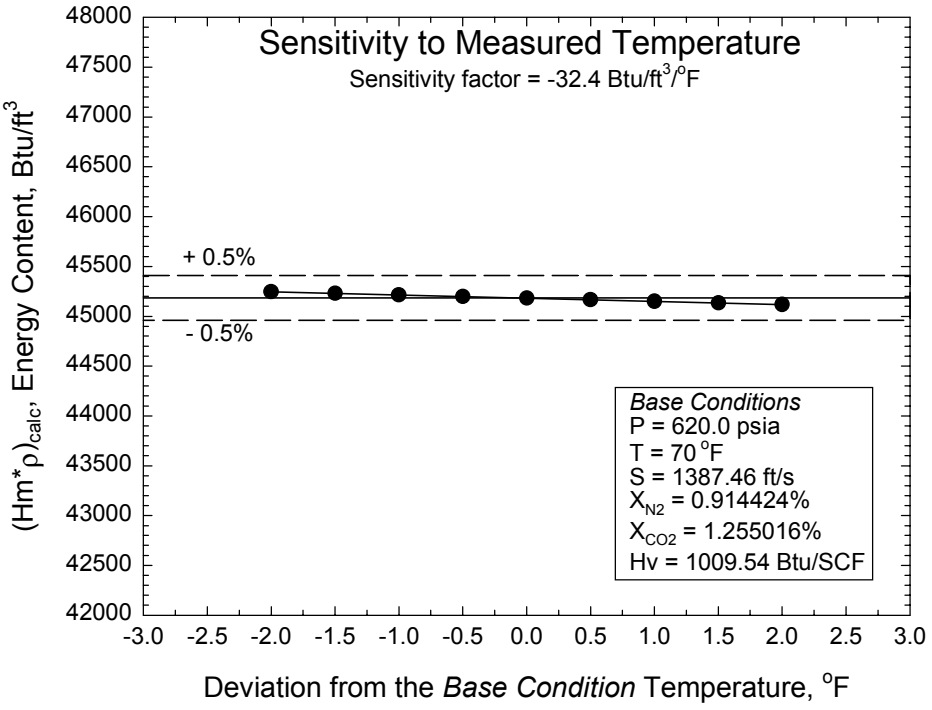


**Figure 17. Sensitivity of the natural gas energy content calculated by the energy meter algorithm to an error in the measured value of temperature.**

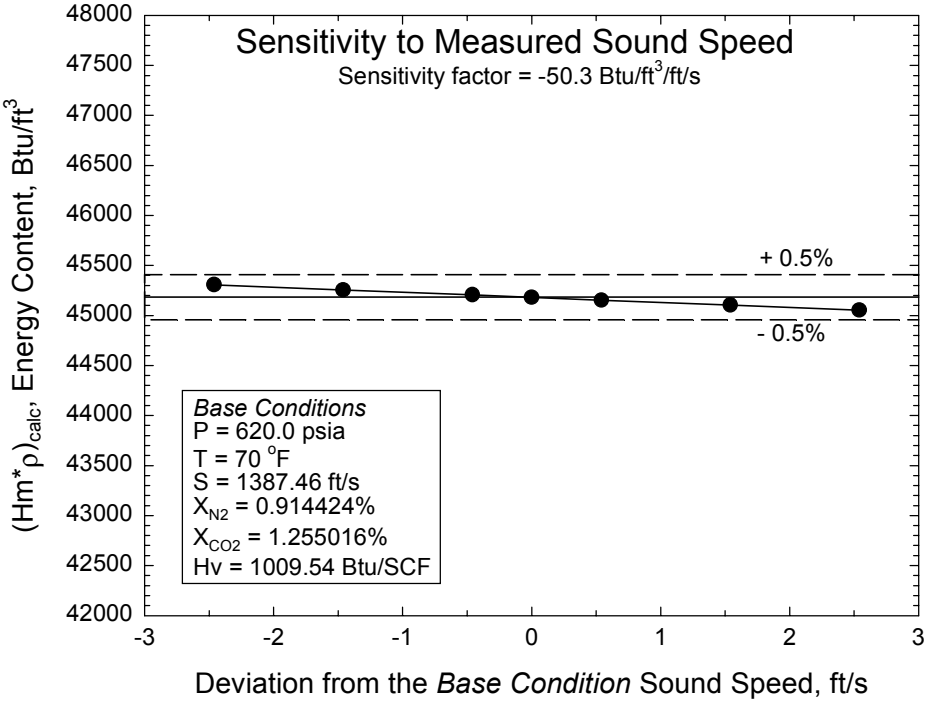


**Figure 18. Sensitivity of the natural gas energy content calculated by the energy meter algorithm to an error in the measured value of sound speed.**

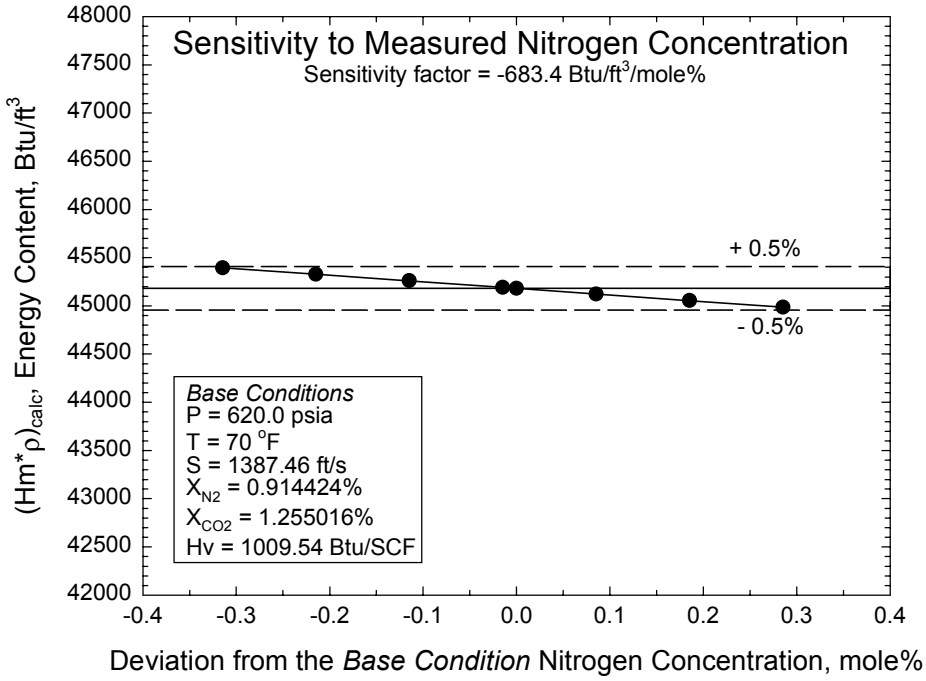


**Figure 19. Sensitivity of the natural gas energy content calculated by the energy meter algorithm to an error in the measured value of nitrogen concentration.**

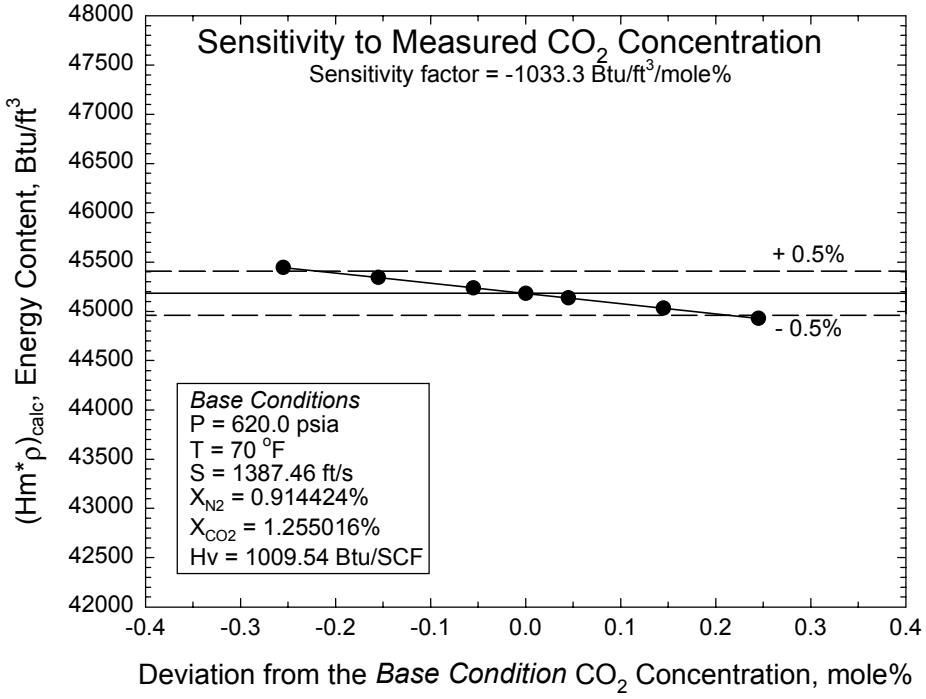


**Figure 20. Sensitivity of the natural gas energy content calculated by the energy meter algorithm to an error in the measured value of carbon dioxide concentration.**

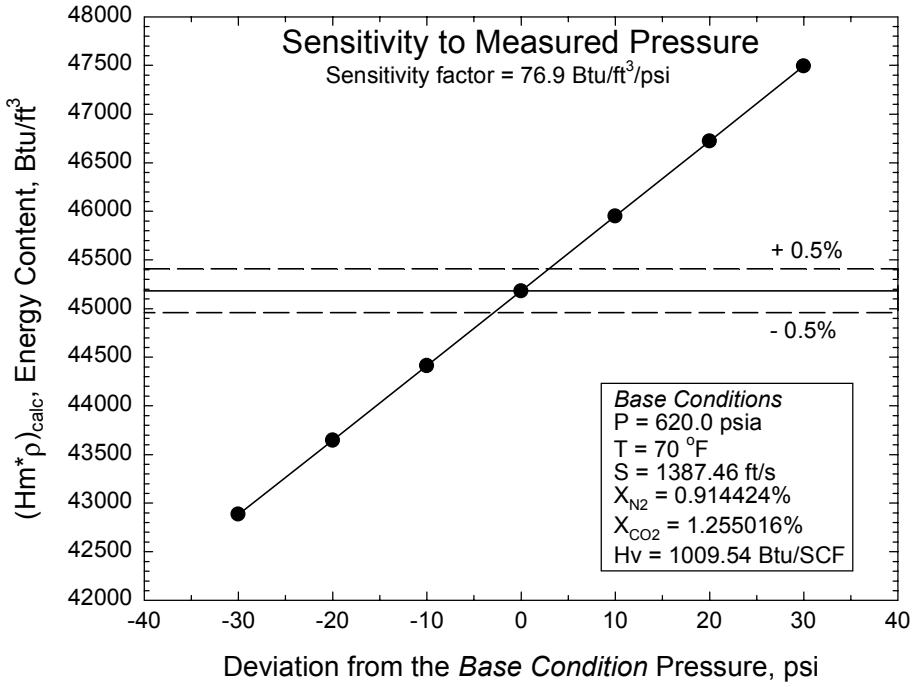


**Figure 21. Sensitivity of the natural gas energy content calculated by the energy meter algorithm to an error in the measured value of gas mixture pressure.**

**Table 7. Sensitivity factors for calculated values of natural gas energy content**

| *Sensitivity to* | *Value* | *Units* |
|---|---|---|
| Temperature | $\partial(\rho * H_m)/\partial T = -32.4$ | (Btu/ft$^3$)/°F |
| Speed of Sound | $\partial(\rho * H_m)/\partial S = -50.3$ | (Btu/ft$^3$)/(ft/s) |
| Nitrogen Concentration | $\partial(\rho * H_m)/\partial X_{N2} = -683.4$ | (Btu/ft$^3$)/mole% |
| Carbon Dioxide Concentration | $\partial(\rho * H_m)/\partial X_{CO2} = -1033.3$ | (Btu/ft$^3$)/mole% |
| Pressure | $\partial(\rho * H_m)/\partial P = 76.9$ | (Btu/ft$^3$)/psi |

product of $\rho * H_m$. The gas mixture temperature would have to be measured to an accuracy of ±7.0°F. For the same uncertainty limit of ±0.5% in the product of $(\rho * H_m)$ the uncertainty limits in the other measured variables are ±4.50 ft/s for the speed of sound, ±0.33 mole% for the nitrogen concentration, ±0.22 mole% for the carbon dioxide concentration, and ±2.9 psi for the gas mixture pressure.

Normally, several measured variables contribute to the experimental uncertainty at the same time. Uncertainty estimates based upon only a single variable can be misleading. Uncertainties in the measurement of temperature, pressure, sound speed, nitrogen concentration and carbon dioxide concentration all contribute to the overall measurement uncertainty. In Section 4.3, the sensitivity factors calculated in this section are used to estimate the overall uncertainty in the standard heating value (Tables 8 and 9) and in the product of density and the mass-based heating value (Tables 10 and 11).

## 4.3 Estimating the Measurement Uncertainty

Coleman and Steele (1989) state that measurement uncertainty is an estimate of experimental error. Uncertainty analysis involves estimating the magnitude of random or precision errors and fixed or bias errors. The textbook by Coleman and Steele (1989) explains the formal basis for estimating measurement uncertainty. In this section, we will make preliminary estimates for the uncertainty in the standard volumetric heating value, $H_v$, and the energy flow rate, $Q_{energy}$.

### 4.3.1 Uncertainty in Standard Volumetric Heating Value, $H_v$

Values of the standard volumetric heating value, $H_v$, can be computed by the energy meter algorithm. The variables that influence the calculated value of $H_v$ are the gas mixture temperature, the speed of sound, the concentration of nitrogen and carbon dioxide in the gas mixture, and the gas mixture pressure. Following Coleman and Steele (1989), we will estimate the measurement uncertainty by the root sum of squares method. That is, the uncertainty in $H_v$ is estimated by taking the square roof of the sum of the squares of the influence factors for all of the variables. The influence factors are simply the sensitivity value multiplied by the uncertainty for each of the independent variables. The uncertainties are assumed to be independent; the sign and magnitude of the uncertainty in temperature are not affected by or correlated to the uncertainty in sound speed or any of the other variables. The uncertainty in standard volumetric heating value can be calculated using equation (20).

$$\Delta H_v = \sqrt{\left(\frac{\partial H_v}{\partial T} * \Delta T\right)^2 + \left(\frac{\partial H_v}{\partial S} * \Delta S\right)^2 + \left(\frac{\partial H_v}{\partial X_{N2}} * \Delta X_{N2}\right)^2 + \left(\frac{\partial H_v}{\partial X_{CO2}} * \Delta X_{CO2}\right)^2 + \left(\frac{\partial H_v}{\partial P} * \Delta P\right)^2} \qquad (20)$$

The values for the sensitivity factors are listed in Table 6 for a single *base condition*. The sensitivity factors may change as a function of the values of the independent variables.

First, let's examine the uncertainty values for each of the independent variables that would lead to an uncertainty in $H_v$ of the order of ±1, ±2, and ±5 Btu/SCF. The results are shown in Table 8.

The uncertainty estimates assumed for the independent variables in Table 8 are somewhat arbitrary. They were selected to show the level of uncertainty that could be tolerated if each variable contributed to the overall uncertainty in standard volumetric heating value.

**Table 8. Uncertainty estimates for standard volumetric heating value, $H_v$.**

| *Uncertainty Source* | | *Base Value* | *Delta* | *Delta/Value* | *Sensitivity* | $U_{95\%}$ | *Units* |
|---|---|---|---|---|---|---|---|
| T | Temperature | 70°F | +/- 0.25°F | 0.00357 | 1.45 | 0.36 | Btu/SCF |
| P | Pressure | 620 psia | +/- 6.2 psi | 0.01000 | -0.036 | -0.22 | Btu/SCF |
| S | Sound Speed | 1387.46 ft/s | +/- 0.5 ft/s | 0.00036 | -0.89 | -0.45 | Btu/SCF |
| $X_{N2}$ | Nitrogen | 0.914424% | +/- 0.05% | 0.05468 | -13.2 | -0.66 | Btu/SCF |
| $X_{CO2}$ | Carbon Dioxide | 1.255016% | +/- 0.025% | 0.01992 | -21.18 | -0.53 | Btu/SCF |
| | | | | | | $\Delta H_v = \pm 1.05$ | Btu/SCF |
| If $H_v$ = 1,009.54 Btu/SCF, then $\Delta H_v / H_v = \pm 0.10\%$ | | | | | | | |
| | | | | | | | |
| *Uncertainty Source* | | *Base Value* | *Delta* | *Delta/Value* | *Sensitivity* | $U_{95\%}$ | *Units* |
| T | Temperature | 70°F | +/- 0.5°F | 0.00714 | 1.45 | 0.73 | Btu/SCF |
| P | Pressure | 620 psia | +/- 6.2 psi | 0.01000 | -0.036 | -0.22 | Btu/SCF |
| S | Sound Speed | 1387.46 ft/s | +/- 1 ft/s | 0.00072 | -0.89 | -0.89 | Btu/SCF |
| $X_{N2}$ | Nitrogen | 0.914424% | +/- 0.1% | 0.10936 | -13.2 | -1.32 | Btu/SCF |
| $X_{CO2}$ | Carbon Dioxide | 1.255016% | +/- 0.05% | 0.03984 | -21.18 | -1.06 | Btu/SCF |
| | | | | | | $\Delta H_v = \pm 2.06$ | Btu/SCF |
| If $H_v$ = 1,009.54 Btu/SCF, then $\Delta H_v / H_v = \pm 0.20\%$ | | | | | | | |
| | | | | | | | |
| *Uncertainty Source* | | *Base Value* | *Delta* | *Delta/Value* | *Sensitivity* | $U_{95\%}$ | *Units* |
| T | Temperature | 70°F | +/- 1.0°F | 0.01429 | 1.45 | 1.45 | Btu/SCF |
| P | Pressure | 620 psia | +/- 6.2 psi | 0.01000 | -0.036 | -0.22 | Btu/SCF |
| S | Sound Speed | 1387.46 ft/s | +/- 2.0 ft/s | 0.00144 | -0.89 | -1.78 | Btu/SCF |
| $X_{N2}$ | Nitrogen | 0.914424% | +/- 0.3% | 0.32808 | -13.2 | -3.96 | Btu/SCF |
| $X_{CO2}$ | Carbon Dioxide | 1.255016% | +/- 0.10% | 0.07968 | -21.18 | -2.12 | Btu/SCF |
| | | | | | | $\Delta H_v = \pm 5.05$ | Btu/SCF |
| If $H_v$ = 1,009.54 Btu/SCF, then $\Delta H_v / H_v = \pm 0.50\%$ | | | | | | | |

Now, let's frame the question differently, and ask what would be the uncertainty in $H_v$ if each variable was measured as accurately as possible within the calibration limitations of the GRI MRF High Pressure Loop (HPL). This will become an estimate of the "pre-test" uncertainty analysis. An estimate of the experimental error that is made before the test is performed. The best case uncertainty estimate for temperature is $\Delta T = \pm 0.2$°F, for pressure, $\Delta P = \pm 0.2$ psi, for sound speed, $\Delta S = \pm 1.5$ ft/s, for carbon dioxide concentration, $\Delta X_{CO2} = \pm 0.05$ mole%, and for nitrogen, $\Delta X_{N2} = \pm 0.05$ mole%. Table 9 shows that the estimated uncertainty in standard volumetric heating value would be of the order of $\Delta H_v = \pm 2.0$ Btu/SCF. The variables that make the largest contribution to the uncertainty are the sound speed, the nitrogen and the carbon dioxide concentrations.

**Table 9. Pre-test uncertainty estimates for standard volumetric heating value, $H_v$.**

| *Uncertainty Source* | | *Base Value* | *Delta* | *Delta/Value* | *Sensitivity* | $U_{95\%}$ | *Units* |
|---|---|---|---|---|---|---|---|
| T | Temperature | 70°F | +/- 0.2°F | 0.00286 | 1.45 | 0.29 | Btu/SCF |
| P | Pressure | 620 psia | +/- 0.2 psi | 0.00032 | -0.036 | -0.01 | Btu/SCF |
| S | Sound Speed | 1387.46 ft/s | +/- 1.5 ft/s | 0.00108 | -0.89 | -1.34 | Btu/SCF |
| $X_{N2}$ | Nitrogen | 0.914424% | +/- 0.05% | 0.05468 | -13.2 | -0.66 | Btu/SCF |
| $X_{CO2}$ | Carbon Dioxide | 1.255016% | +/- 0.05% | 0.03984 | -21.18 | -1.06 | Btu/SCF |
| $\Delta H_v = \pm 1.85$ Btu/SCF | | | | | | | |
| If $H_v$ = 1,009.54 Btu/SCF, then $\Delta H_v / H_v = \pm 0.18\%$ | | | | | | | |

### 4.3.2 Uncertainty in Energy Flow Rate, $Q_{energy}$

As a replacement for a gas chromatograph, it is important that the energy meter module be capable of indicating the correct value of standard heating value with an uncertainty of ±1 or ±2 Btu/SCF. However, as a device used to measure the energy flow rate, the uncertainty of the flow meter must also be considered.

For this example, we shall assume that the energy meter module is to be used with an ultrasonic flow meter to measure the energy flow rate in a transmission gas pipeline. The energy flow rate, $Q_{energy}$, is the product of the actual volumetric flow rate, $Q_v$, the gas density, $\rho$, at pipeline conditions, and the mass-based heating value, $H_m$, as shown in equation (19). For an ultrasonic flow meter, the dry-meter calibration is performed by measuring the distances between the ultrasonic sensors, and the cross-sectional area of the meter body. AGA Report No. 9 (1998) states the uncertainty for a dry-calibrated meter as ±0.7% of reading for meter diameters of 12 inches or larger, and as ±1.0% of reading for meters smaller than 12 inches.

Since the dry-calibration of the ultrasonic flow meter is independent of the variables that affect the energy content of the natural gas mixture, we can estimate the uncertainty of these terms separately.

Let

$$Q_{energy} = (Q_v) * (\rho * H_m)$$

Then,

$$\Delta Q_{energy} = Q_v * \Delta(\rho * H_m) + \rho * H_m * \Delta Q_v$$

Divide both sides by $Q_{energy}$,

$$\frac{\Delta Q_{energy}}{Q_{energy}} = \frac{\Delta(\rho * H_m)}{\rho * H_m} + \frac{\Delta Q_v}{Q_v}$$

Assuming that each term is independent of the other, we can estimate the uncertainty in the energy flow rate as,

$$\frac{\Delta Q_{energy}}{Q_{energy}} = \sqrt{\left(\frac{\Delta(\rho * H_m)}{\rho * H_m}\right)^2 + \left(\frac{\Delta Q_v}{Q_v}\right)^2} \qquad (21)$$

Let's consider a 12-inch diameter ultrasonic flow meter that is dry-calibrated and has an assigned uncertainty of ±0.7% of reading, that is, $\Delta Q_v / Q_v = \pm 0.007$. What level of uncertainty for the independent variables will produce an uncertainty level of ±0.1%, ±0.2% and ±0.5% for the product of $\rho * H_m$? The results are shown in Table 10. Just as in Table 8, the uncertainty estimates assumed for the independent variables in Table 10 are arbitrary. They were selected simply to show the nominal levels of uncertainty that could be tolerated if each variable contributed to the overall uncertainty in the product of $\rho * H_m$. Note that the units of $\rho * H_m$ are Btu/ACF, i.e., Btu/actual cubic ft, **not Btu/SCF**.

Following the example used to develop Table 9, we can estimate the "pre-test" uncertainty by applying an estimate of uncertainty for each variable that is considered to be realistic under good conditions in the GRI MRF HPL. Values of $\rho$ and $H_m$ are calculated for the given conditions of $T$, $P$, $S$, $X_{N2}$, and $X_{CO2}$ listed in the table. Table 11 shows that the estimated uncertainty in $\rho * H_m$ would be of the order of $\Delta(\rho * H_m) = \pm 99$ Btu/ft$^3$, which is equivalent to a value of $\Delta(\rho * H_m)/(\rho * H_m)$ ±0.0022 or ±0.22%.

Finally, let's look at the total uncertainty in energy flow rate that would be calculated from equation (21) using the uncertainty estimates for an ultrasonic meter and for the energy content measured by the energy meter module. We'll consider three different uncertainty levels for the ultrasonic meter.

- $\Delta Q_v / Q_v = \pm 1.00\%$ - dry-calibrated ultrasonic meter smaller than 12 inches in diameter.
- $\Delta Q_v / Q_v = \pm 0.70\%$ - dry-calibrated ultrasonic meter 12-inch diameter or larger.
- $\Delta Q_v / Q_v = \pm 0.30\%$ - ultrasonic meter that has been flow calibrated in a laboratory, as for example, at the GRI MRF.

**Table 10. Uncertainty estimates for the natural gas energy content, $\rho * H_m$.**

| *Uncertainty Source* | | *Base Value* | *Delta* | *Delta/Value* | *Sensitivity* | $U_{95\%}$ | *Units* |
|---|---|---|---|---|---|---|---|
| T | Temperature | 70°F | +/- 0.5°F | 0.00714 | -32.4 | -16.20 | Btu/ft$^3$ |
| P | Pressure | 620 psia | +/- 0.25 psi | 0.00040 | 76.85637 | 19.21 | Btu/ft$^3$ |
| S | Sound Speed | 1387.46 ft/s | +/- 0.5 ft/s | 0.00036 | -50.2703 | -25.14 | Btu/ft$^3$ |
| $X_{N2}$ | Nitrogen | 0.914424% | +/- 0.03% | 0.03281 | -683.404 | -20.50 | Btu/ft$^3$ |
| $X_{CO2}$ | Carbon Dioxide | 1.255016% | +/- 0.025% | 0.01992 | -1033.33 | -25.83 | Btu/ft$^3$ |
| $\Delta(\rho * H_m) = \pm 48.49$ Btu/ft$^3$ | | | | | | | |
| If $\rho * H_m$ = 45,183.09 Btu/ft$^3$, then $\Delta(\rho * H_m)/(\rho * H_m) = \pm 0.11\%$ | | | | | | | |

| *Uncertainty Source* | | *Base Value* | *Delta* | *Delta/Value* | *Sensitivity* | $U_{95\%}$ | *Units* |
|---|---|---|---|---|---|---|---|
| T | Temperature | 70°F | +/- 1.0°F | 0.01429 | -32.4 | -32.40 | Btu/ft$^3$ |
| P | Pressure | 620 psia | +/- 0.5 psi | 0.00081 | 76.85637 | 38.43 | Btu/ft$^3$ |
| S | Sound Speed | 1387.46 ft/s | +/- 1 ft/s | 0.00072 | -50.2703 | -50.27 | Btu/ft$^3$ |
| $X_{N2}$ | Nitrogen | 0.914424% | +/- 0.06% | 0.06562 | -683.404 | -41.00 | Btu/ft$^3$ |
| $X_{CO2}$ | Carbon Dioxide | 1.255016% | +/- 0.05% | 0.03984 | -1033.33 | -51.67 | Btu/ft$^3$ |
| $\Delta(\rho * H_m) = \pm 96.98$ Btu/ft$^3$ | | | | | | | |
| If $\rho * H_m$ = 45,183.09 Btu/ft$^3$, then $\Delta(\rho * H_m)/(\rho * H_m) = \pm 0.21\%$ | | | | | | | |

| *Uncertainty Source* | | *Base Value* | *Delta* | *Delta/Value* | *Sensitivity* | $U_{95\%}$ | *Units* |
|---|---|---|---|---|---|---|---|
| T | Temperature | 70°F | +/- 2.5°F | 0.03571 | -32.4 | -81.00 | Btu/ft$^3$ |
| P | Pressure | 620 psia | +/- 1.5 psi | 0.00323 | 76.85637 | 115.28 | Btu/ft$^3$ |
| S | Sound Speed | 1387.46 ft/s | +/- 2.0 ft/s | 0.00144 | -50.2703 | -100.54 | Btu/ft$^3$ |
| $X_{N2}$ | Nitrogen | 0.914424% | +/- 0.15% | 0.16404 | -683.404 | -102.51 | Btu/ft$^3$ |
| $X_{CO2}$ | Carbon Dioxide | 1.255016% | +/- 0.10% | 0.07968 | -1033.33 | -103.33 | Btu/ft$^3$ |
| $\Delta(\rho * H_m) = \pm 226.15$ Btu/ft$^3$ | | | | | | | |
| If $\rho * H_m$ = 45,183.09 Btu/ft$^3$, then $\Delta(\rho * H_m)/(\rho * H_m) = \pm 0.50\%$ | | | | | | | |

**Table 11. Pre-test uncertainty estimates for natural gas energy content, $(\rho * H_m)$.**

| *Uncertainty Source* | | *Base Value* | *Delta* | *Delta/Value* | *Sensitivity* | $U_{95\%}$ | *Units* |
|---|---|---|---|---|---|---|---|
| T | Temperature | 70°F | +/- 0.2°F | 0.00286 | -32.4 | -6.48 | Btu/ft$^3$ |
| P | Pressure | 620 psia | +/- 0.2 psi | 0.00032 | 76.85637 | 15.37 | Btu/ft$^3$ |
| S | Sound Speed | 1387.46 ft/s | +/- 1.5 ft/s | 0.00108 | -50.2703 | -75.41 | Btu/ft$^3$ |
| $X_{N2}$ | Nitrogen | 0.914424% | +/- 0.05% | 0.05468 | -683.404 | -34.17 | Btu/ft$^3$ |
| $X_{CO2}$ | Carbon Dioxide | 1.255016% | +/- 0.05% | 0.03984 | -1033.33 | -51.67 | Btu/ft$^3$ |
| $\Delta(\rho * H_m) = \pm 99.00$ Btu/ft$^3$ | | | | | | | |
| If $\rho * H_m$ = 45,183.09 Btu/ft$^3$, then $\Delta(\rho * H_m)/(\rho * H_m) = \pm 0.22\%$ | | | | | | | |

Table 10 showed that the uncertainty in natural gas energy content, $\Delta(\rho * H_m)/(\rho * H_m)$, would vary in the range from ±0.11% to ±0.50%. Table 11 gave an example of a pretest uncertainty analysis that calculated an uncertainty value of ±0.22% based upon realistic uncertainty estimates under good conditions in the GRI MRF HPL. Figure 22 shows a graph of the uncertainty in energy flow rate, $\Delta Q_{energy}/Q_{energy}$, as a function of the uncertainty in natural gas energy content, $\Delta(\rho * H_m)/(\rho * H_m)$, and the uncertainty in the actual volumetric flow rate, $\Delta Q_v/Q_v$.

For a flow calibrated ultrasonic meter with $\Delta Q_v/Q_v$ = ±0.30%, increasing the uncertainty in energy content from $\Delta(\rho * H_m)/(\rho * H_m)$ = ±0.11% to ±0.50% increases the uncertainty in energy flow from $\Delta Q_{energy}/Q_{energy}$ = ±0.32% to ±0.58%.

For an ultrasonic meter that was dry-calibrated with $\Delta Q_v/Q_v$ = ±0.70%, increasing the uncertainty in energy content from $\Delta(\rho * H_m)/(\rho * H_m)$ = ±0.11% to ±0.50% increases the uncertainty in energy flow only from $\Delta Q_{energy}/Q_{energy}$ = ±0.71% to ±0.86%.

Finally, for an ultrasonic meter that was dry-calibrated with $\Delta Q_v/Q_v$ = ±1.00%, increasing the uncertainty in energy content from $\Delta(\rho * H_m)/(\rho * H_m)$ = ±0.11% to ±0.50% increases the uncertainty in energy flow only from $\Delta Q_{energy}/Q_{energy}$ = ±1.01% to ±1.12%.

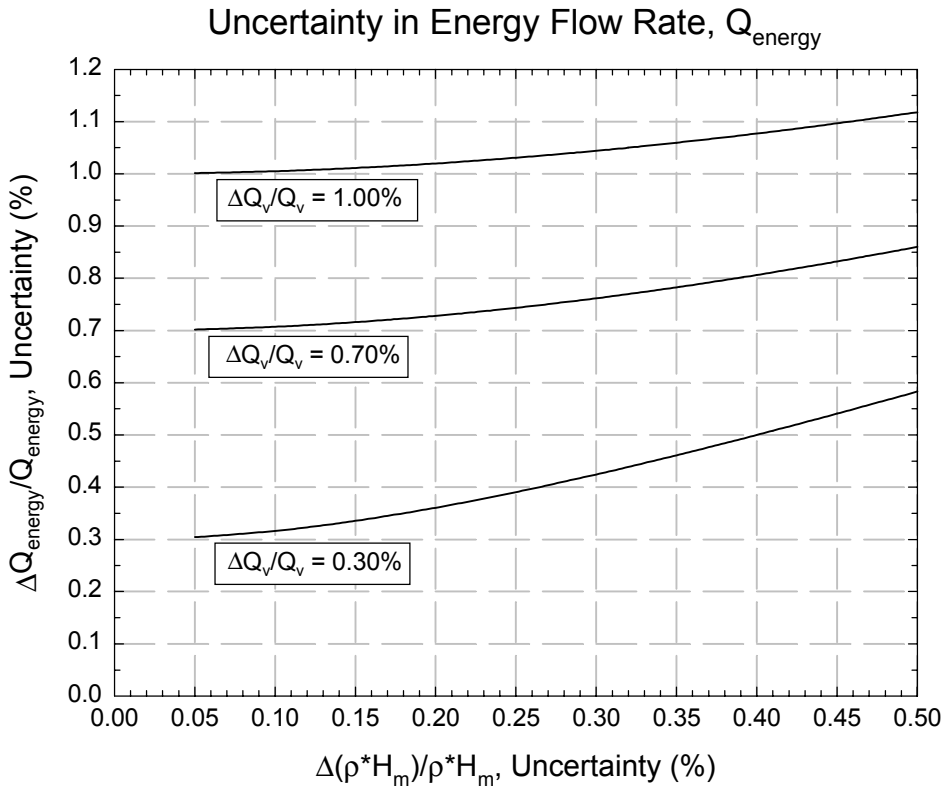


**Figure 22. Uncertainty in energy flow rate, $Q_{energy}$, as a function of the uncertainty in the actual volumetric flow rate, $Q_v$, and the uncertainty in natural gas energy content, $\rho * H_m$.**

*This page is intentionally blank.*

# 5.0 ENERGY METER MODULE DESIGN

## 5.1 Prior Development

Behring et al. (1999) presented the concept of a low-cost energy meter module that would be compatible with existing gas flow meters, e.g. orifice, turbine, ultrasonic and Coriolis meters, and would perform the measurements and calculations needed to quantitatively determine the heating value of the gas stream flowing through the meter. The most promising method evaluated by Behring et al. was to determine the heating value inferentially, by measuring the standard sound speed, the nitrogen and carbon dioxide concentrations, and using the Gross Characterization Method of AGA Report No. 8 (1994).

Behring et al. predicted that "dramatic cost savings over the traditional GC installations can … be achieved by determining new natural gas characterization correlations between properties that are required for energy measurement, and inferential properties that are measured with less costly sensors."

Behring et al. showed that it was feasible to measure the sound speed at standard temperature and pressure using ultrasonic transducers extracted from a Siemens ultrasonic flow meter produced for residential applications. The Siemens ultrasonic meter sells for about $100.

Behring et al. also showed that the carbon dioxide concentration in a natural gas mixture could be measured by a commercial non-dispersive infrared (NDIR) sensor such as the Vaisala Model GMM11C, which sells for about $400. Behring et al. did not identify a most promising route to measuring the nitrogen concentration. That effort was carried forward to the current project along with the objective to assemble instruments for all three measurements into a single package suitable for retrofitting into a natural gas metering station.

## 5.2 Advantages of Sensing at Low Pressure

One of the objectives of the current project was to develop a modification of the measurement methodology recommended by Behring et al. that would allow substituting the measured value of sound speed from an ultrasonic meter installed in a transmission gas pipeline for the sound speed measured at standard pressure and temperature. The extension of the measurement methodology to arbitrary pressure and temperature conditions is discussed in chapter 3 of this report.

This successful development caused us to question the advisability of measuring sound speed at standard temperature and pressure for other types of flow meters. The correlations based on sound speed at standard temperature and pressure had already been developed and published by Behring et al. However, since equivalent correlations could be developed for arbitrary pressure and temperature, it seemed pointless to design a gas sampling system with both pressure reduction and temperature control to maintain the thermodynamic state at 14.73 psia and 60°F.

The design team gave consideration to measuring sound speed, carbon dioxide and nitrogen concentration at the pipeline pressure and temperature. However, the inexpensive instruments for measuring speed of sound and carbon dioxide concentration identified by Behring et al. would have to be modified significantly to withstand pipeline pressure. For purposes of proof testing a prototype design, this would unnecessarily drive up the price and limit the accessibility of the instruments within a high pressure enclosure.

As a result, it was decided that a sample gas stream would be drawn from the pipeline and passed through a pressure reduction valve to reduce the gas stream pressure to a few psi above atmospheric pressure. The temperature and pressure of the gas stream would be measured with commercial transducers, and the sensor output signals converted to numerical values of temperature and pressure in the flow computer. With this technique, the temperature and pressure need not be controlled at 60°F and 14.73 psia, but the temperature and pressure do need to be measured to within typical field measurement accuracy.

The decision to use a sampled gas stream does raise two important issues that must be considered. The first issue is that the gas sampling equipment must be capable of delivering a sample stream whose composition is representative of the entire natural gas flow at the sampling location. Natural gas sampling equipment and procedures have been developed for dry natural gas streams, and these are commonly used in the field. This is not true for wet natural gas streams that consist of a flow of vapor and condensate as a two-phase mixture. The density and average molecular weight of the gas condensate phase is much different from that of the vapor phase. Proper sampling equipment and procedures that provide a representative sample of a two-phase natural gas mixture are not readily available.

The second issue is that the sampled natural gas mixture must not undergo condensation and become a two-phase mixture of vapor and condensate when the pressure is reduced. This stipulation requires more care. If the fluid stream can pass beyond the dew point line during depressurization, it will be necessary to pre-heat the gas stream to insure that condensation does not occur. A special procedure for gas sampling and sample stream treatment will be needed if condensation of the sampled gas stream is possible.

## 5.3 Module with Acoustic Sound Speed Sensing

Figure 23 is a photograph of the system developed for measuring the sound speed, carbon dioxide concentration, pressure and temperature of the natural gas mixture. Gas is drawn off from the pipeline in the vicinity of the flow meter, and is passed through a pressure reduction valve (not shown). The low pressure gas stream enters the energy meter module enclosure at the lower left of the photograph. The sampled gas stream flows into the speed of sound sensor, where the gas temperature and the gas temperature are measured using field grade natural gas smart transmitters. Upon leaving the speed of sound sensor, the sampled gas stream flows into and through the carbon dioxide sensor. On leaving the carbon dioxide sensor, the sampled gas stream exits at the upper left of center of the energy meter module enclosure.

Because neither a nitrogen sensor nor a system for determining the nitrogen concentration inferentially from other thermodynamic properties of the natural gas mixture has yet been identified, the nitrogen concentration was determined from a gas chromatograph analysis. The numerical value indicated by the gas chromatograph was entered directly into the Bristol Babcock flow computer shown in Figure 24.

Time did not permit programming a code in ACCOL for the flow computer to convert the signals from the ultrasonic transducer in the speed of sound sensor to sound speed readings. Therefore, a computer program in LabView was developed and run on a laptop PC located close to the energy meter module in the MRF LPL. The PC furnished a Modbus signal, similar in format to that produced by the Daniel model 3400 ultrasonic flow meter, that could be read directly by the Bristol Babcock flow computer.

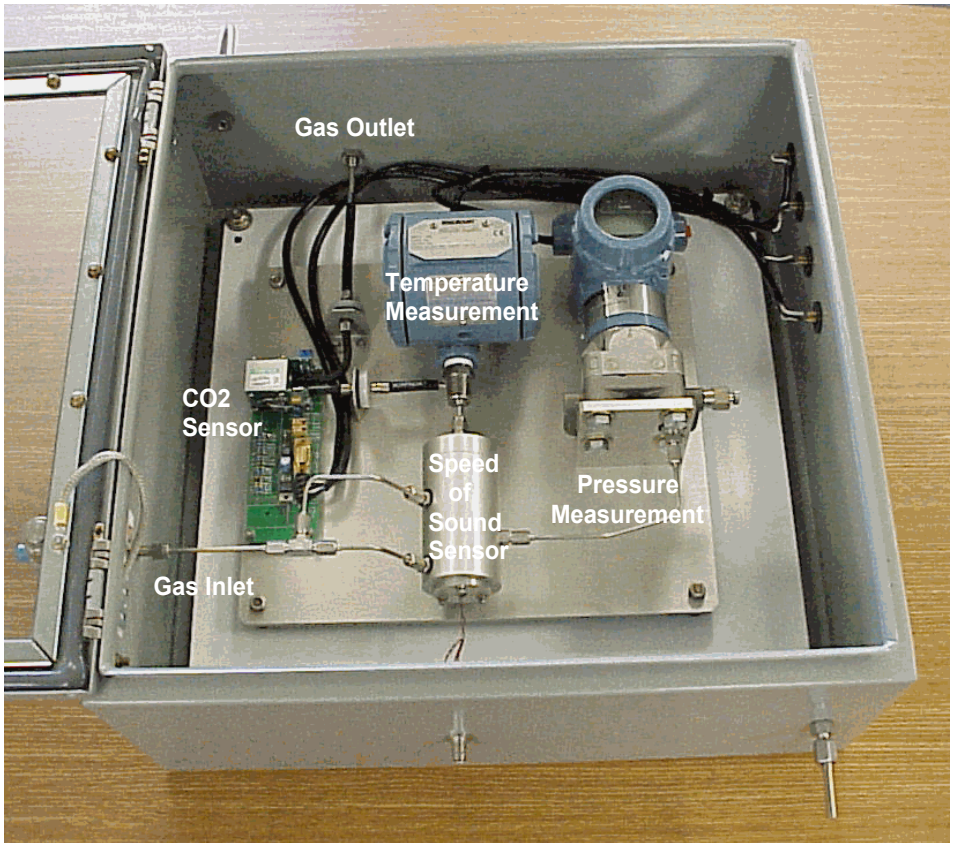


**Figure 23. Photograph of energy meter module components installed in low pressure enclosure.**

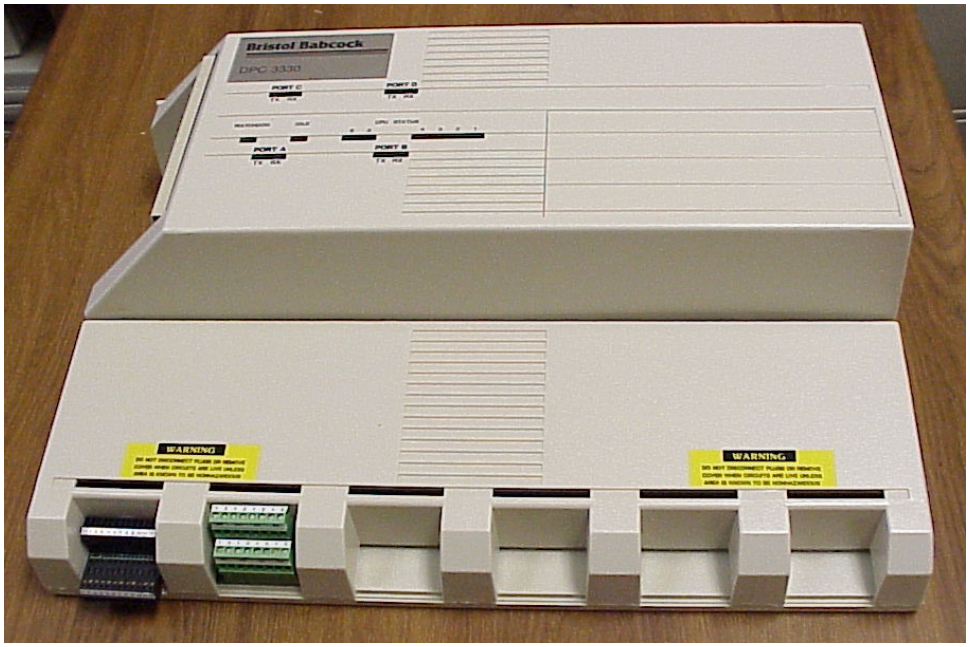


**Figure 24. Photograph of the Bristol Babcock flow computer.**

A version of the energy module computer program, translated into ACCOL, was loaded into the Bristol Babcock flow computer. This version of the code accepts values of the speed of sound and carbon dioxide concentration measured at the pressure and temperature in the energy meter module. Then, together with a value for the nitrogen concentration entered manually, the ACCOL computer code calculates the density and molecular weight of the gas in the energy meter module, the density, mass-based heating value, and standard volumetric heating value of the gas at standard temperature and pressure. Data for the orifice meter tube diameter and the orifice bore diameter are entered manually into the flow computer. Values of orifice meter static pressure (at the downstream pressure tap), the orifice meter pressure differential, and the orifice meter downstream static temperature are read by the flow computer from smart transducers installed in the LPL. Then the flow computer can calculate the gas density, the Reynolds number, the orifice coefficient, and the actual volumetric flow rate through the orifice meter. Finally, the flow computer calculates the product of the actual volumetric flow rate, the gas density, and the mass-based heating value to calculate the energy flow rate.

## 5.4 Module Compatible with Ultrasonic Flow Meter

An ultrasonic meter measures the speed of sound directly at pipeline pressure and temperature. The values of sound speed, pressure, and temperature can be read directly by the flow computer shown in Figure 24. The energy meter module shown in Figure 23 would still be used to measure the concentration of carbon dioxide. Therefore, a small sample gas stream would be taken from the pipeline, passed through a pressure reduction value, and allowed to flow into the energy meter module. Because the carbon dioxide sensor is sensitive to density, the pressure and temperature values measured in the energy meter module are used to correct the carbon dioxide reading to standard pressure and temperature. When a reliable system for determining nitrogen concentration is demonstrated, that system will also be placed within the energy meter module enclosure.

A second version of the energy meter module computer program, translated into ACCOL, was loaded into the Bristol Babcock flow computer. This version of the code accepts the speed of sound, actual volumetric flow rate (or at least the cross-sectional average velocity), pressure, and temperature from the ultrasonic flow meter. The computer program accepts the carbon dioxide concentration, and the pressure and temperature from the energy meter module. The value of nitrogen concentration is read from the gas chromatograph analysis and entered manually into the flow computer.

The flow computer program uses this information to calculate the gas density at pipeline conditions and the molecular weight of the gas mixture. Next, the value of standard sound speed is calculated, together with the mass-based heating value and the standard volumetric heating value. Finally, the flow computer calculates the energy rate as the product of the actual volumetric flow rate multiplied by the pipeline density and the mass-based heating value.

# 6.0 GAS SENSORS

## 6.1 Speed of Sound Measurement

There are several methods that can be used to measure the speed of sound in natural gas. The method selected for use on this project to develop an energy meter module is the ultrasonic method.

### 6.1.1 Ultrasonic Method

Ultrasound has a wide range application in medicine and nondestructive inspection of materials. This technique uses high frequency acoustic waves that are not audible to the human ears (typically the frequency range of 50 kHz to 50 MHz). Recently, the lower frequency ultrasonic technique is being used in natural gas industry to measure the gas flow rate.

The ultrasonic waves are usually generated and received by piezoelectric transducers. In this kind of transducer, the piezoelectric element generates mechanical vibration when charged. The same element can produce electric signals when impacted by ultrasonic waves. However, these ultrasonic transducers are capable of generating and receiving only a small range of frequencies. The piezoelectric element determines the frequency and other characteristics of a transducer.

Although ultrasound can easily propagate through solid materials, the low densities of gases provide a poor environment for ultrasonic propagation. The rate of absorption of ultrasound in gases increases with frequency. Thus, lower frequency ultrasonic transducers are used for propagation in gases (typically less than 1 MHz). On the other hand, low frequency ultrasound reduces the resolution and accuracy of the measurement. Therefore, a balance must be kept between adequate propagation and the degree of accuracy desired.

### 6.1.2 Speed of Sound Measurement Technique

Two methods can be used to measure the speed of sound in both solids and gases. The first approach is called pitch-catch method. In this method, two ultrasonic transducers are placed face-to-face in front of each other. One transducer is used to generate the ultrasonic waves, and the other transducer is used to receive them (see Figure 25). By knowing the distance between the two transducers and measuring the time it takes for the ultrasonic wave to travel from the generating transducer to the receiving transducer, one can determine the speed of sound on the medium between the two transducers. As shown in Figure 25, the transducers are separated by a known distance, $D$, and the time it takes for ultrasonic waves to travel from the transmitting transducer to the receiving transducer is measured to be $t$. Then, the speed of sound is calculated by:

$$S = D/t \tag{22}$$

where $S$ is the speed of sound in the medium between the two transducers. This method of measuring the speed of sound has the advantage of being very simple. Also, due to the fact that the ultrasonic signal travels directly from the transmitting transducer to the receiving transducer without any loss associated with reflections, the received signal is generally very strong.

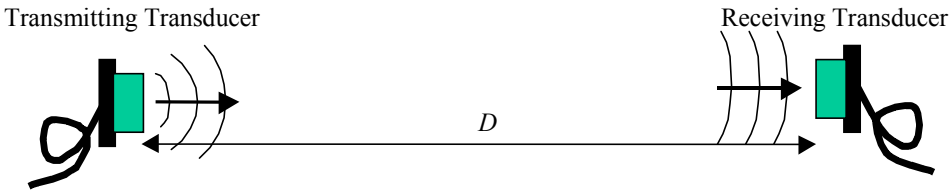


**Figure 25. Schematic drawing of the pitch-catch method.**

The other approach for measuring the speed of sound is called pulse-echo method. In this technique, a transducer is used as both the transmitter and the receiver. Figure 26 shows the schematic drawing of the pulse-echo technique. In the pulse-echo technique the generated wave is reflected back from a target with a known distance from the transducer, and is received by the same transmitting transducer. If the distance between the transducer and the target is $D$, and the measured time is $t$, then the speed of sound is calculated by:

$$S = 2D/t \tag{23}$$

This method is also very simple to apply and has the additional advantage of using only one transducer. However, due to the reflection of the ultrasonic beam from the reflector, some losses in the signal can occur.

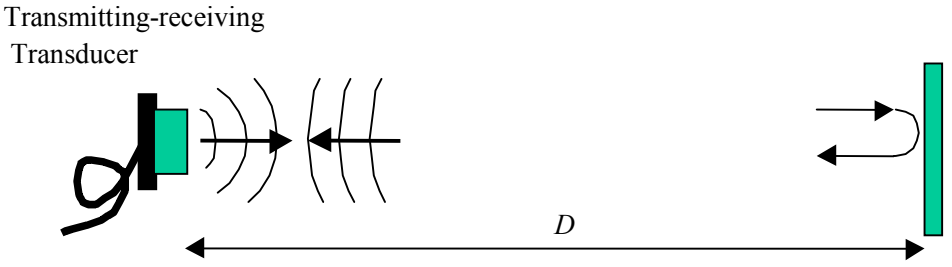


**Figure 26. Schematic drawing of the pulse-echo method.**

### 6.1.3 Time Delay Error

Both of the above methods can generate some inaccuracy in the speed of sound measurement. This inaccuracy mainly comes from the uncertainty in measuring the time of the received signal. The uncertainty in starting time of both initial pulse and the received signal produces this *time delay* error.

At the initial pulse, the starting point of the signal where time, $t$, is zero can not be determined accurately. Furthermore, the timing of the received waveform signal can not be measured accurately. Therefore, the uncertainty in these two measurements generates the time delay error.

To eliminate the time delay error, one can measure the time difference between the two received signals. Figure 27 shows the experimental setup for measuring the speed of sound using pulse-echo technique and reflections from two targets. In this method, the speed of sound is measured by:

$$S = 2D/\Delta t \tag{24}$$

where $D$ is the known distance between the two targets and $\Delta t$ is the time difference between the two received signals. By measuring this time difference, we eliminate the time delay error. This method has proven to be the most reliable way to measure the speed of sound accurately.

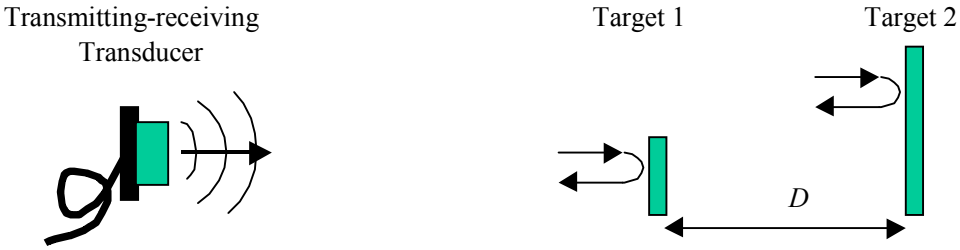


**Figure 27. Schematic drawing of the pulse-echo method using two reflectors.**

### 6.1.4 Chamber Design for SOS measurement

To measure the speed of sound of natural gas, a chamber was designed to have two reflectors. Figure 28 shows the schematic drawing of the chamber. The reflectors are two semi-circle faces of a cylinder that has been cut along the cylinder axis. The distance between the transducer and the front reflector is approximately 50 mm. This distance is not used in speed of sound measurement. However, the distance between the two reflectors was measured accurately. In our design the distance between the two targets were measured to be 25.451 mm.

The transducer used in this study has a nominal frequency of 200 kHz and was driven by a tone-burst signal generator. The pulser-receiver card that was used to drive the transducer and receive the reflected signals is a Matec TB1000 ISA card.

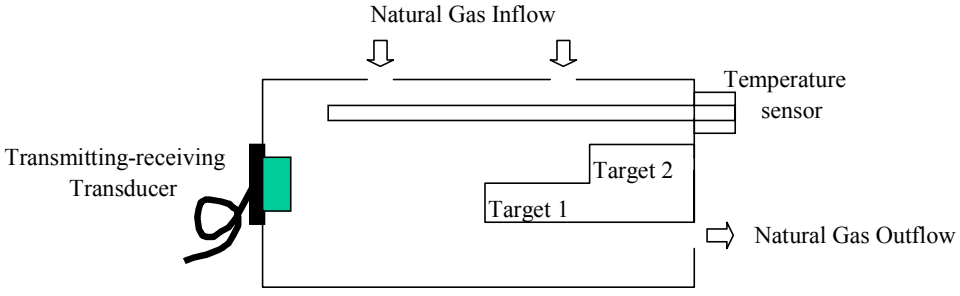


**Figure 28. Schematic drawing of the chamber.**

### 6.1.5 Time Measurement

To measure the time difference between the two reflected signals from the two targets, the following procedure was used. First, the waveform signal of the reflected waves is acquired. Figure 29 shows a typical waveform signal from the reflections of the two targets. The first signal in the waveform is the reflection from the front target (Target 1), and the second signal in the waveform is the reflection from back target (Target 2). To measure the time difference between these two signals, the first signal is correlated against the second signal. Figure 30 shows the correlation of these two signals. The point where the maximum correlation occurs determines the time difference between the two signals.

The correlation technique is accurate when the shapes of the two signals are not changed. If the shapes of the two signals change due to the absorption of ultrasound in natural gas, the correlation method can produce some uncertainty in the results. In our measurements, both signals retained their frequency contents, and the shapes of the two signals were similar.

## 6.2 Carbon Dioxide Concentration

The presence of carbon dioxide in a mixture of other gases may be directly sensed by its unique infrared absorption characteristics. Infrared radiation is the region of the electromagnetic spectrum with wavelengths ranging from about 0.1 cm (0.039 in.) to $7.0 \times 10^{-5}$ cm ($2.8 \times 10^{-5}$ in.). In terms of the wavenumber, which is the inverse of wavelength, the range is from 10 $cm^{-1}$ (26 $in^{-1}$) to 14,000 $cm^{-1}$ (36,000 $in^{-1}$). The region is bounded by microwaves on the low end and visible waves on the high end. Figure 31 shows the electromagnetic spectrum relative to other electromagnetic energy domains.

Infrared absorption characteristics of some gases may be exploited to measure concentration because (1) infrared signatures of some gases are unique, and (2) the level of absorption is related to the concentration present. A gas sample is exposed to infrared radiation (which may be broadband) at one end of a sample cell; then the intensity at a particular wavelength (wavenumber) is measured by a narrow-band detector at the other end of the cell. Absorption of infrared energy occurs when molecular vibrations are resonated by a particular wavelength (wavenumber). These absorbed wavelengths provide a "signature" of the molecule in the form of an absorption spectrum. Such a spectrum is summarized in Figure 32 for carbon dioxide. The most prominent absorption peak occurs at a wavenumber of about 2360 $cm^{-1}$. This is the principal wavenumber that is exploited by (infrared) carbon dioxide sensor manufacturers. The Vaisala GMM11 non-dispersive infrared (NDIR) carbon dioxide sensor is one such instrument.

Note that in Figure 32 that a transmittance of 1.0 means that the infrared energy passes without absorption.

Behring et al. (1999) reported the results of previous tests conducted at SwRI that used a Vaisala model #GMM11 NDIR carbon dioxide sensor with a design range of 0-10 mole% carbon dioxide. The results indicated that (1) no major interference bands were seen for the n-Paraffin hydrocarbons from methane to n-decane, and (2) the sensor predicted known concentrations of carbon dioxide to within about 0.2 mole%. This result established the general technical feasibility of using an NDIR carbon dioxide sensor.

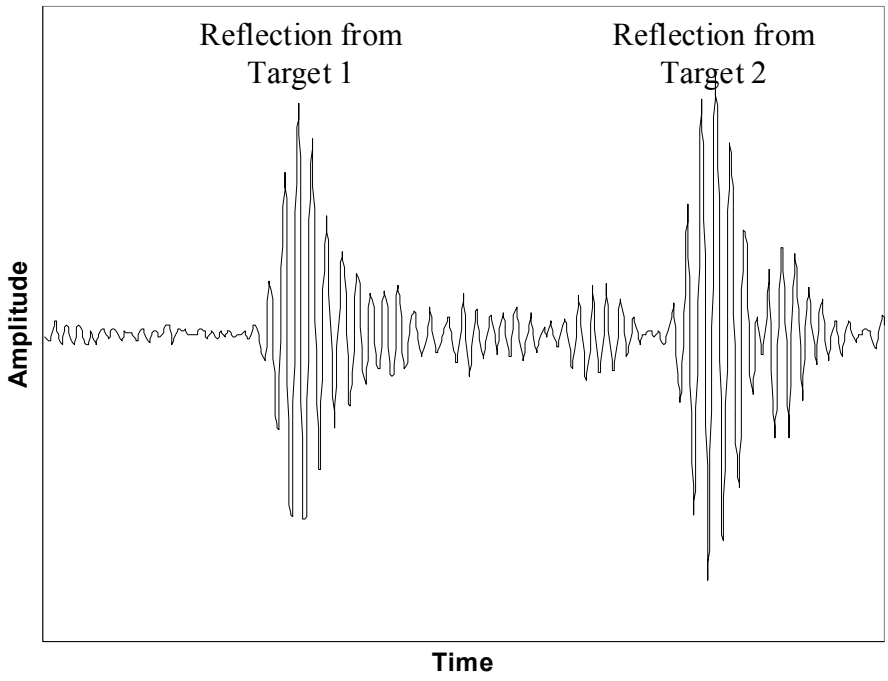


**Figure 29. The two reflected signals from target 1 and target 2.**

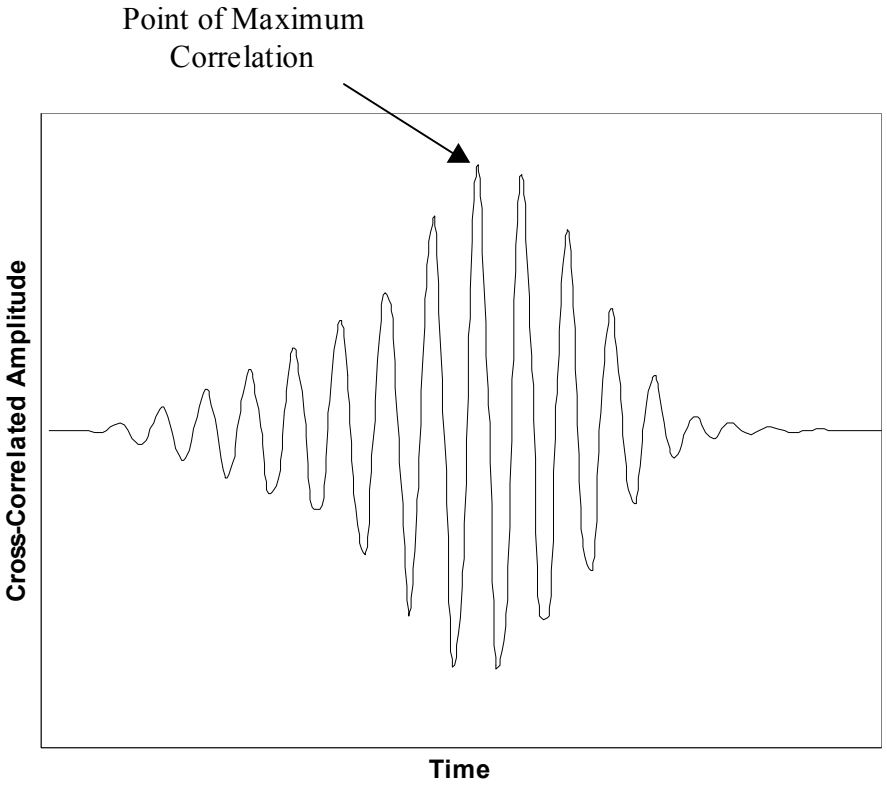


**Figure 30. The correlation signal between reflections of target 1 and target 2.**

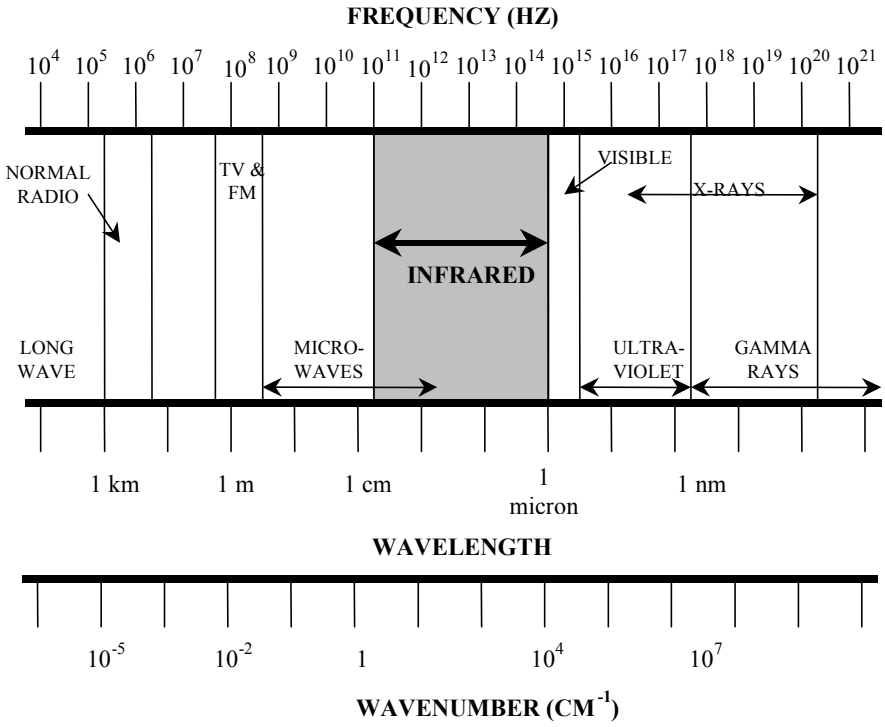


**Figure 31. The infrared region of the electromagnetic spectrum relative to other familiar wave regions.**

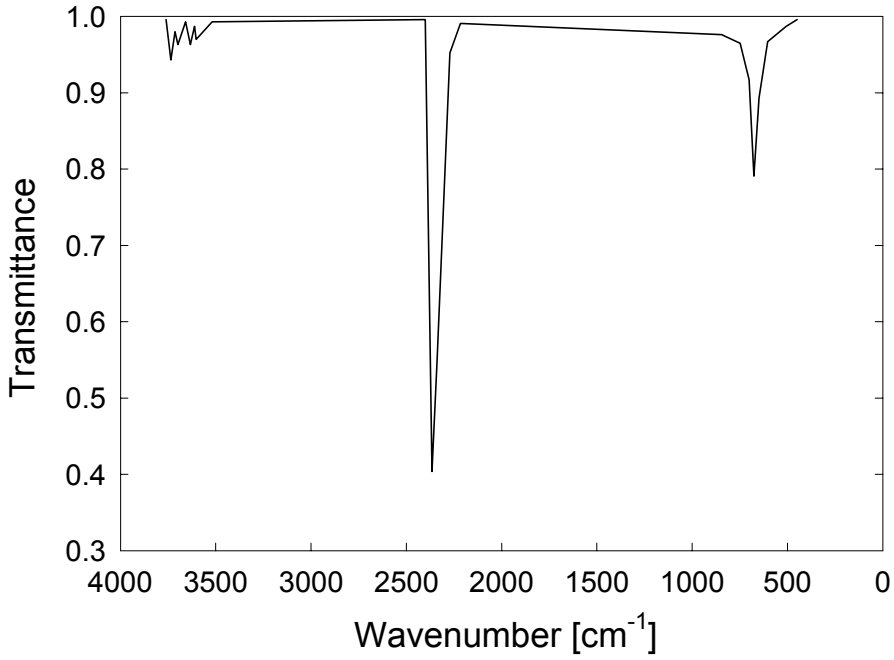


**Figure 32. The infrared absorption (transmittance) behavior of carbon dioxide, showing unique wavenumber regions that are preferentially absorbed by the gas.**

For the current project, a similar NDIR carbon dioxide sensor, the Vaisala model GMM12B, with a design range of 0 to 3 mole% carbon dioxide and 4-20 milliamp output was used.

## 6.3 Nitrogen Concentration

Behring et al. noted that the nitrogen concentration within a natural gas mixture is more difficult to measure directly than carbon dioxide. Nitrogen has low infrared absorption characteristics, and it is likely that infrared sensor technology will not work. Nitrogen is relatively inert chemically, and electrochemical sensors will not work either. Behring et al. estimated that the nitrogen concentration would have to be determined to within ±0.3 mole% for a 0.5% shift in the mass-based heating value or the density. In fact, Figure 19 shows that a ±0.3 mole% shift in nitrogen concentration will produce an equivalent shift of ∓0.5% in the product of the mass-based heating value and the gas mixture density.* Behring et al. claimed that the standard volumetric heating value was insensitive to the nitrogen concentration. This claim is contradicted by Figure 14, which shows that a ±0.075 mole% shift in nitrogen concentration will produce a ∓1.0 Btu/SCF shift in standard volumetric heating value.

Behring et al. suggest that direct measurement of nitrogen may not be necessary and that indirect methods for determining nitrogen concentration should be considered. These methods require either that measurements be made at two thermodynamic states or that another thermodynamic property, such as a specific heat, be measured. Both schemes have been investigated, although neither has lead to a workable experimental system at this time.

### 6.3.1 Molecular Weight at Two Thermodynamic States

This scheme would be the easiest to implement because only the pressure, temperature, carbon dioxide concentration, and speed of sound are measured. Because measurements are required at two different thermodynamic states, some method is needed to control either the pressure or temperature. Since the pressure upstream of the energy meter module is set and controlled by a pressure regulation valve, it should be feasible to select two different pressures.

Equation (13) is the key to this method.

$$MW_{calc} = \left( A_{MW} + B_{MW}/S + C_{MW}/S^2 \right) * \left(1 + D_{MW} * X_{CO2} + E_{MW} * X_{N2}\right) \qquad (13)$$

where $D_{MW} = D_{MW1} + D_{MW2}/S + D_{MW3}/S^2$, and $E_{MW} = E_{MW1} + E_{MW2}/S + E_{MW3}/S^2$.

The coefficients in this equation, such as $A_{MW}$, are functions of the temperature and pressure, and can be calculated for two thermodynamic states, *State One* and *State Two*. Values of sound speed, $S$, are measured for both states. The value of carbon dioxide concentration, $X_{CO2}$, is expected to be the same at both states, as are the nitrogen concentration, $X_{N2}$, and the molecular weight, $MW_{calc}$. Therefore, we have two independent equations for molecular weight that can be solved for the nitrogen concentration, $X_{N2}$.

---

*An increase (positive shift) in nitrogen concentration reduces (produces a negative change) in the product of the mass-based heating value and the density, and vice-versa.

It seems reasonable to suppose that the two equations for $MW_{calc}$ will be independent as long as the coefficients are sufficiently different. If *State One* and *State Two* were adjacent to each other, the coefficients would be nearly identical and the solution for $X_{N2}$ would be indeterminate. A series of calculations was performed with varying conditions for *State One* and setting *State Two* to be $P_2$ = 14.73 psia and $T_2$ = 60°F. The temperature at *State One* was taken to be either $T_1$ = 70°F, $T_1$ = 65°F, or $T_1$ = 60°F. The pressure $P_1$ was allowed to take different values between $P_1$ = 14.73 psia and $P_1$ = 200 psia. The results of the calculations are shown in Figure 33. $P_1$ must be at least 50 psia, and preferably greater than 100 psia for the value of $X_{N2}$ to be within ±0.3 mole% of the correct value.

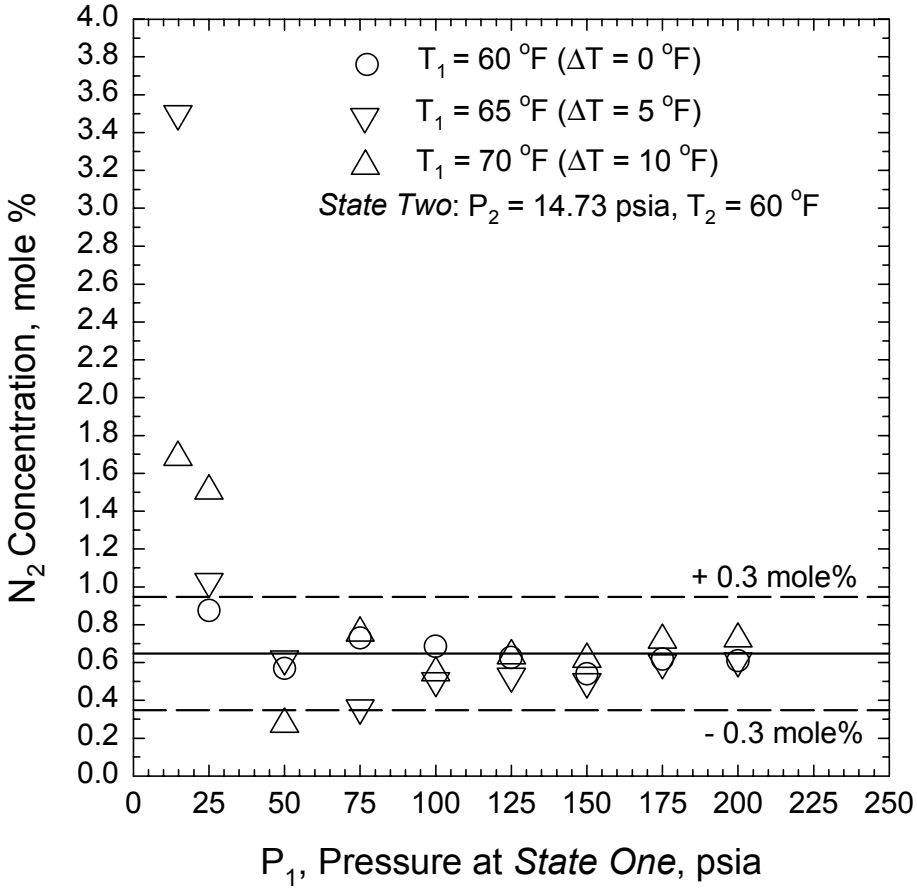


**Figure 33. Nitrogen concentration calculated from speed of sound measurements at two thermodynamic states.**

At first glance, this appears to be a promising method. Unfortunately, the "scatter" shown in Figure 33 is caused by numerical round-off error when the values of $S_1$, $S_2$, and $X_{CO2}$ are known as accurately as possible. For this procedure to calculate the nitrogen concentration correctly, the values of sound speed at *State One* and *State Two* and the value of $X_{CO2}$ should be known as accurately as possible. Experimental uncertainty in the values of sound speed and/or in the measured value of $X_{CO2}$ may produce physically unrealistic values for $X_{N2}$.

For example, consider a hydrocarbon gas mixture with a carbon dioxide concentration of $X_{CO2}$ = 1.042910 mole%, and a nitrogen concentration of $X_{N2}$ = 0.646753 mole%. *State One* is $P_1$ = 200 psia and $T_1$ = 60°F, where the speed of sound is $S_1$ = 1406.8 ft/s. *State Two* is $P_2$ = 14.73 psia and $T_2$ = 60°F, where the speed of sound is $S_2$ = 1422.3 ft/s. Using these values of $S_1$, $S_2$, and $X_{CO2}$, we can calculate a value of $X_{N2}$ = 0.608637 mole%. The error is –0.038116 mole%, well within the desired uncertainty of ±0.30 mole%. However, if the sound speed at *State One* is measured to be $S_1$ = 1407.3 ft/s (0.5 ft/s higher than the actual value), then the calculated value of the nitrogen concentration becomes $X_{N2}$ = 1.400631 mole%, an error of +0.753878 mole% and well outside the desired uncertainty interval. If the sound speed at *State One* is measured to be $S_1$ = 1406.3 ft/s (0.5 ft/s lower than the actual value), then the calculated value of the nitrogen concentration becomes $X_{N2}$ = -0.18114 mole%, an error of –0.827893 mole%. Not only is the error outside the desired uncertainty interval, the negative value calculated for $X_{N2}$ is physically impossible. Figure 34 shows the variation of the calculated value of $X_{N2}$ as a function of the error in the measured value of sound speed at *State One*. We can conclude that the sound speed measurement would have to have an uncertainty of ±0.2 ft/s or less for the uncertainty in nitrogen concentration, $\Delta X_{N2}$, to be within ±0.3 mole%. The uncertainty in sound speed measurement of current ultrasonic meters is within the range of ±1 ft/s to ±2 ft/s, approximately one order of magnitude larger than that required for the inferential measurement of nitrogen concentration.

### 6.3.2 Determining Temperature Rise After Heating

Behring et al. discussed the discussed the potential for the indirect determination of nitrogen concentration by correlating the isentropic exponent, $k_{std}$, at standard temperature (60°F) and standard pressure (14.7 psia) to the inferential variables, $S_{std}$, $X_{CO2}$, $X_{N2}$, and $S_{std}$. For an ideal gas, the isentropic exponent is the same as the ratio of the specific heats at constant pressure and constant volume, $k = c_p / c_v$. The ideal gas assumption is reasonable in the region of low pressure and high temperature, well away from the dew point line for a natural gas mixture.

The Lomic SonicWare® (1997) computer program was used to calculate values of $c_p$, $c_v$ and sound speed, $S_{std}$, for 86 distinct natural gas compositions at standard temperature and pressure. Values of $k_{std}$ were calculated simply as the ratio of the two specific heats. Figure 35 is a graph of $k_{std}$ as a function of standard sound speed. For diluent concentrations less than 2%, $k_{std}$ varies in an approximately linear manner as a function of standard sound speed. For diluent concentrations greater than 3%, values of $k_{std}$ are about 1% higher.

Since $k_{std}$ varies with the diluent concentrations, both $c_p$ and $c_v$ at standard temperature and pressure must also vary with the diluent concentration. The values of $c_v$ and $c_p$ calculated by the Lomic SonicWare software are plotted against the standard sound speed in Figure 36a and Figure 36b below. Note that the darkened symbols represent gas mixtures with total diluent concentrations that exceed 4%. The specific heat values calculated by Lomic SonicWare have units of Btu/lbmole*$^o$F. To express the specific heat in units of Btu/lbmass*$^o$F, the calculated values must be divided by the molecular weight of the gas mixture. Note that increasing the diluent concentration reduces the specific heat values. However, it has the effect of increasing $k = c_p / c_v$. The values of $c_v$ and $c_p$ are approximately 5% to 6% lower for $X_{N2}$ and $X_{CO2}$ concentrations in the range of 5%.

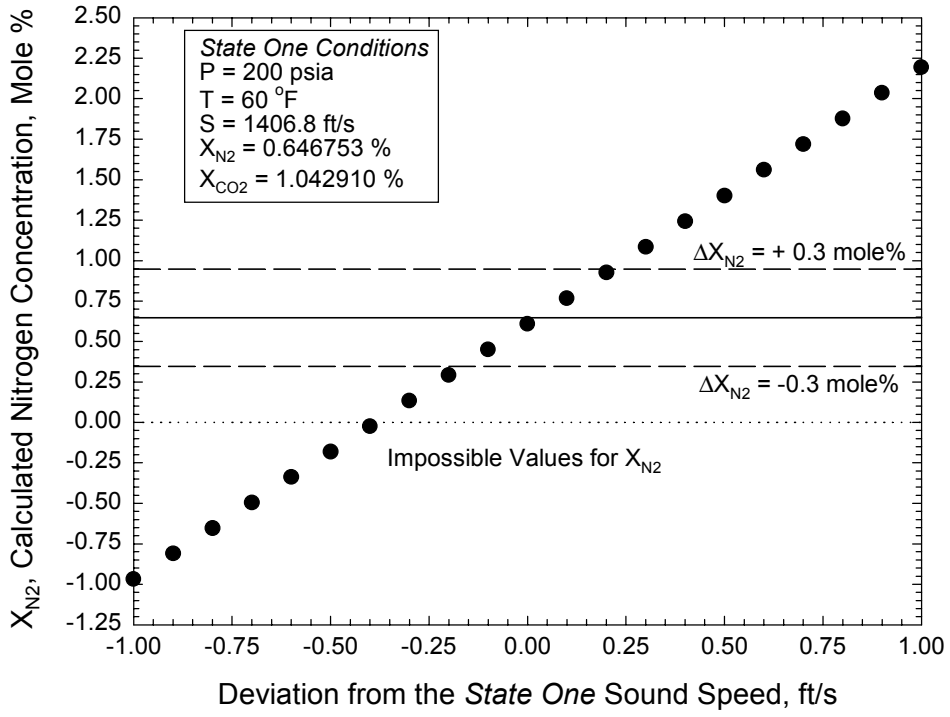


**Figure 34. Sensitivity of the nitrogen concentration calculated from speed of sound measurements at two thermodynamic states to an error in the measured value of sound speed at *State One*.**

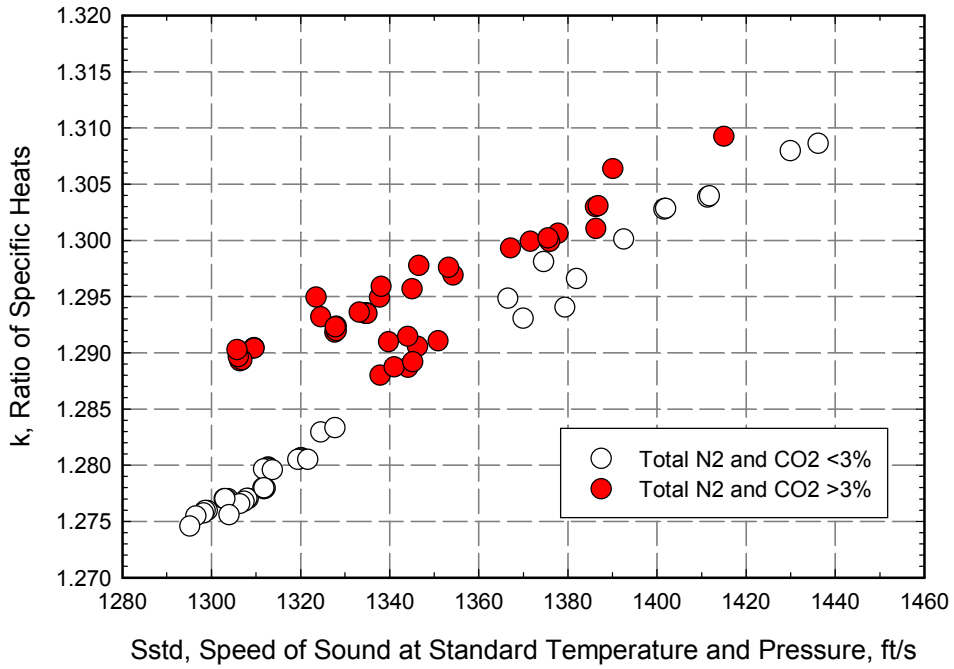


**Figure 35. Graph of the ratio of specific heats, $k_{std}$, versus sound speed at standard temperature and pressure.**

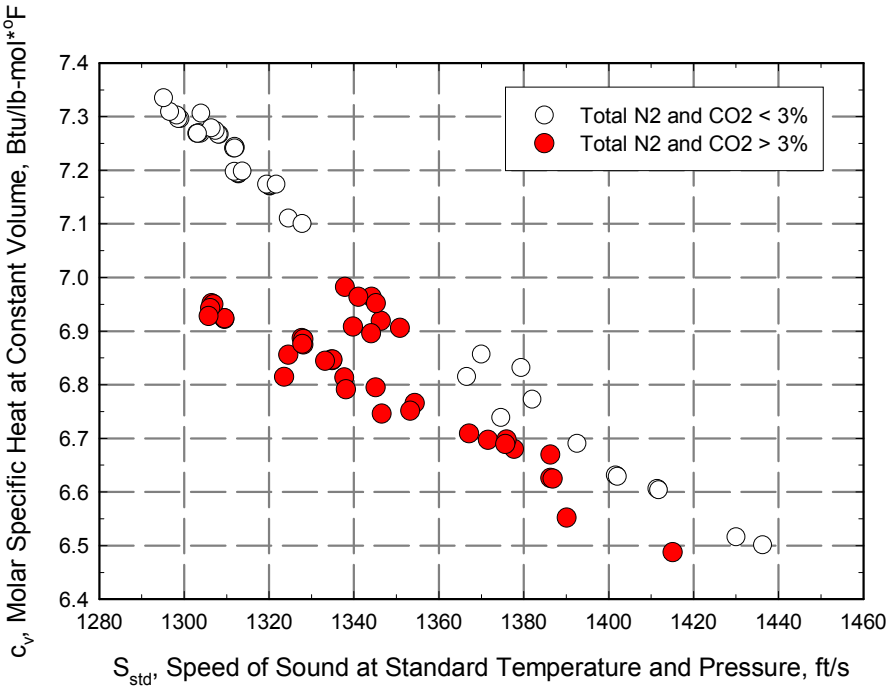


**Figure 36a. Graph of $c_v$, specific heat at constant volume, versus sound speed at standard temperature and pressure for 86 distinct mixtures of paraffin hydrocarbons, nitrogen, and carbon dioxide.**

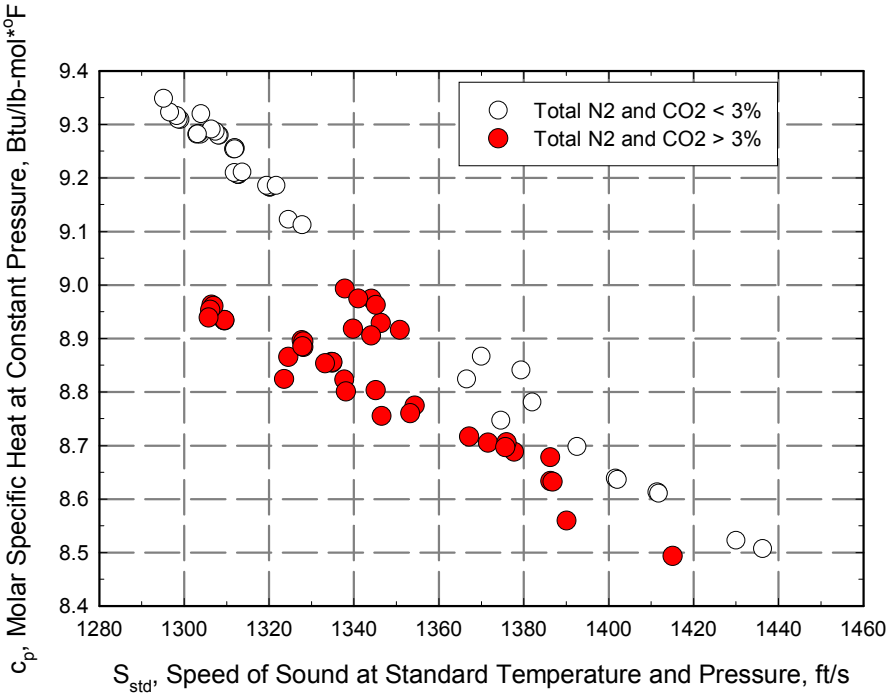


**Figure 36b. Graph of $c_p$, specific heat at constant pressure, versus sound speed at standard temperature and pressure for 86 distinct mixtures of paraffin hydrocarbons, nitrogen, and carbon dioxide.**

The measurement of thermodynamic properties such as $k$, $c_p$, and $c_v$ is not necessarily straightforward. The property values at standard temperature and pressure are obviously functions of standard sound speed and diluent concentration. But in order to infer the nitrogen concentration, $X_{N2}$, we need a property or a combination of properties that can be measured simply and inexpensively. One route that may work is to infer the nitrogen concentration from the product of the standard density and the standard specific heat at constant volume.

Suppose that we fill a container with a gas mixture at standard temperature and pressure. The mass of the gas mixture inside the container is $m = V * \rho_{std}$ where $V$ is the container volume in units of ft$^3$, and $\rho_{std}$ is the gas mixture density in units of lbmass/ft$^3$. Next, we heat the gas using an electrical heater to raise the temperature by $\Delta T$. The quantity of electrical energy used to heat the gas can be measured as the product of the voltage across the heater times the electrical current through the heater times the duration of heating in seconds. The gas in the container will be heated at constant volume, and the gas pressure will rise slightly as a result of the temperature rise. The gas density within the container will not change since neither the container volume nor the mass of the gas has been changed. The amount of heat energy, $Q$, added to the gas in the container (neglecting losses through the cylinder wall) will be: $Q = \rho_{std} * V * (c_v / MW) * \Delta T$. If we measure $Q$, the quantity of heat energy dissipated, and measure $\Delta T$, the temperature rise of the gas, then since we know the volume of the container:

$$\left( \rho_{std} * {c_v}/{MW} \right) = {Q}/{(V * \Delta T)} \tag{25}$$

In order to use this equation, we need to show that the product of $(\rho_{std} * c_v / MW)$ is a function of standard sound speed and diluent concentration. Figure 37 shows the values for the product of the standard density and the specific heat at constant volume for the 86 distinct gas mixtures in Table 1. It is apparent that this product does vary with standard sound speed, and that the values are affected by the diluent concentration.

We can model the variation of the quantity $(\rho_{std} * c_v / MW)$ product as a function of the standard sound speed and the diluent concentrations. The model parameters can be determined by regression analysis.

$$\left( \rho_{std} * {c_v}/{MW} \right) = A + {B}/{S_{std}} + {C}/{S_{std}^{\,2}} \tag{26}$$

where

$$A = A_0 + A_1 * X_{N2} + A_2 * X_{CO2}$$
$$B = B_0 + B_1 * X_{N2} + B_2 * X_{CO2}$$
$$C = C_0 + C_1 * X_{N2} + C_2 * X_{CO2}$$

The regression fit feature in SigmaPlot® 5.0 (1998) was used to calculate values for the nine regression parameters. The values are:

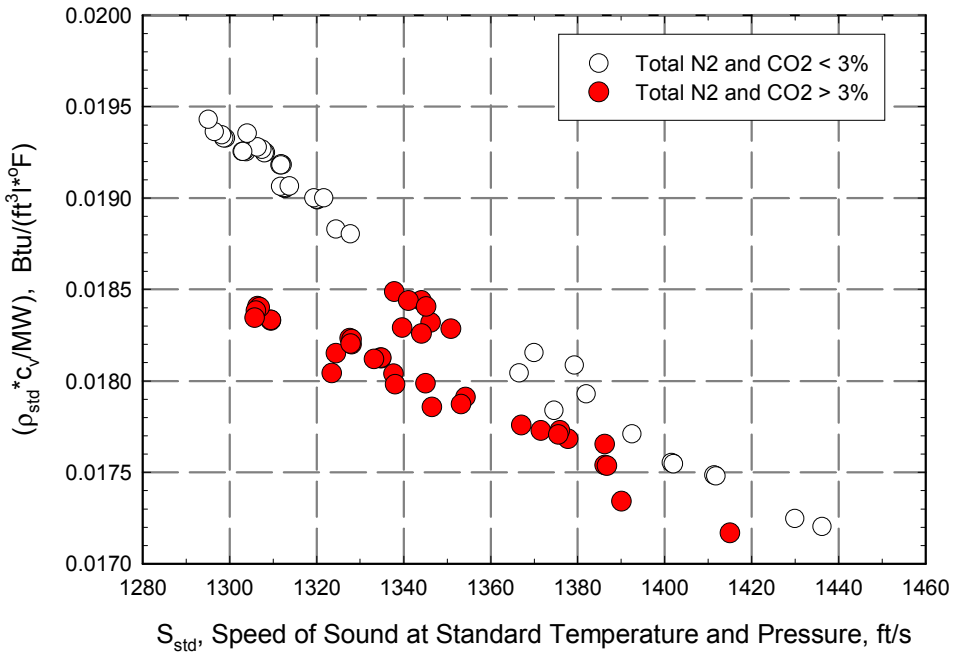


**Figure 37. Graph of the product of density and specific heat at constant volume at standard temperature and pressure versus sound speed at standard temperature and pressure for 86 distinct mixtures of paraffin hydrocarbons, nitrogen, and carbon dioxide.**

$$A_0 = 0.00248359\,,\ A_1 = 0.000475082\,,\ A_2 = 0.000653587$$

$$B_0 = 11.0257\,,\ B_1 = -1.67547\,,\ B_2 = -2.3125$$

$$C_0 = 14707.8\,,\ C_1 = 1185.97\,,\ C_2 = 1598.$$

Now, the regression model can be rearranged to predict the value of nitrogen concentration given values for the standard sound speed and the concentration of carbon dioxide.

$$X_{N2} = \frac{\left[\left(Q/V * \Delta T\right) - \left(A_0 + B_0/S_{std} + C_0/S_{std}^{\,2}\right) - X_{CO2} * \left(A_2 + B_2/S_{std} + C_2/S_{std}^{\,2}\right)\right]}{\left(A_1 + B_1/S_{std} + C_1/S_{std}^{\,2}\right)} \qquad (27)$$

This equation may be used to determine nitrogen concentration from measurements of (1) the amount of energy transferred as heat to the gas mixture, (2) the volume of the container, (3) the temperature rise of the gas mixture before and after heating, (4) the standard sound speed, and (5) the concentration of carbon dioxide. The effectiveness of this approach is shown in Figure 38. Actual values of the product $(\rho_{std} * c_v / MW)$, actual values of standard sound speed, and actual values of carbon dioxide concentration were used to calculate values of nitrogen concentration using the inferential equation given above for 86 distinct gas mixtures. The calculated values of nitrogen concentration are compared to the actual value of nitrogen concentration for each gas mixture. Agreement between the calculated and the actual values is good.

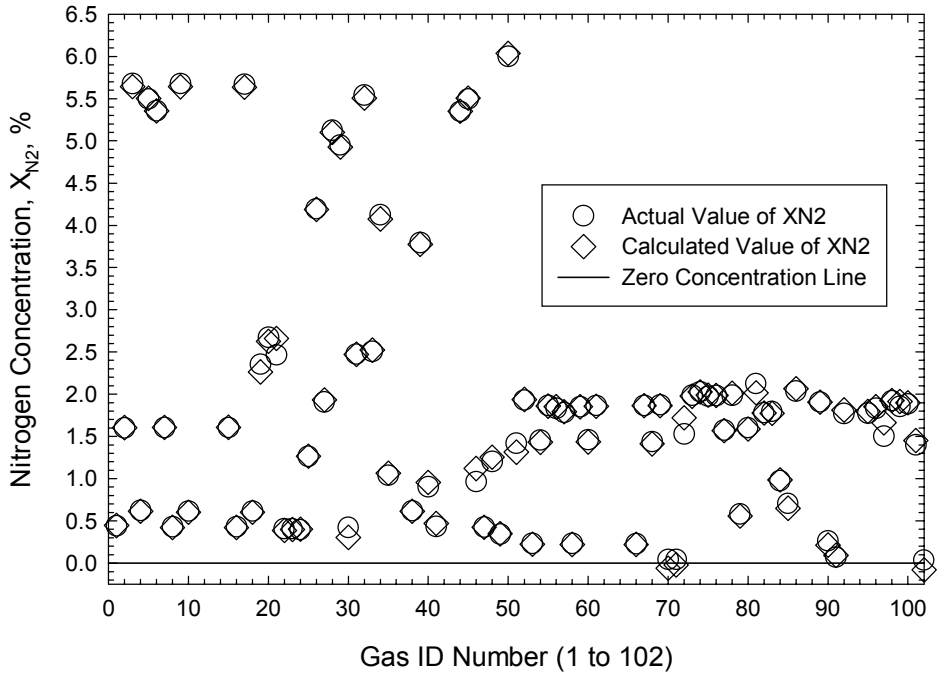


**Figure 38. Graph of actual and predicted values of nitrogen concentration for 86 distinct mixtures of paraffin hydrocarbons, nitrogen and carbon dioxide.**

A very similar inferential procedure may be developed on the premise that the natural gas mixture flows through a heating tube in steady flow and the steady state temperature rise is measured. In both methods, some of the energy transferred from the heating coil may be transferred to the container or heating tube and not to the gas mixture. This parasitic loss should be minimized if possible, and/or "calibrated out" of the data reduction equation (27) so that $Q$ represents only the heat energy transferred to the gas. The final development of an inferential procedure for the determination of nitrogen concentration must include an analysis of the effects of the uncertainty in the experimental measurement of sound speed and carbon dioxide concentration.

# 7.0 MRF TESTS OF ENERGY METER MODULE

The energy meter module, shown in Figure 23, was fabricated, assembled, and checked out in mid-May. All testing was performed outdoors during hot weather in San Antonio, Texas, with ambient air temperatures that exceeded 90ºF.

The evaluation of the energy meter module performance was initiated in conjunction with a scheduled test on a different flow meter installed in the High Pressure Loop (HPL) test manifold.

- **Test 1** - Test the Bristol Babcock flow computer and the energy meter module algorithm with a 12-inch ultrasonic flow meter shown in Figure 39. The ultrasonic flow meter furnishes three digital Modbus coded signals for (1) speed of sound, (2) pipeline pressure, and (3) pipeline temperature. Values of (4) carbon dioxide concentration, and (5) nitrogen concentration will be read separately from the MRF gas chromatograph and input manually into the flow computer. The flow computer will perform the calculations for standard volumetric heating value. This value will be compared to the value computed from the detailed gas composition measured by the gas chromatograph.

Tests with a 4-inch diameter Daniel Senior fitting orifice meter were scheduled in the Low Pressure Loop (LPL) for the week of Tuesday, May 30, following the Memorial Day Holiday. These tests were designed to evaluate the ability of the energy meter module to determine the carbon dioxide concentration, the natural gas heating value, and the energy flow rate. The orifice meter test plan called for:

- **Test 2** - Test the ability of the energy meter module to produce an analog signal proportional to the carbon dioxide concentration in a sample of gas taken under pressure from the LPL. The carbon dioxide concentration measured by the energy meter module will be compared to the concentration indicated by the MRF gas chromatograph.
- **Test 3** - Test the Bristol Babcock flow computer, the energy meter module speed of sound sensor and the energy meter module algorithm with a 4-inch orifice flow meter shown in Figure 40. The speed of sound sensor shown in Figure 23 sends its signals to a laptop computer that, in turn, sends a Modbus coded signal to the Bristol Babcock flow computer. Therefore, the flow computer will receive a digital Modbus signal for speed of sound, and two analog signals for (2) pressure and (3) temperature in the energy meter module. Values of (4) carbon dioxide concentration, and (5) nitrogen concentration will be read separately from the MRF gas chromatograph and input manually into the flow computer. The flow computer will perform the calculations for standard volumetric heating value. This value will be compared to the value computed from the detailed gas composition measured by the gas chromatograph.
- **Test 4** – Repeat Test 3 with the analog signal for carbon dioxide concentration from the energy meter module replacing the manually input value from the gas chromatograph in Test 3.
- **Test 5** – Repeat Test 4, but provide the Bristol Babcock flow computer with additional analog signals for (6) static pressure measured at the downstream pressure tap of the orifice meter, (7) differential pressure measured between the upstream and downstream pressure taps of the orifice meter, and (8) static temperature measured downstream of the orifice plate. The energy meter module algorithm will calculate the standard volumetric heating value, as

in Tests 3 and 4, but will also calculate the natural gas density upstream of the orifice plate. The flow computer will calculate the volumetric flow rate through the orifice meter and will multiply it by the calculated values of density and mass-based heating value to calculate the energy flow rate.

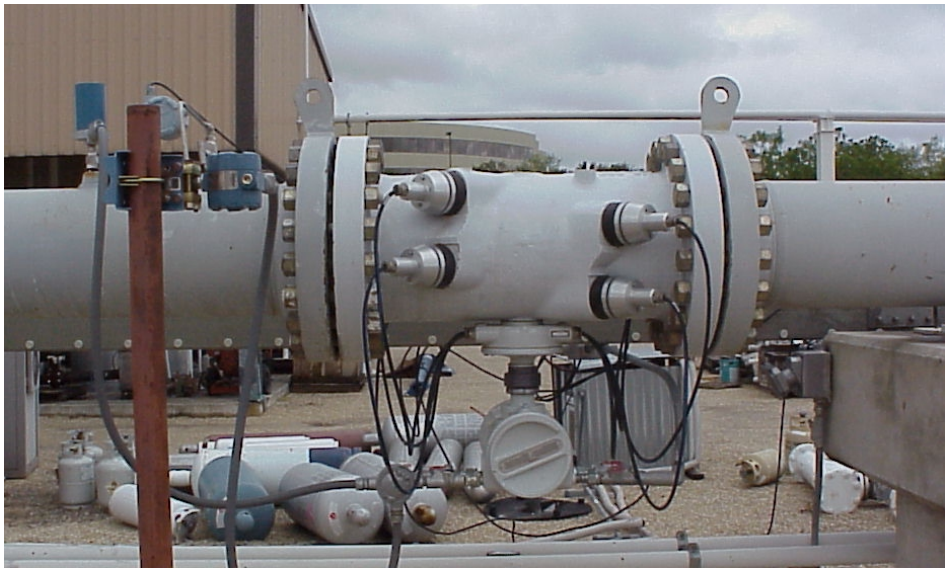

**Figure 39. Daniel Model 3400 ultrasonic flow meter.**

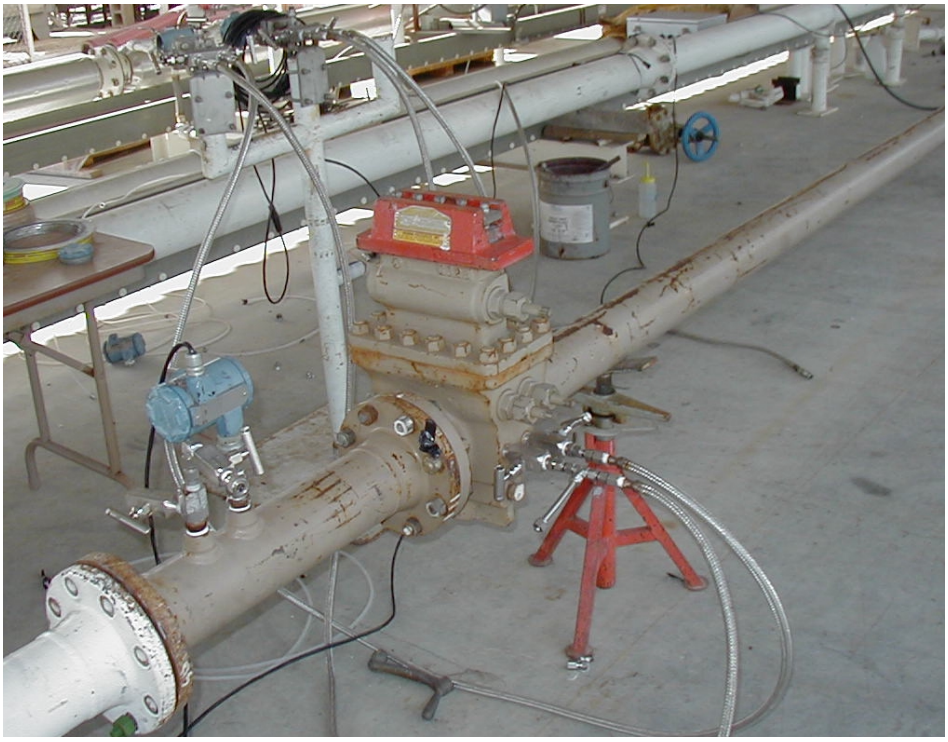

**Figure 40. Four-inch diameter orifice meter installed in MRF LPL for test of the energy meter module.**

Test 1 was performed on June 1st. Test 2 was performed in the LPL during the week of June 12th. Tests 3, 4, and 5 were combined and modified due to the outcome of preliminary testing. Section 7.2 includes a discussion of the changes in the test plan.

## 7.1 Test with 12-inch Daniel Model 3400 Ultrasonic Flow Meter

Energy meter module performance tests were scheduled to be performed during the week of May 22nd with a Daniel 3400 ultrasonic flow meter (see Figure 39) installed in the reference leg of the GRI MRF High Pressure Loop. On May 22nd, the ACCOL software for the energy meter module was loaded into the Bristol Babcock flow computer. A Modbus communication line linked the flow computer to the ultrasonic flow meter. Surprisingly, the flow computer would not communicate with the flow meter, and no data were acquired. The data communication problem resisted solution at the MRF, and the Bristol Babcock engineer returned to his office with the flow computer to run additional checks.

After consulting with the ultrasonic flow meter manufacturer, the Bristol Babcock engineer was able to resolve the communication problem on May 31st. He returned to the MRF the next day and communication was established successfully between the Daniel ultrasonic flow meter in the HPL and the flow computer on June 1st. Two limited sets of data were acquired on June 1st with the Daniel ultrasonic flow meter.

During the morning of June 1st, gas flowed through the Daniel ultrasonic flow meter while an unrelated test was performed on another flow meter in the HPL test section manifold. Table 12 shows one set of pressure, temperature and sound speed values that was recorded by hand, together with the value of standard volumetric heating value calculated by the energy meter module computer code. Values of nitrogen and carbon dioxide concentration were taken from the detailed gas composition printout from the gas chromatograph at 10:30 a.m. Lomic SonicWare® (1997) was used to calculate a value for the sound speed of 1386.01 ft/s using the detailed gas composition from the gas chromatograph and the measured values of temperature and pressure. This value is within ±1 ft/s of the value measured by the ultrasonic flow meter at the same value of temperature and pressure. The value of standard volumetric heating value determined by the gas chromatograph was 1009.4 Btu/SCF. This value is slightly outside an interval of ±1 Btu/SCF from the value calculated by the energy meter module algorithm.

**Table 12. HPL data recorded under flowing gas conditions on June 1, 2000.**

| *Temperature, (°F)* | *Pressure, (psia)* | *Sound Speed, (ft/s)* | *$H_v$, (Btu/SCF)* |
|---|---|---|---|
| 70.27 | 665.4 | 1386.95 | 1008.4 |

A second set of data was taken later in the day on June 1st using the data logging feature of the flow computer. Unfortunately, gas was not being circulated through the HPL at the time because a new flow meter was being installed in the HPL test manifold. The data that were collected under zero flow conditions are shown in Table 13 and in Figures 41a and 41b. During this period the temperature recorded at the ultrasonic meter increased from 80.5°F to 84.6°F, the gas pressure increased by 1.7 psia, and the sound speed increased from 1403.26 ft/s to 1408.52 ft/s. However, as Figure 41b shows, the calculated value of standard volumetric heating

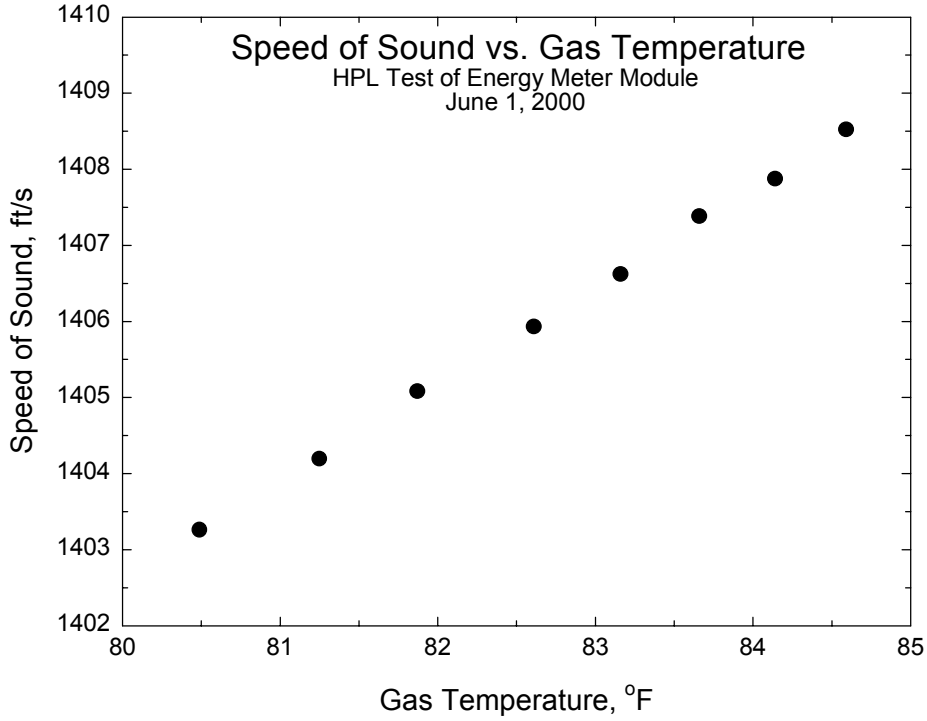


**Figure 41a. Graph of measured sound speed versus measured value of gas temperature with no gas flow in GRI MRF HPL.**

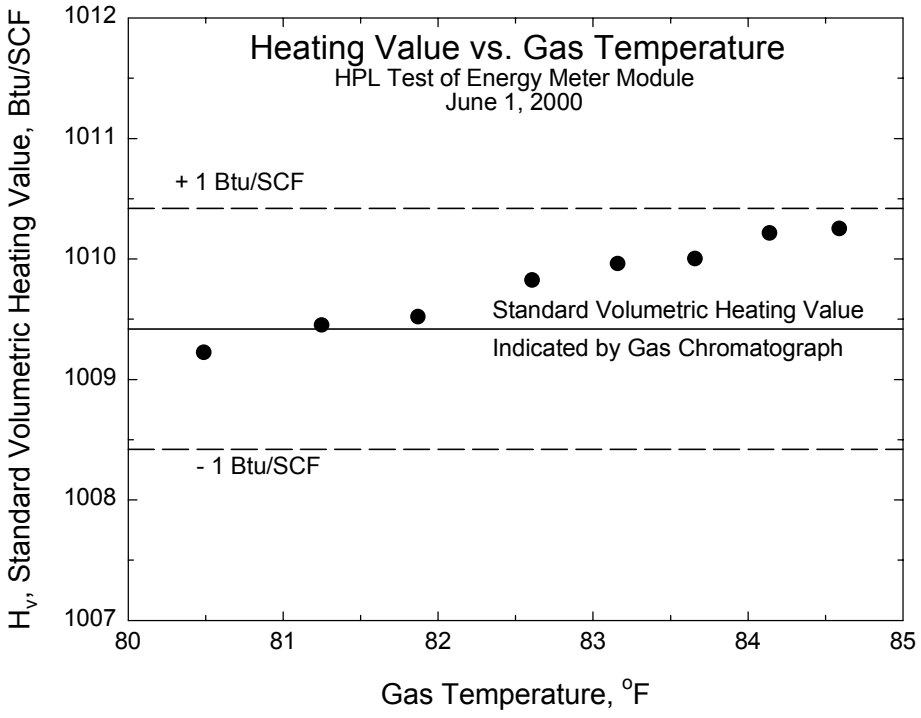


**Figure 41b. Graph of calculated value of standard volumetric heating value versus measured value of gas temperature with no gas flow in GRI MRF HPL.**

value, $H_v$, changed by about +1 Btu/SCF and remained within an interval of ±1 Btu/SCF of the value indicated by the gas chromatograph analysis.

Of course, the actual value of $H_v$ was 1009.4 Btu/SCF and did not change during this time. The increase of 1 Btu/SCF observed in the calculated value of $H_v$ suggests that the recorded values of temperature, pressure, and sound speed were not in equilibrium. Note that a value of +1.2 Btu/SCF would be predicted using the sensitivity factors in Section 4.1 and the upper and lower limits of temperature, pressure, and sound speed in Table 13. Since the temperature is measured inside a thermowell, it is subject to an error due to thermal conduction through the pipe wall and thermowell casing. A temperature measurement error as small as +0.7°F would cause an error of 1 Btu/SCF in $H_v$.

$$\Delta H_v = 1.45\frac{Btu}{SCF*°F}*4.1°F - 0.89\frac{Btu}{SCF*ft/s}*5.26\,ft/s - 0.036\frac{Btu}{SCF*psi}*1.6\,psi = 1.21\frac{Btu}{SCF}$$

**Table 13. HPL data recorded under conditions of no gas flow on June 1, 2000.**

| *Temperature, (°F)* | *Pressure, (psia)* | *Sound Speed, (ft/s)* | *$H_v$, (Btu/SCF)* |
|---|---|---|---|
| 80.49 | 648.2 | 1403.26 | 1009.2 |
| 81.25 | 648.4 | 1404.19 | 1009.5 |
| 81.87 | 648.8 | 1405.08 | 1009.5 |
| 82.61 | 648.2 | 1405.93 | 1009.8 |
| 83.16 | 649.2 | 1406.62 | 1010.0 |
| 83.66 | 649.3 | 1407.38 | 1010.0 |
| 84.14 | 649.8 | 1407.87 | 1010.2 |
| 84.59 | 649.8 | 1408.52 | 1010.3 |

The two sets of tests performed with the Daniel ultrasonic meter and the energy meter module are too limited to be considered as a definitive demonstration of performance of the energy meter module when used with an ultrasonic meter. Additional tests are needed with gas flowing through the ultrasonic flow meter. Also, the carbon dioxide and nitrogen concentrations should be measured instead of determined by a gas chromatograph.

## 7.2 Test with 4-inch Daniel Senior Orifice Meter Fitting in MRF LPL

A 4-inch diameter orifice meter with a Daniel Senior orifice fitting was installed in one leg of the MRF Low Pressure Loop as shown in Figure 40. The energy meter module performance tests with an orifice meter were originally scheduled for the week of May 30th. However, the delay caused by the problem with reading the speed of sound signal from the Daniel ultrasonic signal affected the schedule for the orifice meter tests also.

On the afternoon of June 1st and June 2nd, the flow computer was disconnected from the 12-inch Daniel 3400 ultrasonic flow meter and connected to the SwRI energy meter module (containing ultrasonic sensors and a $CO_2$ sensor) in the LPL. Although the electronic signals from the ultrasonic sensors had been transformed to resemble a Modbus signal from an ultrasonic flow meter, a problem was experienced in communication between the energy meter module and the flow computer. The problem was found in the program source code and resolved. On the morning of June 2nd, time was spent in training SwRI staff to set up and use the flow computer software without onsite support from the Bristol Babcock engineer. Once training was completed, the afternoon was used to continue to investigate the communication and speed of sound sensing problems.

Lomic SonicWare was used to calculate the speed of sound from the gas chromatograph analysis of the gas flowing in the LPL and the temperature and pressure measured in the energy meter module. There was an approximately 15 m/s difference between the speeds of sound that we obtained during the test and those computed using Lomic SonicWare software. These differences were surprising since the speed of sound values measured during instrument checkout tests with pure nitrogen gas in the sound speed sensor had agreed with accepted speed of sound values.

Test 2 began on June 13, 2000. The initial results from the $CO_2$ measurement tests indicated that the concentration of $CO_2$ was being measured to within an average of 0.054 mole% of the value determined by gas chromatography, without pressure or temperature correction (Figure 42). Furthermore, the $CO_2$ sensor provided a steady output. At this point, it was decided to modify Test 3, Test 4 and Test 5.

In the modified test plan, Test 3 was deleted because the results of the $CO_2$ concentration tests indicated that it was not necessary. Tests 4 and 5 were combined into a single flowing test providing the determination of flow rate and energy content. This test was conducted on June 13, 2000.

During the initial flowing tests on June 13, 2000, the heating value determined using the energy module was approximately 18 Btu/SCF higher than the heating value determined using a gas chromatographic analysis and GPA Standard #2172. Further analyses of raw data indicated that there was a significant difference between the indicated gas temperature at the orifice and the indicated gas temperature at the SOS sensor (Figure 43). This difference was considered too large to be accounted for by heat transfer from the sample delivery/energy module system to the flowing gas. It was also observed that the indicated gas temperature at the sound speed sensor increased throughout the day.

Flowing tests conducted in the LPL on June 14, 2000, were intended to assess the impact of changes in indicated gas temperature at the SOS sensor and in the measured sound speed. Discussions within the design team resulted in the following four test scenarios: (1) use the measured temperature at the SOS sensor and use the measured ultrasonic signal transit time; (2) use a corrected temperature at the SOS sensor and use the measured ultrasonic signal transit time; (3) use a corrected temperature at the SOS sensor and decrease the measured ultrasonic transit time by 5 μseconds; (4) use the measured temperature at the SOS sensor and decrease the measured ultrasonic transit time by 5 μseconds.

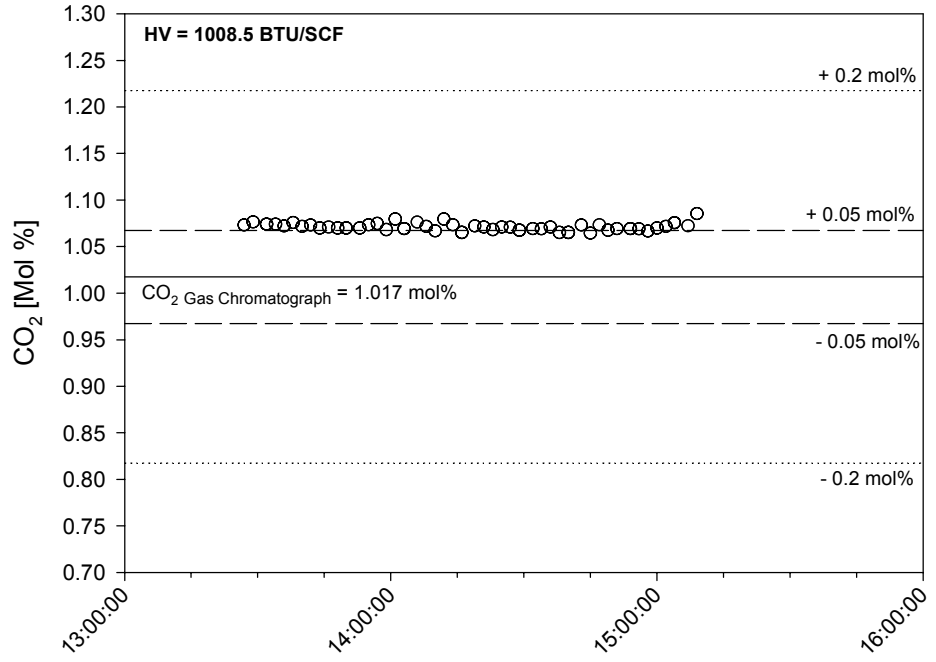


**Figure 42. Mole% difference between the $CO_2$ concentration measured by the energy meter module and the $CO_2$ concentration measured by the gas chromatograph on June 13, 2000.**

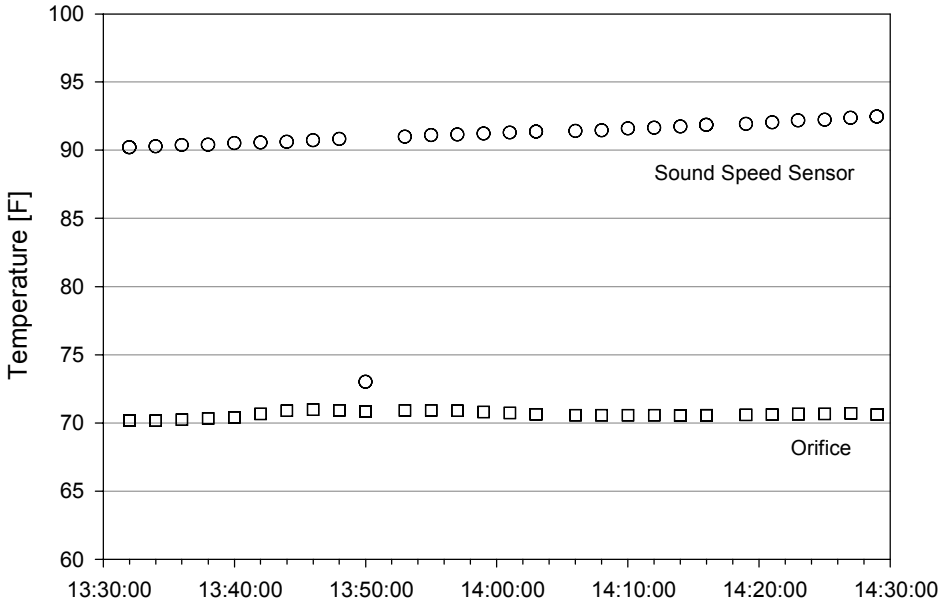


**Figure 43. Indicated temperature at the orifice meter and at the sound speed sensor in the energy meter module. (The low sound speed sensor temperature at approximately 13:50:00 is probably an anomaly.)**

The corrected (fixed) temperature was set at 73°F to reflect heating along the sample line from the sample point to the SOS chamber. It was assumed that the Joules-Thomson cooling effect was offset by the temperature of the energy module components (approximately 90°F), and the sample delivery system, resulting in a small net increase in gas temperature.

A –5-μsecond adjustment in ultrasonic signal transit time was selected to reflect an assumed error in the measured time between the 2 signals of 1 cycle (1/200 kHz = 5 μs). The adjustment signifies an increase in measured sound speed.

Table 14 shows the average heating values calculated during the June 14th LPL flowing tests. The largest deviation occurred when the measured gas temperature at the sound speed sensor and the measured ultrasonic signal transit time were used without correction or adjustment. The lowest deviation occurred when the temperature was set at 73°F and the ultrasonic signal transit-time was reduced to provide a velocity of sound consistent with Lomic SonicWare at the assumed temperature.

**Table 14. Average heating values calculated from LPL energy meter tests.**

| *Test* | *Test Conditions* | *Sensor Heating Value (Btu/SCF)* | *Reference Heating Value (Btu/SCF)* | *Difference (Btu/SCF)* |
|---|---|---|---|---|
| 1 | Measured Temperature & Measured Transit Time | 1056.6 | 1009.3 | 47.3 |
| 2 | Corrected Temperature & Measured Transit Time | 1041.7 | 1009.3 | 32.4 |
| 3 | Corrected Temperature & Reduced Transit Time | 1007.0 | 1009.3 | -2.3 |
| 4 | Measured Temperature & Reduced Transit Time | 1024.5 | 1009.3 | 15.2 |

The data suggest that the temperature indicated at the sound speed sensor is affected by the ambient temperature. It is speculated that heat transfer from the outside environment warms the sound speed sensor, thereby subjecting the temperature measurement device to heat transfer via the mechanisms of conduction and radiation, and affecting the indicated gas temperature.

The error in the speed of sound measurement may be due to one, or a combination of the following: signal processing, insufficient purging of the sensor (i.e. air contamination), and indicated gas temperature (used to look up SonicWare calculated sound velocities for comparison with the measurement). The reflected signals, viewed with an oscilloscope, provide no reason to suspect target interference.

# 8.0 RECOMMENDATIONS FOR FURTHER WORK

The scheduled test period was limited, and the unforeseen problems in communication between the ultrasonic flow meter and the flow computer limited the amount of performance information acquired. Both the ultrasonic meter test and the orifice meter test should be repeated before new research tasks are initiated.

## 8.1 Speed of Sound Measurement Improvement

Recently, a new, commercially available ultrasonic transducer was received under loan from the manufacturer. The new transducer operates at a higher frequency, 500 kHz, compared to 200 kHz for the transducer that we tested. The new transducer has a higher efficiency to generate ultrasound in natural gas. The manufacturer is willing to loan the transducer to SwRI for evaluation. If the evaluation is satisfactory, the transducer can be purchased for application to this project. It is anticipated that the results obtained with the new transducer may help to determine the causes of discrepancies between the sound speed results obtained in the LPL and the results computed using Lomic SonicWare® (1997).

The design of the sound speed sensor should be reviewed, and the sensor chamber should be tested to ensure that air is not entering the system and that there is a sufficient purge to remove any air in the system after initialization.

## 8.2 Nitrogen Concentration Sensing

The "on paper" design and evaluation of potential systems for measuring or inferring nitrogen concentration discussed in section 6.3 must be completed, and a candidate system fabricated for evaluation in the LPL. A candidate inferential system must be capable of measuring a property such as a specific heat that is sensitive to the concentration of the diluent gases, nitrogen and carbon dioxide. Although it wasn't considered in this report, the apparatus and method described in Drayton et al. (1999) should be considered if further work is undertaken.

This reference is a United States patent, assigned to GRI, that describes a method for determining thermophysical properties such as the specific heat at constant volume and the specific heat at constant pressure, without knowing the gas mixture composition. If the value of specific heat is determined accurately by applying the GRI patent, and if the specific heat is modeled as a function of pressure, temperature, speed of sound, nitrogen concentration, and carbon dioxide concentration, then it will be possible to inferentially determine the nitrogen concentration and the heating values of a gas mixture of unknown composition.

## 8.3 Temperature Measurement in Energy Meter Module

It is plausible that the temperature indicated by the sound speed sensor may be different from the actual gas temperature at that location due to heat transfer from the environment to the resistance temperature device via the mechanisms of conduction and radiation. If so, the sensor design should be modified to ensure that the indicated gas temperature is the true gas temperature. Tests should be conducted to verify the effect of the modifications. If the gas temperature is changing within the energy meter module, it may also be necessary to stabilize the

gas temperature using small diameter coiled tubing or a compact heat exchanger, before the gas stream enters the sound speed sensor.

## 8.4 Evaluate Performance for Range of Gas Mixtures

Although we are confident that the energy meter module will work well for a range of natural gas molecular weights and standard volumetric heating values, this capability should be demonstrated. We will add a quantity of propane to the natural gas in the LPL to increase the heating value to a value approaching 1100 Btu/SCF. Orifice meter tests will be performed. Analysis by the MRF gas chromatograph will confirm the gas mixture composition and provide reference data on heating value. Values of sound speed will be predicted using Lomic SonicWare and compared to measured values. A separate test should be performed with elevated levels of "inerts." We will add a quantity of carbon dioxide to the LPL that will bring the total inert gas composition to about 6 %, and perform tests with the energy meter module. Again, the MRF gas chromatograph will be used to confirm the gas mixture composition and provide reference data on heating value for comparison with values determined by the energy meter module.

## 8.5 Field Test of Energy Meter Module

Following successful tests in the MRF, the GRI MTAG membership will be solicited to assist with a field test of the energy meter module. Ideally, two types of tests would be scheduled at field sites. The first would be a test with an ultrasonic flow meter, similar to the test that will be completed in the MRF HPL. The second test would involve another class of meter such as a turbine meter, orifice meter, or Coriolis meter.

## 8.6 Market Research and Commercialization

Behring et al. (1999) operated on the presumption that a commercial niche exists for a natural gas energy meter module that is significantly less expensive and less complex than a traditional gas chromatograph for energy measurement. The market potential for a retrofit energy meter module, suitable for use with any type of natural gas flow meter, should now be confirmed.

The method could be implemented soon in ultrasonic meters, if the diluent concentrations could be input as constant values, or if only the $CO_2$ concentration is measured and the $N_2$ concentration is input as a constant value.

## 8.7 Recruit a Commercial Partner

Naturally, it will make good sense to bring a commercialization partner on board to assess the commercial potential of the energy meter module. A U.S. patent application has been filed to protect the intellectual property disclosed in this report and the previous report by Behring et al. Discussions may now be held with both potential users and manufacturers to develop a commercialization plan for the energy meter module. From a research point of view, the work outlined in sections 8.1 through 8.4 should be completed first, so that it may be reviewed with GRI/DOE and the information shared with potential commercialization partners.

# 9.0 REFERENCES


AGA (1994). Compressibility factors of natural gas and other related hydrocarbon gases. American Gas Association Transmission Measurement Committee Report No. 8, Arlington, VA.

AGA (1998). Measurement of gas by multipath ultrasonic meters. American Gas Association Transmission Measurement Committee Report No. 9, Arlington, VA.

Behring II, Kendricks A., Kelner, Eric, Minachi, Ali, Sparks, Cecil R., Morrow, Thomas B., Svedeman, Steven J. (1999). A technology assessment and feasibility evaluation of natural gas energy flow measurement alternatives, Final Report, Tasks A and B, DOE Cooperative Agreement No. DE-FC21-96MC33033, U.S. Department of Energy, Morgantown, WV. Southwest Research Institute, San Antonio, TX.

Coleman, Hugh W., Steele, W. Glenn (1989). *Experimentation and uncertainty analysis for engineers.* John Wiley & Sons, New York.

Drayton, Troy, Beyerlein, Steve, Savidge, Jeffrey L., Goodwin, Anthony R. H. (1999). Apparatus and method for determining thermophysical properties using an isochoric approach. United States Patent 5,932,793. Date of Patent: August 3, 1999. U. S. Patent Office, Washington, DC.

Ferziger, Joel H. (1981). *Numerical methods for engineering application*. John Wiley & Sons, New York.

Gas Processors Association (1994). Table of physical constants of paraffin hydrocarbons and other components of natural gas. GPA Standard 2145-94. Gas Processors Association, Tulsa, OK.

Kristensen, Bard D., Lofseik, Cecilie, Froysa, Kjell-Eivind (1998). An overview of projects related to the KOS FMU 700 6 path ultrasonic gas flow meter, American Gas Association Operations Conference, Seattle, WA, May 17-19, 1998.

Lomic (1997). SonicWare® computer program, Ver. 2.0, Lomic Inc., State College, PA.

Lueptow, Richard M., Phillips, Scott (1994). Acoustic sensor for determining combustion properties of natural gas, Measurement Science and Technology, Vol. 5, pp. 1374-1381.

Miller, Jr., Judd (1995). Grid integration project gas quality task force final report. Exxon Company, USA, Houston, TX.

Savidge, Jeffrey L. (1989). "GRI Extended Thermodynamic Properties Computer Program," Gas Research Institute, Chicago, IL, March 1989.

SigmaPlot 5.0 (1998). SPSS Inc, Chicago, IL.

Starling, K.E., Fitz, C.W., Chen, Y.C., Rondon, E., Jacobsen, R.T., Beyerlein, S.W., Clarke, W.P., Lemmon, E. (1991). GRI high accuracy natural gas equation of state for gas measurement applications. Annual Report, May 1990 – April 1991, for Gas Research Institute, Chicago, IL.

Watson, J. W., White, F. A. (1981). Acoustic measurement of natural gas Btu content, 1981 International Gas Research Conference, Los Angeles, CA, Sept. 28 – Oct. 1, 1981, pp. 1793-1802.

*This page is intentionally blank.*